

POLITECNICO DI TORINO

Department Of Structural, Building, And Geotechnical Engineering

Masters Course in Civil Engineering



Masters course thesis

Analysis of the state of conservation of the ferrocement structures by Eng. Pier Luigi Nervi: numerical and experimental study.

Supervisor

Prof. Ing. Francesco Tondolo

Candidate

Qazi Mohammad Swaleh

Assistant supervisor

Prof. Erica Lenticchia

Prof. Ing. Rosario Ceravolo

A.Y 2021/2022

TABLE OF CONTENTS

1. INTRODUCTION.....	5
2. WHAT IS FERROCEMENT.....	7
2.1. Origin of ferrocement.....	7
2.2. Application And Recent Prespectives Of Ferrocement.....	9
2.3. Marine Application.....	11
2.4. Repair And Rehabilitation.....	11
2.5. Boats.....	14
2.6. Use In Sydney Opera House.....	17
3. USE OF FERROCEMENT BY ENG. PIER LUIGI NERVI.....	20
3.1. Pier Luigi Nervi works.....	21
3.1.1. Palazzetto dello Sport, Roma.....	21
3.1.2. Stadio Artemio Franchi 1930.....	24
3.1.3. Torino Esposizioni Complex Centre.....	26
3.2. Construction Phase Of The Exhibition Centre.....	26
3.3. Hall B.....	28
3.4. HALL C.....	30
3.5. Current Use of Pavilions Today.....	34
4. CASE STUDY.....	38
4.1. Pier Luigi Nervi: Shell and Spatial Structure Construction System.....	38
4.2. Ferrocement Slabs.....	38
4.3. Shape resisting structures.....	40
5. MECHANICAL BEHAVIOR OF FERROCEMENTS.....	45
5.1. Constituent Materials of Ferrocement.....	45
5.2. Behaviour Of Ferrocement In Tension.....	50
5.3. Stress Strain Law.....	52
5.3.1. Elastic modulus of cracked and uncracked section.....	53
5.3.2. Prediction of stress strain response for the ferrocement mockup.....	54
5.4. Typical moment-curvature response.....	59
5.5. Calculation Of Cracking Bending Moment.....	60
6. SELECTING THE TYPE OF MOCK-UP.....	64
6.1 Realization of smaller mock-ups.....	64
6.2 Realization of bigger Mock-up.....	66

6.3	Practical implementation of bigger mock-up.....	70
6.3.1.	Aluminium Curved Sheet Placement	73
6.3.2.	Shaping and placement of the reinforcements	75
6.3.3.	Trial testing of the beam.	78
6.3.4.	Making Of Diaphragms	80
7.	ANALYSIS OF CURVED SHAPED BEAM	81
7.1	Modelling the beam in RHINO	81
7.2	4-point bending test.	83
7.3	Finite Element Modelling and Analysis	84
7.3.1	Numerical Modelling and Analysis.	85
8.	CONCLUSION AND FUTURE DEVELOPMENTS	89
	References	91
	INDEX OF FIGURE	94
	INDEX FOR TABLE	97

1. INTRODUCTION

As the architectural history in Italy and around the world makes up a sizeable portion of the existing structures and is in increased danger, the topic of structural conservation, or the preservation of modern 20th-century buildings, is becoming a more common one. The idea behind structural restoration is what is opening new avenues for study and collaboration between public and commercial organizations. This results from a crucial need to deal with the upkeep of several prominent and historic buildings throughout the world. But these works continue to be undervalued and underappreciated, and there is also a lot of disinformation about these crucial issues.

Unfortunately, there is also a lack of effective technique and a shortage of information on the resources and interventions that address these difficult problems. Research and experimentation into methods and materials for rehabilitating concrete structures, the material used in construction the most frequently worldwide, are notably lacking at the moment. There is a practical lack of linear and functional solutions to the issue, which is consistent with environmental sustainability issues. Therefore, the main goal is to explore and learn about the most important factors affecting structures by working with and developing relationships with significant global institutions.

The Getty Foundation's "Keeping it Modern" Project has focused its attention on the reuse and structural rehabilitation of historically and architecturally prestigious concrete buildings from the 20th century. [1] Through the cast-in-place and prefabrication of pieces in reinforced concrete or ferrocement, a substance he created and patented during the war, Pier Luigi Nervi has long explored the potential of concrete. The Halls of the Palazzo di Torino Esposizioni in Turin, the UNESCO buildings in Paris, the Palazzetto dello Sport in Rome, and the Aula per le Udinese in the Vatican are just a few of his most well-known works. Pier Luigi Nervi was a prolific engineer and architect who pushed the boundaries of reinforced concrete with daring innovations and expressive concepts. [1] All of these structures represent an important chapter in the history of twentieth-century architecture, structure, and construction. The volume carefully examines Nervi's enthusiasm for the fabrication of formwork and concrete.

The buildings and artwork that make up the rich architectural history of Italy date from many different historical eras, so planning for their proper upkeep frequently takes precedence over the construction of new structures. A few of the elements that make up maintenance planning include study and evaluation of the work, analysis of the laws in force at the time of construction, and the creation of tests for determining the current state of conservation.

This thesis is a work of project which aims at preserving the existing works of Eng. Pier Luigi Nervi, in the present work explored in this thesis mainly focus on the analysis and the state of conservation of the ferrocement structures of the Torino Esposizioni in Turin, The Nervi's System's building possibilities have been investigated and studied, and the construction steps have been replicated, ensuring a thorough grasp of the structure in order to make a miniature model and analyze how it would behave under the given deteriorating circumstances.. [2]

Also in July 2019 The Getty Foundation in Los Angeles has selected Torino Esposizioni, the exhibition complex designed and built by Pier Luigi Nervi between 1947 and 1954, to enter the list of over 60 works of world architecture of the twentieth century of the "Keeping It Modern" program, which since 2014 chooses and finances conservation projects of iconic buildings of the twentieth century in order to develop recovery models for contemporary architecture, The grant of about 200 thousand dollars comes as a result of a multidisciplinary work that involves Italian, European and American researchers led by the Polytechnic of Turin and coordinated by professors in concert with the City of Turin, [2].

This thesis seeks to pinpoint a thorough investigation of the building with the goal of identifying the structural conception and the construction philosophy used by Nervi in order to recover and repurpose these structures, which are currently abandoned. The project of 1:1 scale construction of the ferrocement mock-ups, replicating a corrugated beam from the Torino Esposizioni pavilion C's perimeter floor. To achieve this, materials with geometric and mechanical properties as close to those used in 1949 as possible have been analysed and purchased after a comprehensive examination of archival documentation from the period of construction. And last, a hardwood formwork with the appropriate shape for casting pieces with original geometries The next step is to observe how mock-ups behave after intentionally creating a condition of deterioration brought on by corrosion of the steel reinforcing also

building up the model in a FEA software such as ANSYS and predict the behaviour of the corrugated beam 4 point bending test and later use the results for the real testing of beam.

2. WHAT IS FERROCEMENT

2.1. Origin of ferrocement

An "armature" of metal mesh, woven, expanded metal, or metal-fibres and closely spaced thin steel rods, such as rebar, is used as a foundation for reinforced mortar or plaster (lime or cement, sand, and water). Iron or a form of steel is the most used metal, and wire with a diameter of between 0.5 mm and 1 mm is utilized to create the mesh. When used to make boards, the cement is normally a highly rich mixture of sand and cement in a 3:1 ratio; because no gravel is used, the substance is not concrete. [3]

Ferrocement is used to build a variety of forms and relatively thin, hard, robust surfaces, including water tanks, shell roofs, and boat hulls. Ferrocement, the precursor of reinforced concrete, was developed in France and the Netherlands in the 1840s. It may also be used for a variety of other things, such sculpture and prefabricated construction parts. [3]

Because ferrocement is reinforced in two dimensions as opposed to the traditional reinforced concrete, it exhibits homogenous-isotropic qualities in both directions. Ferrocement typically has a high reinforcing ratio, which contributes to its high tensile strength and high rupture modulus. Additionally, because ferrocement's specific surface of reinforcement is one to two orders of magnitude higher than that of reinforced concrete, larger bond forces with the matrix form, resulting in an average crack spacing and width that is more than an order of magnitude smaller than in conventional reinforced concrete. The simplicity of prefabrication and cheap cost of maintenance and repair are further enticing qualities of ferro cement.

The renaissance of ferrocement in recent two decades has led to the ACI design guideline "Guide for the Design, Construction, and Repair of Ferrocement, [4], and publications such as "Ferrocement Design, Techniques, and Application" [5] and "Ferrocement and Laminated Cementitious Composites, [6] , which provide comprehensive understanding and detailed design method of contemporary ferrocement. However, the rapid development in reinforcing

meshes and matrix design requires continuous research to characterize the new material and improve the overall performance of ferrocement.

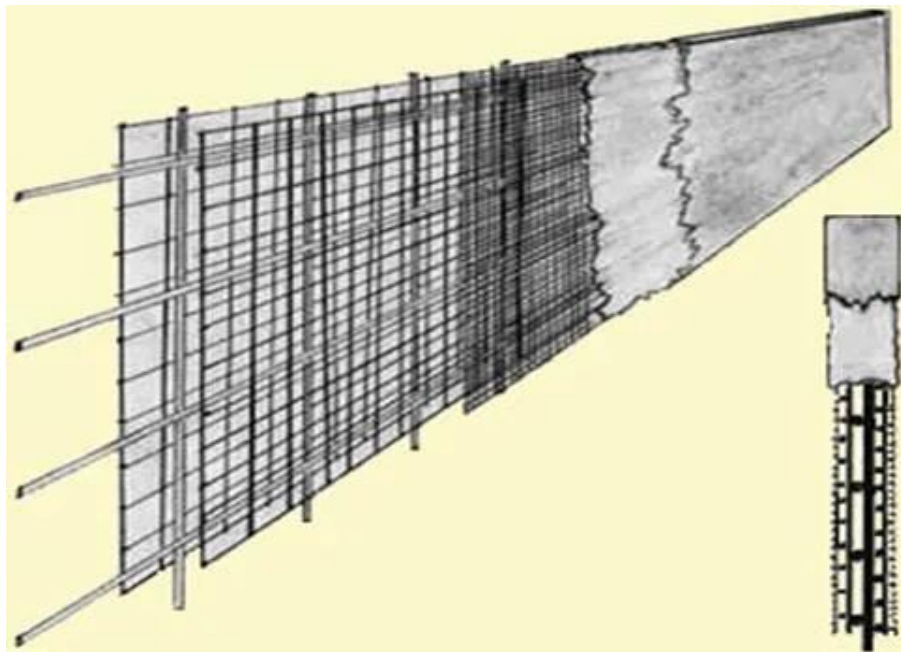


Figure 1 typical cross section of ferrocement beam [7]

The effective manufacture of meshes was not possible with the technology of the second half of the 19th century, and tiny diameter wires were very costly compared to larger diameter rods. As a result, the usage of bigger diameter iron or steel rods increased, which caused ferrocement construction to give way to conventional reinforced concrete building. After then, reinforced concrete was the preferred material. Due to a lack of supplies, notably steel, reinforced concrete was once again tried to build ships and barges during the First World War. This time, it failed. In essence, reinforced and prestressed concrete took the role of ferrocement.



Figure 2 joseph loius labot (right) ferrocement boat (left)

2.2. Application And Recent Prespectives Of Ferrocement

The earliest known kind of reinforced concrete, known as ferrocement, was initially employed two centuries ago in France and Italy, mostly for the building of boats. It is constructed from mortar and steel wire mesh and is often cast in very thin pieces, allowing for the creation of any desired design, as seen in Figure 1. Ferrocement sections typically have a thickness of 2 to 3 cm. Ferrocement is a fascinating and adaptable substance that has not received much attention and has a wide range of potential uses. It is a composite material made of mortar matrix and steel wire mesh. Depending on the needs of the application, several mesh types may be utilized to create ferrocement sheets. [4]



Figure 3 Having been given a cylindrical shape, cement and its components, mortar and steel

When comparing the behavior of the two materials in terms of tension and flexure, the State-of-the-art report on ferrocement from ACI [1] separates ferrocement from standard concrete. Since the mortar matrix splits during the first stages of stress, the wire mesh is responsible for the tensile and flexural strength of ferrocement. The compression behavior of traditional concrete is comparable. The cracking, impact, and load-deformation behaviors of this material are among of its positive qualities. Despite tiny fractures being present in the matrix even before loading, ferrocement can restrict crack growth due to the reinforcement's

excellent distribution. Due to insufficient curing or cover thickness, these little fractures may appear.

As indicated in Figure 2, the primary mesh types employed in ferrocement applications include hexagonal mesh, woven mesh, welded mesh, and expanded metal. In general, it can be said that the kind and orientation of the reinforcement utilized have a significant impact on the qualities of the ferrocement. The welded mesh, which has two powerful directions that are equally strengthened, provides the optimum performance for practically all attributes. Despite having a weaker 45° direction than expanded metal (unidirectional mesh), woven, or hexagonal mesh, this form of mesh nonetheless produces superior results. [6]



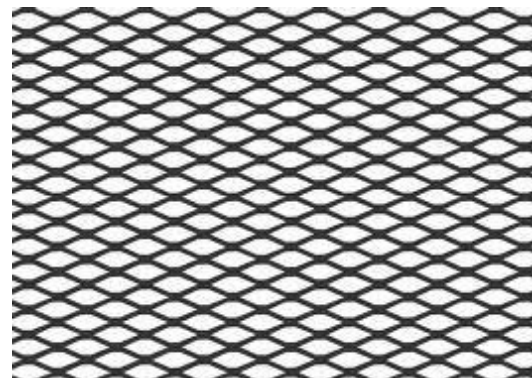
(a)



(b)



(c)



(d)

Figure 4 Types of wire mesh used in ferrocement applications; (a) welded wire mesh; (b) hexagonal wire mesh; (c) woven wire mesh; (d) expanded metal [6]

The original use of ferrocement is the construction of mediums size boats, marine application, Terrestrial Applications, Repair and Rehabilitation though other usages related to the agricultural applications have emerged with time.

2.3. Marine Application

Boats, fishing ferries, barges, docks, cargo tugs, flotation buoys, and water or fuel tanks are just a few examples of marine applications for ferro cement. Thickness, impact resistance, watertightness, and low weight are the main requirements for these applications. Fishing boats, transport boats with flat bottoms used mostly for inland transit, catamarans, yachts, ancient schooner replicas, farming boats, and oil tankers are just a few of the several types of boats that have been constructed out of ferro cement.

2.4. Repair And Rehabilitation

Ferrocement is perfect for patching and other minor repairs due to its simplicity and inexpensive cost of application. Important examples, however, are lining for existing swimming pools, lining for corroded steel water tanks, confinement jackets for reinforced concrete columns to increase their seismic resistance, skin reinforcement for unreinforced brick or masonry walls to increase their seismic response.

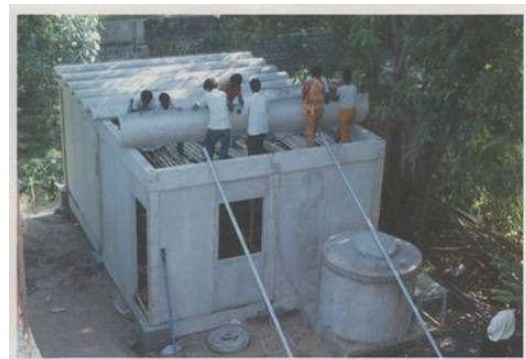
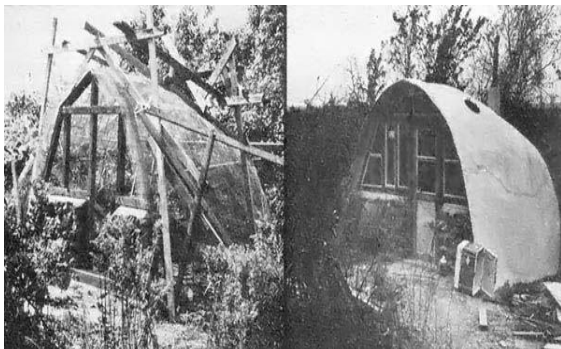




Figure 5 typical ferrocement housing units

Ferrocement is most widely utilized in the construction industry for famous architectural works like Antoni Gaudi's buildings, as well as smaller projects like modest cottages or granaries for agricultural purposes. [8]

The ease of availability of the material, the low level of technology needed for construction, and the relatively inexpensive cost of the finished product all contribute to the success of using ferro cement in many terrestrial applications. One of the major benefits of adopting it is that, depending on the budget and plan, it may be constructed with a wide range of mechanical qualities, quality, and costs. The potential for industrialization, which would result in the production of panels in various sizes that are subsequently installed on site, is another advantage that has encouraged its usage for the construction of single-family homes in America. [6]

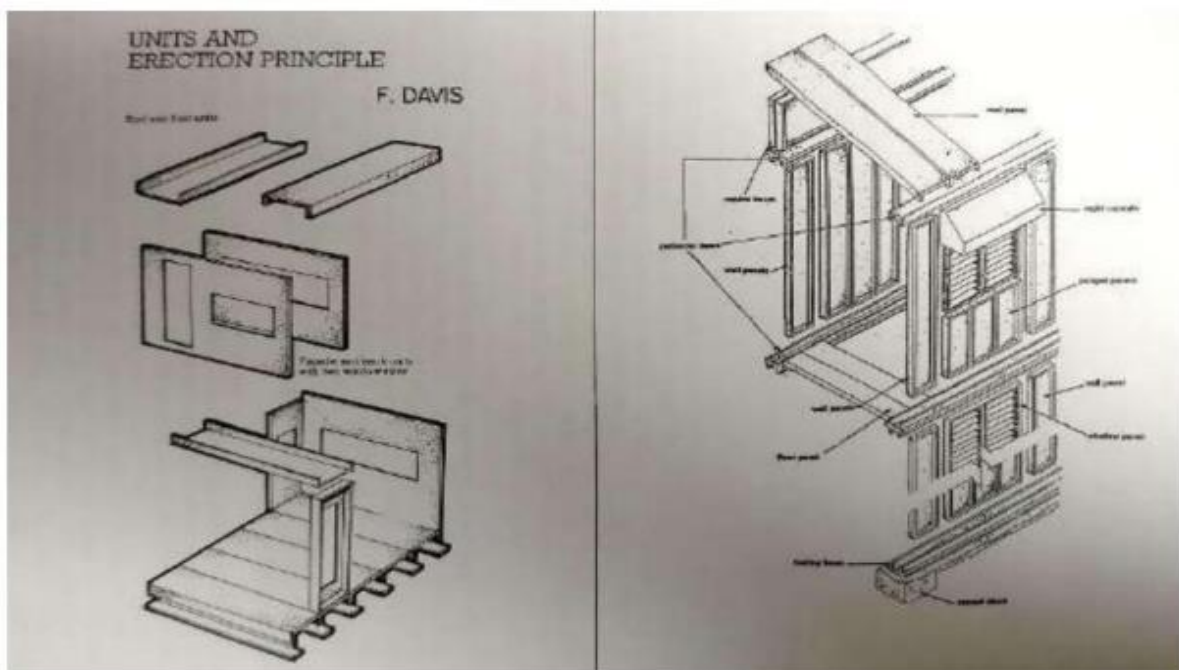


Figure 6 ferro-cement panels that have been prefabricated and installed for a house [6]

A ferrocement structure is formed by fabricating the mesh reinforcement to the shape and size of the structure first and then mortared and cured. A skeleton of steel bars is welded to the exact geometrical shape and size of the structure. This provides a rigid framework for the structure. Mesh reinforcement is tightly tied over this skeleton of steel bars. Multiple layers can be used to achieve the required density of steel. Cement Mortar is applied over this reinforcement. The mortar can be applied either by hand or shot through a spray gun. The reinforcement should be completely covered with mortar to prevent any corrosion. Curing is necessary to develop the required strength of the structure and a curing period of 28 days is suggested. However a minimum of 14 days of curing is essential. Clean water should be used for curing and should start 24hrs after the application of mortar.



Figure 7 ferrocement wall in construction [7]





Figure 8 ferrocement walls and shell in India [9]



Figure 9 ferrocement dome shaped house [7]

2.5. Boats

A boat-building technique that uses steel wires wrapped in a sand and cement plaster and was developed by the French in 1855 is known in English-speaking countries as ferro-cement. There are still ferrocement boats around, and at least one of them is still afloat, from before 1855. The construction technique was known as Ferro-cemento by the Italians. Ferro-cement, also known as "concrete," was the name given to the technique for do-it-yourself construction by the British, New Zealanders, and Canadians. For boats longer than 25 feet, it is the simplest and least expensive type of construction. Additionally, without the need for specialized

equipment or a weatherproof structure, it is the only material for big round-bilge boats that is practical for amateurs, with the exception of strip-plank composite construction. Because of ferrocement's low strength to weight ratio, however, application has been limited to low performance displacement craft over 30-feet. [6]

Pier Luigi Nervi repurposed the ferrocement, Study idea in the early 1940s in order to apply it to the building of fishing boats. He emphasized how the placement of the reinforcement meshes results in a concrete material with largely homogenous mechanical characteristics that can bear a heavy impact. He put the slab-making material through tests, demonstrating that ferrocement had outstanding strength, flexibility, elasticity, and crack resistance. The Italian Navy also granted ferrocement permission in 1943. [6]

He put the slab-making material through testing, demonstrating the excellent elasticity, flexibility, strength, and crack resistance of ferrocement. The Italian Navy also granted ferrocement the pass in 1943. Soon after, Nervi constructed "Irene," a 165-ton motor yacht with a 35 mm thick ferrocement hull, to show off the material's possibilities.

Extremely pleased with "Irene" Nervi's accomplishment, he significantly deepened the usage of ferrocement by focusing on construction.



Figure 10 Ferro-cement fishing boat 'La Giuseppa', designed by Nervi, 1967 Image source: ericafirpo.com (left): ferrocement boat name PRISCILLA (right) [10]

In the UK, New Zealand, Canada, and Australia, ferrocement for boat building ultimately attained widespread recognition in the early 1960s. The United Nations' Food and Agriculture Organization (FAO) began ferro-concrete boat building initiatives in Asia, Africa, and Latin America in 1968. Other nations, such as the Soviet Union, China, and a number of South-East

Asian nations, followed. A group was established by the US National Academy of Science in 1972 to study the use of ferrocement in developing nations. [6].

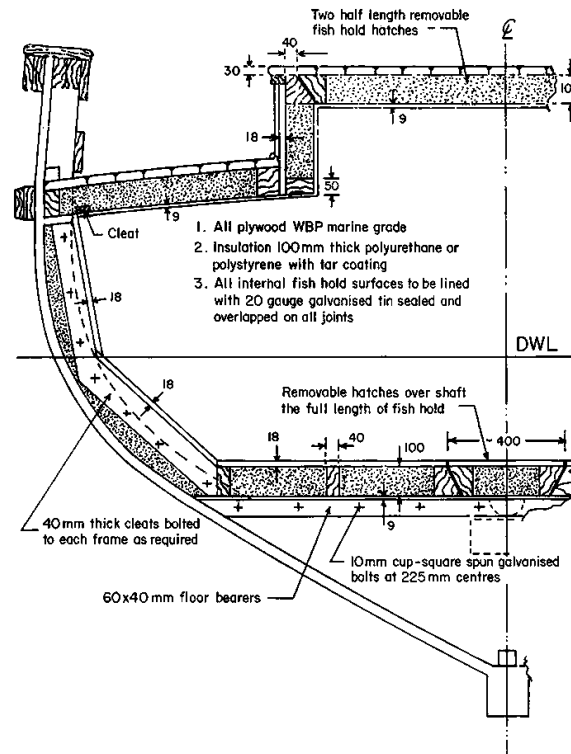


Figure 11 Typical section through bulwark showing fitting out detail



Figure 12 ferrocement boat Ambrym dating 1985 [10]



Figure 13 large size boat of ferrocement in China (left); medium size ferrocement boats (right) source A Naman [6]

2.6. Use In Sydney Opera House

The Sydney Opera House is one of the most well-known examples of ferrocement. Despite not being entirely comprised of ferrocement, the roof is made up of ferrocement panels that fit together. Many challenges were faced in constructing the Sydney Opera House, which was thought by many at the time to be ‘unbuildable’. The design competition was won by Jorn Utzon in 1957 but the building was not completed until mid-1973. [11]

A significant engineering challenge related to the design of the enormous pre-cast concrete shells. This was successfully achieved through the analyses of its structure by the use of pioneering computer programs:

As said by Ove Arup “The roofs were considered shell structures, as four pairs of triangular shells, but they had to be considered in longitudinal stability as a whole system of four pairs of shells as one... It is one of those not infrequent cases where the best architectural form and the best structural form are not the same” [12]

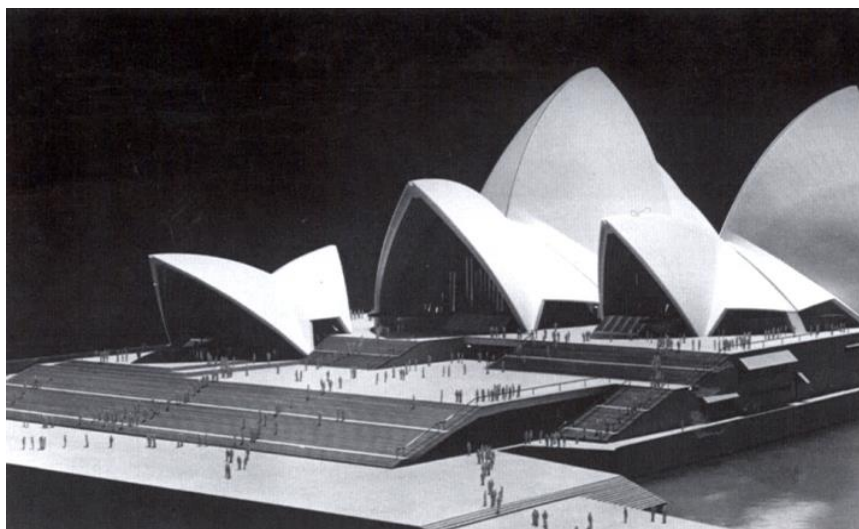
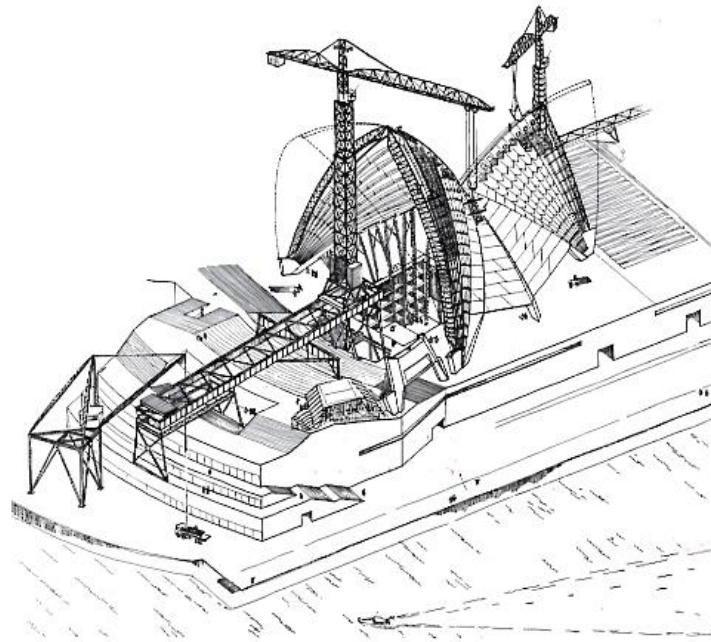


Figure 14 Sydney opera house built with ferrocement shell elements [13]

The chosen method involved creating each shell unit from a single sphere. This allowed the pre-cast concrete ribs to be comparable in length, set at varied angles, and adhered to the neighbouring units with epoxy glue. This gave the units a means of evenly distributing the weight.

Ceramic tiles placed face down in a mould and a ferro-cement mixture cast on the back with built-in reinforcing ribs are used to create the roof covering. A 30 mm thick galvanized steel reinforcing mesh is used with mortar to create ferro-cement. Against increase the resistance of the panels to wind-blown salt ingress, epoxy glue was poured into the joints between the tiles, providing a 1 mm thick barrier layer. Due to the diurnal temperature changes, the joints between the panels were prone to complicated movement patterns and needed to be filled with a high performance sealant. [13]

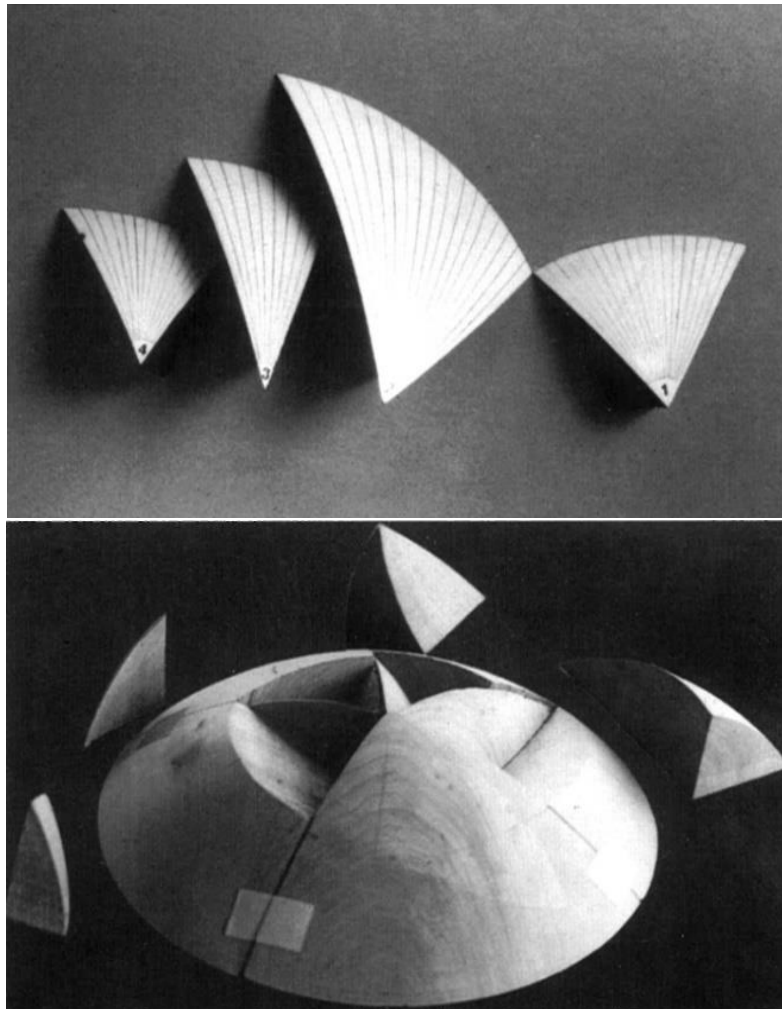


Figure 15 Sydney opera house (Australia) [13]

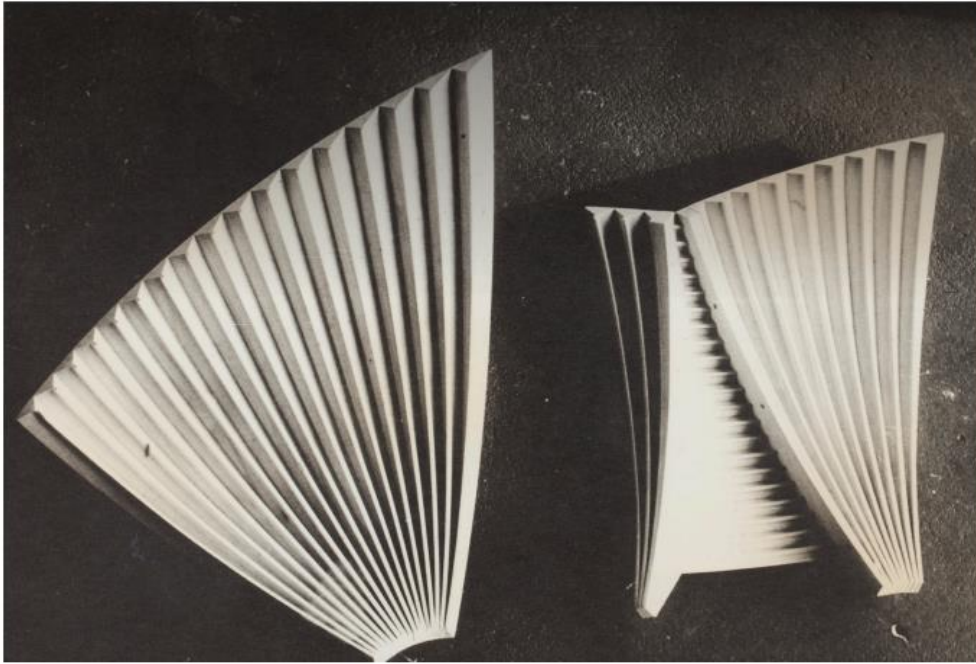


Figure 16 Arup, O and Zunz, J 1969, 'Sydney Opera House', *Structural Engineer*, March 1969. Reprinted in *The Arup* [13]

3. USE OF FERROCEMENT BY ENG. PIER LUIGI NERVI

Pier Luigi Nervi was an Italian engineer and architect who lived from 21 June 1891 until 9 January 1979. His time at the University of Bologna culminated with a 1913 graduation. From 1946 to 1961, Nervi served as an engineering professor at Rome University. He is renowned internationally as a structural engineer, architect, and for his inventive use of reinforced concrete, particularly with regard to a number of well-known thin shell structures. [11]

In Italy, Nervi received his education and worked as an *ingegnere edile*, or "construction engineer." An architect might also be regarded a building engineer during the time, and to a lesser extent today. His artistically attractive designs were adopted for significant projects after 1932. This was because there were so many construction projects using concrete and steel at the period in Europe, and the focus shifted from architecture to the possibilities of engineering. In his time, Nervi was successful in making reinforced concrete the primary structural material. In four books and numerous scholarly works, Nervi developed his theories on construction. [11]

Archaeological digs indicated that he might be in charge of the Flaminio stadium's foundations, which pass through old Roman tombs. His creations also appeared in the 1936 Summer Olympics art competition's building category. [14]

Although he worked on projects abroad, the majority of the buildings he built were in his own Italy. The George Washington Bridge Bus Station, for which Nervi created the roof made of triangular parts that were formed in place, was his first project in the United States. Currently, more than 700 buses and their passengers use this structure.

Without ever losing sight of the structure's functionality, Pier Luigi Nervi based his designs on their ability to be intuitive. He was inspired to create strong ideas by the harmony of structure and shape, which he executed using readily available materials like reinforced concrete. Other architects throughout Europe were greatly influenced by and inspired by this idea. He often made extensive use of prefabricated materials, such as his invention of **Ferrocement**, a construction system that used reinforced mortar or plaster, applied over a metal "armature," and closely spaced thin steel rods, such as rebar. He was driven by the desire to express the beauty and the clever implementation of this material in his works.

3.1. Pier Luigi Nervi works.

3.1.1. Palazzetto dello Sport, Roma

The dome architecture was popularized throughout the world by this innovative undertaking. Palazzetto Dello Sport straddles the line between a restrained design and a formal taste. It was created in the 1950s as a prototype for a sporting palace made of affordable materials by Pier Luigi Nervi and Annibale Vitellozzi; the dome was constructed of prefabricated ferrocement and distinguished by a smooth surface and an embroidered interior. It was one of the earliest uses of the so-called "Nervi System," Pier Luigi Nervi's go-to strategy for controlling expenses. This building became a representation of the revitalization of a once-deserted area while also putting out a fresh approach to architectural design. [15]

In 1954, the Italian National Olympic Committee commissioned the project to the architect Annibale Vitellozzi who called Nervi for the roof structure. The conception is essential: a large dome with a circular plan of 60 meters in diameter raised on inclined trestles set on an external circumference of 78 meters. Having abolished the wooden rib, Nervi, as already starting from the second series of hangars, breaks down the canopy into pieces to be assembled on site, then assembled on a light and discontinuous scaffolding; the reinforcement is thus arranged in the channels between the planks and the completion casting is carried out. [16]

The roof is supported by 36 Y-shaped trestles that are placed along the plant's perimeter at an angle of 10 degrees and a linear distance of 6.30 meters from one another. The trestles are inclined in accordance with the tangent to the point of intersection with the concrete cap. This roof is entirely made of reinforced concrete and is prefabricated according to wedge-shaped modules, wider towards the outside and then tightening towards the centre of the cap. [17]



Figure 17 Palazzetto dello Sport (Rome) [15]

The building has a first-aid station, four groups of locker rooms, an official's locker room, a medical sports centre, a management office, a press room with 12 phone booths, two storerooms, and heating and air conditioning equipment that is placed in the basement. The seating may be arranged to accommodate 3,500 basketball fans and up to 5,600 for fans of boxing or wrestling. The arena is built with a 61-meter-diameter ribbed concrete shell dome that is made of 1,620

prefabricated concrete pieces and is supported by concrete flying buttresses. The dome was built in 40 days because a large portion of the structure was prefabricated. [15]



(A)



(B)



(C)



(D)



(E)



(F)

Figure 18 (A) interior view Palazzetto dello Sport; (B) Exterior view of the Palazzetto (Source: Pier Luigi Nervi Project); Aerial view of the Flaminio Stadium; (D) Flaminio shelters; (E) Interior view of the Palazzetto; (F) Aerial view of the Sports Palace [18]

The dome of the Palazzetto dello Sport was constructed entirely out of precast "rhomboidal components." The thickness of each of the 12 sorts of elements is the same (2,5 cm). They were mass produced in advance using a mold made from a model. The reinforcement was then put in the channels and the cast was completed when these components were set on the scaffolding, only resting on 2 places. The extrados of the dome, where a 3 cm thick layer

of concrete was poured, are also included in the reinforcement. The intrados of the ring gallery at the Palazzo dello Sport were also painted using the same style. The moulds were prepared in six separate steps using a model here as well in order to prefabricate the necessary 240 parts. [19]

3.1.2. Stadio Artemio Franchi 1930

The In the heart of Tuscany's most priceless city, the Artemio Franchi Stadium is a truly hidden treasure. It is the first piece of work created by Italian architect Pier Luigi Nervi. This stadium, which was originally built as a memorial to a young Florentine fascist who was assassinated for political reasons, is a lovely example of how Nervi quickly rose to become one of the greatest Italian architects of the twentieth century. The president of the newly formed Fiorentina, the Marquis Luigi Ridolfi da Verrazzano, ordered the construction of a new stadium in 1930. Construction didn't finish until 1932, and the stadium held 39,000 spectators. [20]

In order to create the comparatively light forms of the cantilevered roof and helical staircases, strong steel reinforcing and moment connections for lateral stability were used throughout the stadium's construction. [21] Starting with the "D" form of the building, which was specifically wanted by the fascist authorities as part of a comprehensive exercise in design and ideological fanaticism, there are numerous characteristics of this structure. It stands for a unique thing in the globe. The grandstand's canopy was an amazing feat of engineering, with a formal design, a 22-meter overhang, and no structural supports of any type, allow for a full view of the playing field. [20]

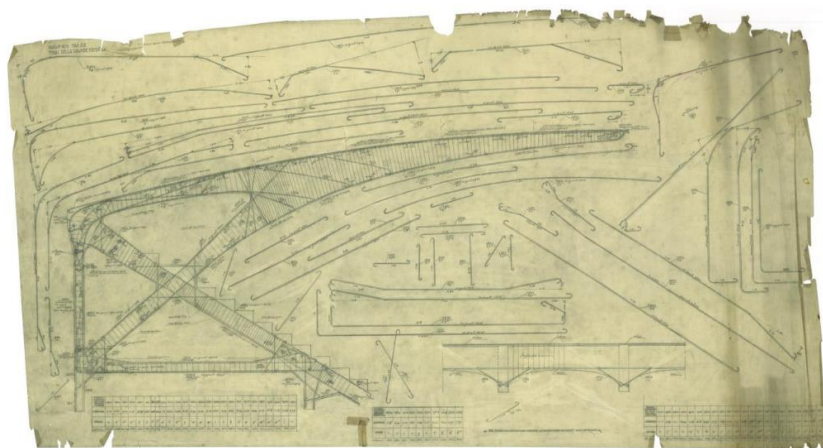


Figure 19 Pier Luigi Nervi, drawing of the covered stand, section of the heading part, undated (1931). Private Archive of Pier Luigi Nervi, Rome [21]

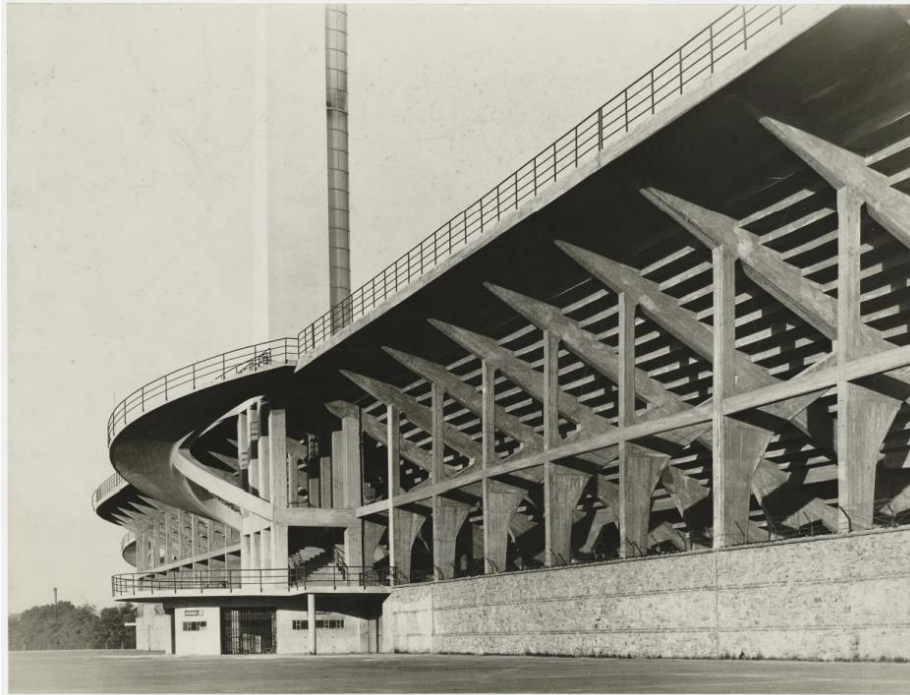


Figure 20 External view of the Stadium shortly after its completion, © Ferdinando Barsotti, 1932 [21]

Nervi's designs for the grandstands, the grandstand roof, and the helicoidal staircases demonstrate his growing self-assurance in both his design and construction skills. Their global publication served as an inspiration to engineers and architects all over the world. The grandstand roof is a cantilevered essay, with a created diagram showing the "proper" bending moment profile in the shape of its tapering, curving profile. The three functionally-driven stairs on the east stand are even more poetic; Nervi stabilized them with a second helical support that cuts through the stair spiral in the middle. His experimental approach and the freeing impact of his new cooperation with Bartoli on his creative sense are shown by the daring form and thin profiles. [21]

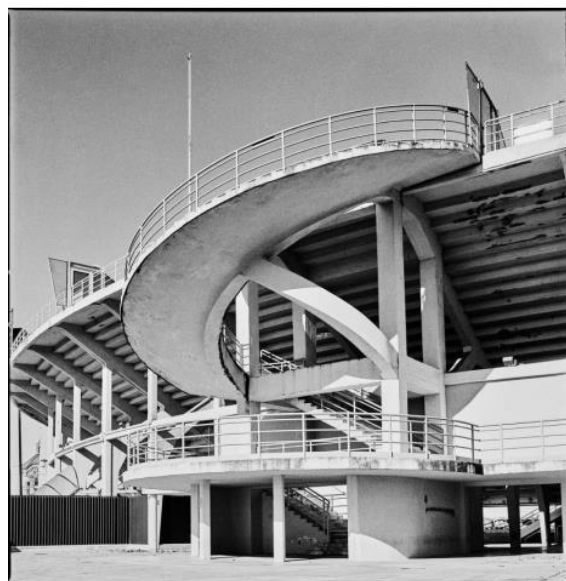


Figure 21 One of the helicoidal staircases, ©Marco Menghi, 2018 [21]

3.1.3. Torino Esposizioni Complex Centre

The Palazzo della Moda, completed in 1936 by Ettore Sottsass Jr. and damaged during the War, was to be demolished and replaced with a new exhibition hall by engineer Roberto Biscaretti di Ruffia as a showcase for Turin's automotive industry. The project by Biscaretti, which was based on a large hall with an apse, underwent two significant revisions in 1947 after Nervi & Bartoli won the invited competitive tender: inclined lateral columns to raise the vault above grade and a thin, flattened semi-dome in place of a flat roof for the terminal apse. The Hall B at the Turin Exhibition was Nervi's first actual chance to put the idea of structural prefabrication into practice. It was conceived and constructed shortly after the War. In one substantial vaulted building, it blended his very individual use of ferro concrete—steel mesh and tiny diameter steel rods formed in a thin concrete pour—with the wide use of prefabricated components. Additionally, it was the first effort that connected Nervi to Fiat and Turin's important industrial customers. [22]

Nervi designed both the Turin Exhibition Center's large Hall B and the smaller, nearby Hall C. (1947-1948, and 1950). As he is in the great majority of his works, Nervi was both the Exhibition Center's designer and constructor via its construction firm. The Hall B (1947–1948) features a striking apse with a ribbed hemispherical dome and an impressive broad nave with a cylindrical barrel vault. It is designed like a spectacular contemporary cathedral. For the construction of the vault's arches, Nervi devised wave-like prefabricated reinforced concrete pieces that were connected by reinforced concrete ribs that were constructed on site. Elegant fans link the arcs with the angled columns. The apsidal semi-dome was built using lozenge-shaped ferrocement tiles connected by reinforced concrete cast in the lateral ribs and on their tops. The Hall C (1950) stands out for having the same system of ferrocement tiles and a fascinating, ribbed roof supported by four inclined arches with sculptural designs. [23]

3.2. Construction Phase Of The Exhibition Centre

The arched vault of Hall B is created by the joining of 15 prefabricated, thin, undulating pieces of ferrocement, each weighing 1500 kg. Its center line is getting close to the limit of permanent loads. Cement mortar must be used to fill a 4 cm gap left by diaphragms when their ends solidify. The method is completed by installing locally cast reinforced cement ribs in the wave's ridges and troughs. Before being moved to its final location, each component

was elevated using an elevator and put on rails that were positioned above the scaffolding. The slanted pillars supporting the vault and absorbing the thrust are connected to the wavy ceiling by three extremely elegant, fanned arms. The prefabricated ferro-cement tile components of the hemispherical dome of the apse are linked by on-site reinforced concrete that was cast in the lateral ribs and on their tops.

Nervi used the same method to build the extremely beautiful, ribbed ceiling of Hall C (with lozenge-shaped tiles) and its supporting sculpturally designed slanted arch frames.

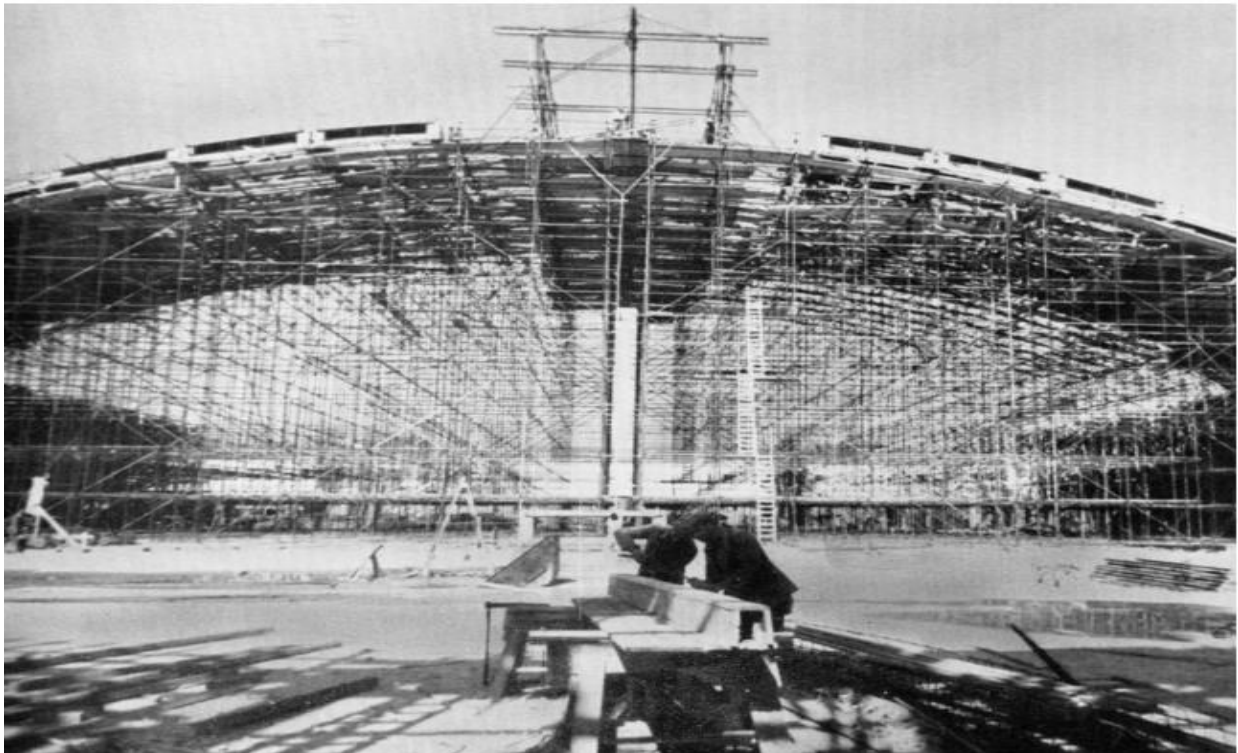


Figure 22 scaffolding for the building's prefabricated components (from The Norton Lectures, Courtesy Pier Luigi Nervi Knowledge and Management project Asbl) [24]

3.3. Hall B

Based on a Fiat Construction and Plant, the Torino Esposizioni body established in 1947 commissioned Pier Luigi Nervi and his company to reconstruct the Palazzo della Moda: some portions (hall A and the theatre) were merely rebuilt; however, with Salone B (later Salone Agnelli), Nervi conceived the largest iron construction in the world: a basilica measuring 110.5 m wide by 95 m long (f), with a free rectangular surface of 81, The Salone B and its extraordinary coverage, which was

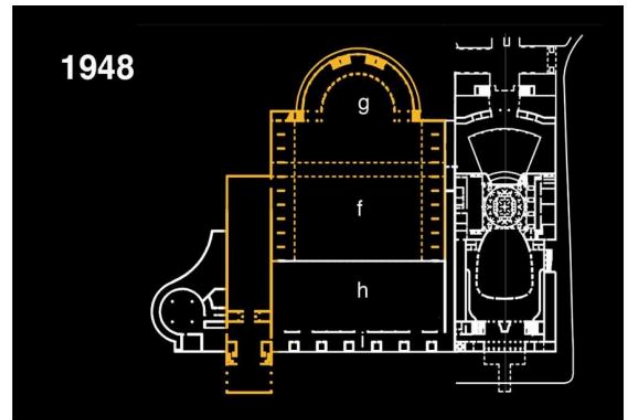


Figure 23 Proposed hall b in 1948

reflected in the automobiles on show, as well as the new Torino Esposizioni building, which was opened on September 15, 1948, stunned the globe. However, the entrance is closed by a glazed apse in the opposite way (g). The main front with the enormous vestibule and the rotunda, as well as the filter between the city and the park: a separate garden (h) spanning 100x35 m (45 originally) from the course with a 15 m wide portico were all kept in Nervi's project (s).

The corrugated vault is made up of innumerable little components known as "wavy ashlar," which ensured the overall strength of the ceiling of Hall B due to their slimness but also remarkable rigidity due to the substantial internal and exterior reinforcement and the shape of the element chosen. With transitional features known as "fans," these undulating sections—which also had skylights in the sloping sides providing considerable illumination to the exhibition center—formed arches of 13 elements that converged in an order of three arches towards the lateral piers sustraining the entire structure. [22]

In order to satisfy the structural hypothesis of a two-hinged arch, which is entirely consistent with the chosen calculation scheme, the undulation reaches its maximum level at the ridge and gradually diminishes near the supports until it disappears. Because of this, the arch that creates the vault only has openings on two thirds of its length. In order to have the contrast on the ground in the direction of the vault thrust, it was initially decided to slant the pillars that crossed the aisles and rested on shaped plinths. The engineer gave this vaultpillar

transition a great deal of thought and study because it was so challenging to solve. However, he decided to use a vee-shaped fan made of three wavy prefabricated pieces as the transition element because it worked well with the reinforcement and the finished concrete slab to bind the piers.

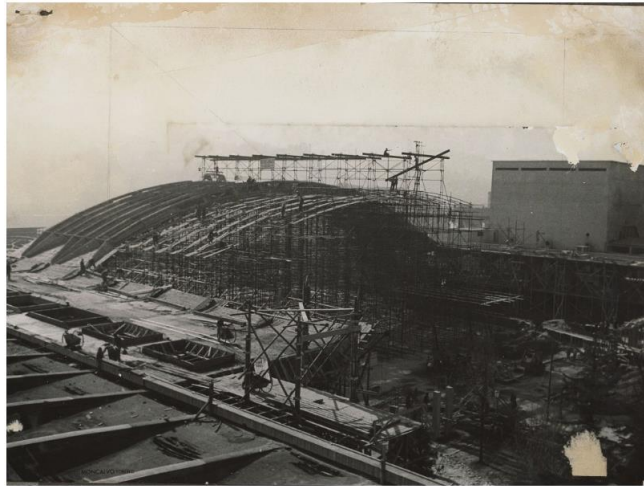


Figure 24 The Salone B of Torino Esposizioni under construction in 1948: assembly of the prefabricated ferro-cement waves that make up the arches of the great vault. [24]

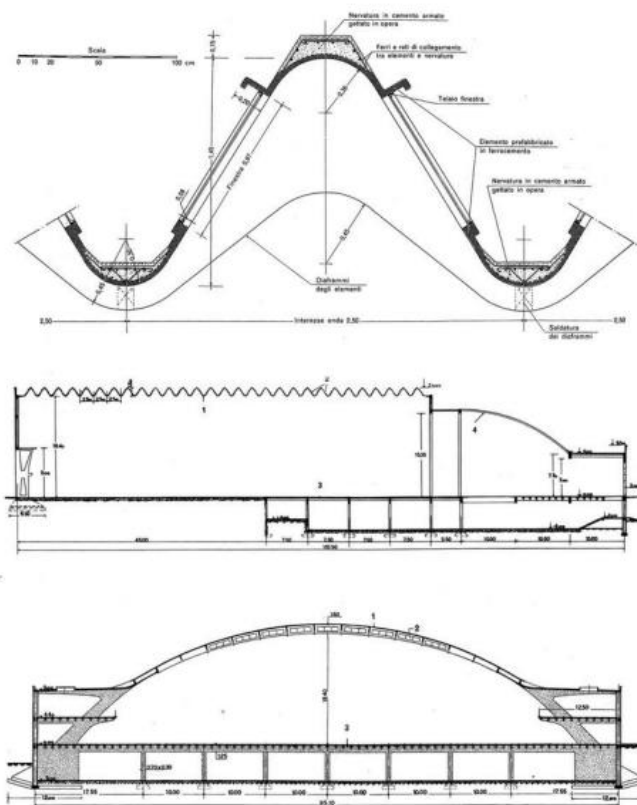
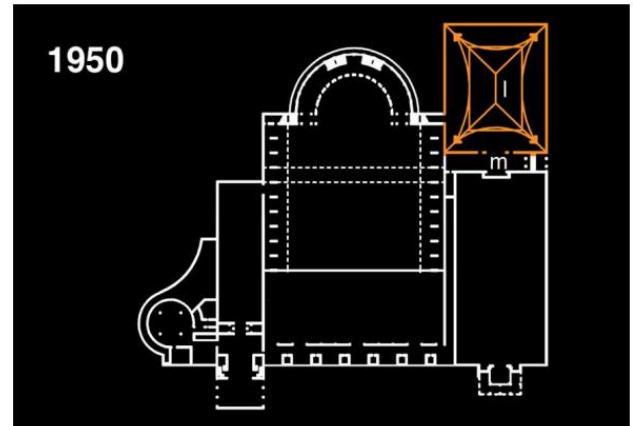


Figure 25 prefabricated system illustrations from The Norton Lectures, courtesy of Pier Luigi Nervi Knowledge and Management project asbl) [24]

3.4. HALL C

The Turin Exhibition's directors made the decision to create Salone C as a new hall in 1949 in order to expand the structure. They gave Nervi the design once more, and he was confronted with two major issues. First, just a limited amount of time was available to construct the 65 by 50-meter Hall. After the Exhibition closed, construction was supposed to



begin in the fall, and it had to be finished by the following June. Second, the conceptual challenges of maintaining the spirit of the original work while without replicating its forms. Nervi tried a cross vault throughout his many tries before settling on a vaulted roof with a slab of Perimetric material that was around 10 meters in length. A part of Hall C and the layout are shown in Fig 23. The roof is a pavilion vault, where natural light makes up about a third of its height. vault supported by four arches, which, like the half-dome of Hall B's apse, was constructed using lozenge-shaped ferrocement tiles that were manufactured in moulds that served as temporary formworks. The Torino Esposizioni complex now has a new entrance perpendicular to the street. This gallery connects Salone C to the sizable Hall B and has a roof that includes the new pavilion's system of crossed ribs.

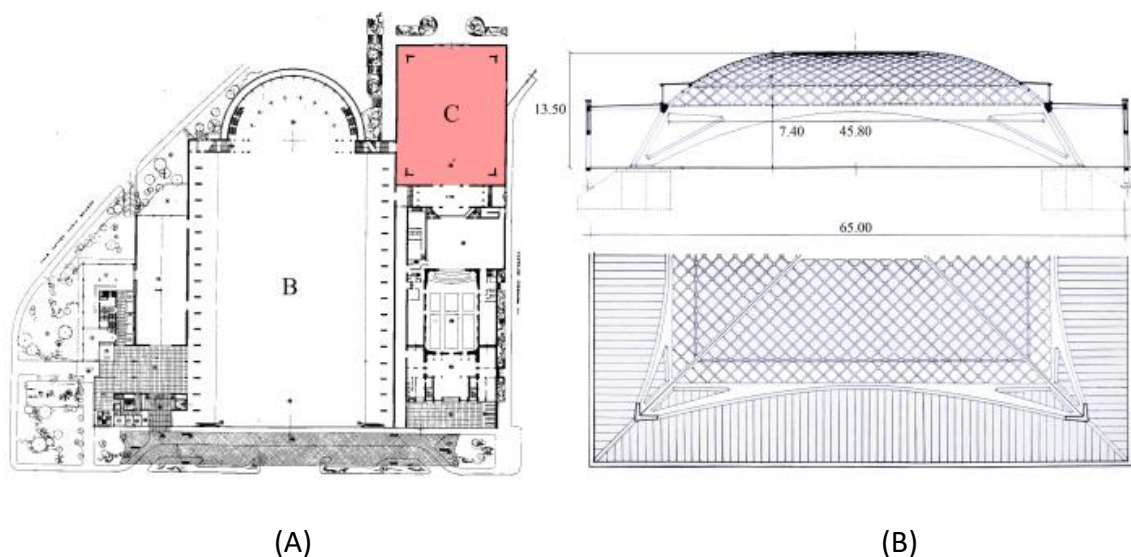


Figure 25 Plan of the Turin Exhibition: Hall B, the huge rectangular area in the; Hall C, the smaller rectangular shape in the upper right corner, was constructed a year later; (B) Pier Luigi Nervi's plan and section of Hall C from the (*Rassegna tecnica della Società degli ingegneri e architetti in Torino.*) [25]

Nervi tested a cross vault during his many experiments before settling on a vaulted ceiling with a roughly 10-meter-long perimetric slab as its final piece. The layout and a portion of Hall C are shown in Figure 23 (b). With the solution obtained by Nervi used in hall B it was also imposed in the construction of hall C where during the construction the diamond shaped elements in ferrocement composites can be seen. [25] Moreover, this solution was chosen because it demonstrated the benefit of a more expressive and organic static formula as well as a sizable budgetary benefit. Nervi, who had previously thought about using undulated ferrocement beams for the perimeter several times, finally put them to use. Immediately following the pavilion's completion, Nervi filed for patent no. 465636 in Rome on May 19, 1950, with the title "Building procedure for creating flat or curved load-resisting surfaces consisting of grids of reinforced concrete ribs, possibly finished with connecting concrete slabs between the ribs." [26]. Along with the patent no 445781 with which gradual improvement was observed in the construction of Turin exhibition centre. Halls resulted in their final configuration. These patents would be used by Pier Luigi Nervi throughout the ensuing decades, eventually becoming a standard element of the now-famous Nervi's style.

Like pavilion B's roof, the roof of pavilion C was built using ferrocement slabs that were then assembled on ribs and finished with concrete castings to create the traditional ribs. A coating of cement mortar was spread on the slabs created using stiff moulds for the roof's construction, and then the cage constructed of reinforcing nets and tiny diameter reinforcing bars was placed inside. Everything was then properly covered with mortar that was highly plastic and stored with the other components that had previously been created using the same technique.

The hall is 65 meters long and 50 meters wide. It is covered with a pavilion vault that is supported by four descending arches set on slanted planes. By supporting the weight of the perimeter floor slab, the arches' inclination develops to resist the resulting incoming loads. There are two different kinds of arches: a long arch that spans 56 meters and a short arch that spans 34 meters.

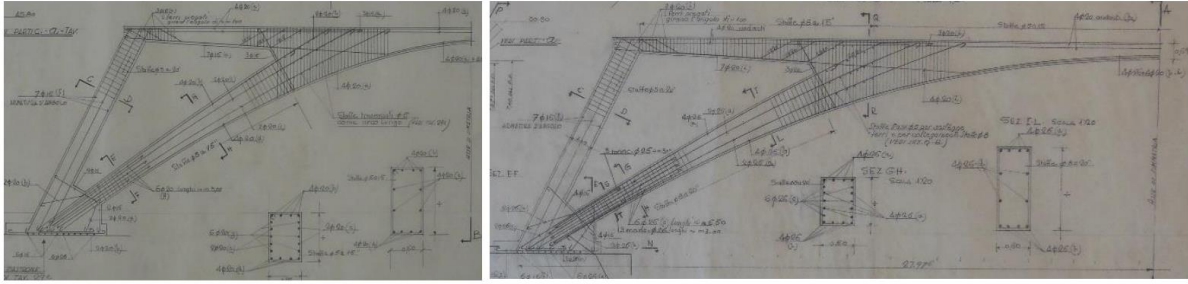


Figure 26 original drawings of the short bow (left) and longbow (right) reinforcement design [27]



Figure 27 phase of assembling the diamond shape slabs on the vault before casting the ribs [28]

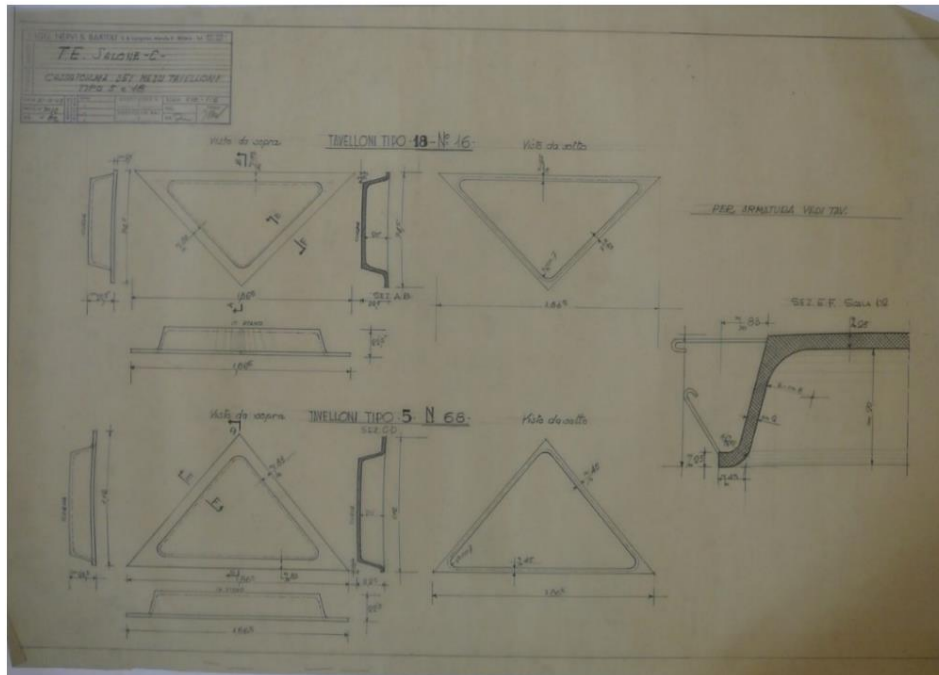


Figure 28 Hall C's half-plank outline as seen in the source : CSAC Parma Archives

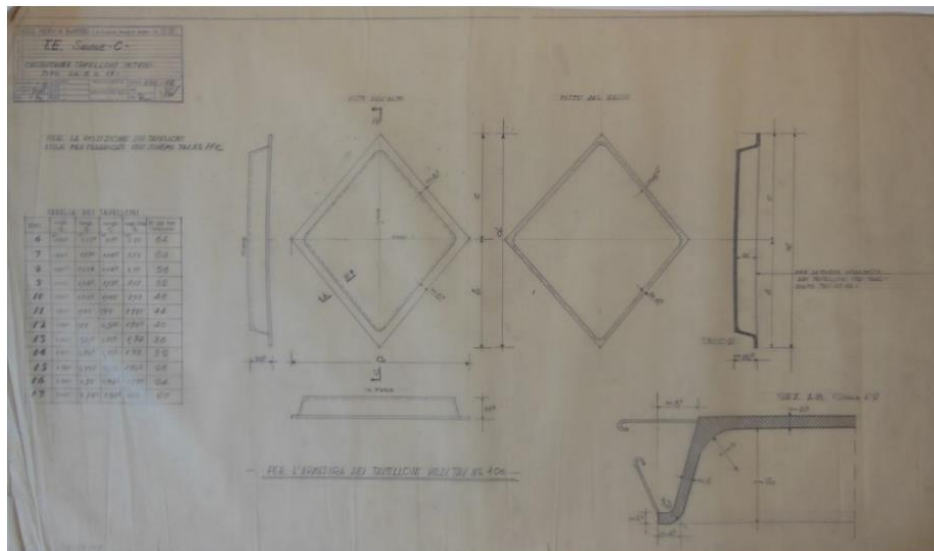


Figure 29 Planks in Hall C are shown in silhouette in this image from the CSAC Parma Archives.

The perimeter floor, on the other hand, is formed of thin, wavy ferroceмент beams with a 94 cm transverse spacing, larger at the connection with the internal beam and decreasing towards the wall perimeter; the entire structure is finished by a 4 cm cast-in-place slab. Its primary static role is to rectify the vault's horizontal thrust so that it may be transferred to the inclining arches and mixed with the vertical forces, straining them in their plane.

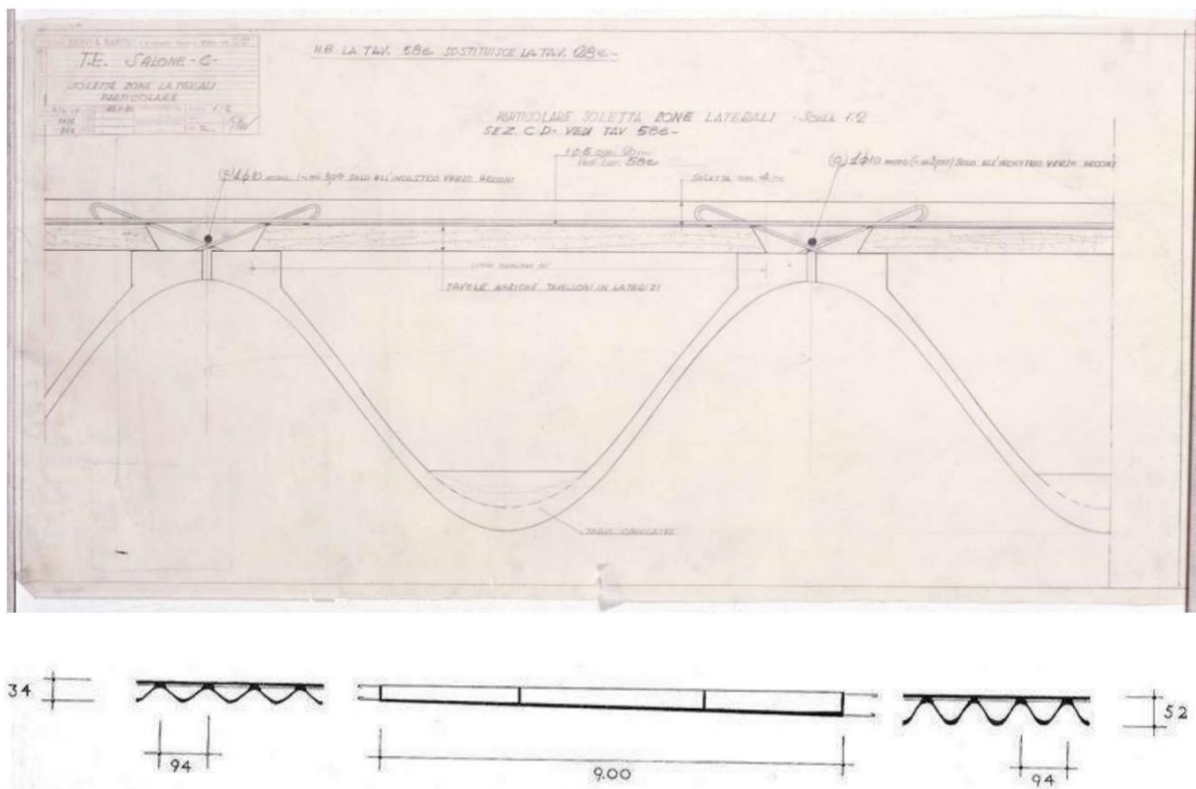


Figure 30 Section of the perimeter floor in ferroceмент source CSAC Archive Parma

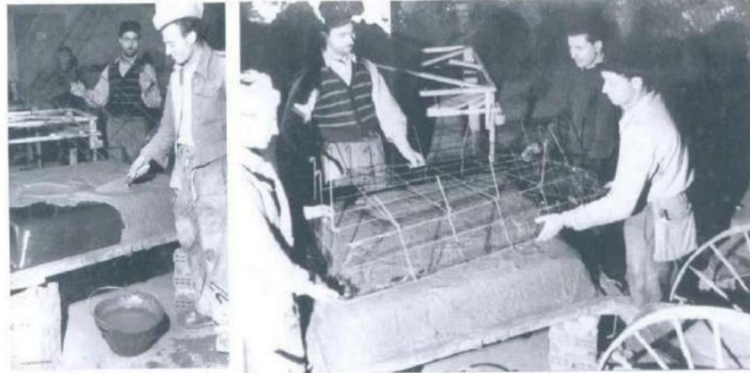


Figure 31 Realization of a practical roofing board

3.5. Current Use of Pavilions Today

The Società del Palazzo delle Esposizioni commissioned the engineer Roberto Biscaretti di Ruffia to construct a new exposition hall to serve as a showcase for Turin's automobile industry on top of the wreckage of the Palazzo della Moda, which Ettore Sottsass Sr. built in 1936 and was bombed during the War. After making two significant changes to Biscaretti's plan, which was based on a large hall with an apse, Nervi & Bartoli won the invited competitive tender in 1947. These changes included inclined lateral columns to raise the vault above grade and a thin, flattened semi-dome in place of a flat roof for the terminal apse. The Hall B of the Turin Exhibition, which Nervi planned and constructed immediately after the War, was his first chance to utilize the concept of structural prefabrication in practice. In one substantial vaulted building, it blended his very individual use of ferro concrete—steel mesh and tiny diameter steel rods formed in a thin concrete pour—with the wide use of prefabricated components. Additionally, it was the first effort to connect Nervi to Fiat and Turin's important industrial customers.

Not only was Torino Esposizioni Turin's "fair building," but it was also a significant architectural complex that grew from 1911 through the twentieth century. Those exquisite structures, which were among those created by Ettore Sottsass senior and Pier Luigi Nervi, are now partially abandoned and the subject of vandalism.

Only Pavilion 1, which houses university classrooms, the New Theater, and Pavilion 5, underground, which serves as a parking lot, have been used recently, up until the start of the health emergency. However, it transforms into a venue for "Christmas in the carousel," a custom that has been popular since 1978, at the beginning of the winter holidays.

Due to normal maintenance done over the years by the original management company for exhibits, the halls were in rather excellent preservation conditions. Although the original color (yellow and grey) was changed to white, the original lighting arrangement that followed the ribs was removed, and new air conditioning installations were installed to the balconies. The 2,700 roof windows in Hall B, however, were darkly painted in the 1990s to lessen zenith illumination, which resulted in high temperatures and substantial glass element breaking. Over time, there was a need to replace bitumen waterproofing due to significant rainwater penetration. The main renovation task completed in 2006 for the Olympic Games was the installation of air conditioning. Since indoor summer temperature conditions proved to be uncomfortable, this was done to satisfy the short-term demands of winter sports and, more crucially, to enable for future permanent displays. The related pipework was placed outside the roof. Due to safety restrictions for inspection and maintenance, the ceiling windows had to be separated into smaller components, losing some of their original aesthetic charm.



Figure 32 The Palazzo delle Esposizioni ITALIA 61 turin olympic games 2006 [29] [30]

The hall was later briefly converted into an annex to the Turin Modern Art Gallery, where the collection from Turin's National Automobile Museum was housed. Till 2011, this system was in place. The building's most recent modification has the benefit of partly reverting to its original function with the exhibition of historic cars. While the exhibit installations utterly disregarded the original architectural plan, the interior space was ruined and the apse vista towards the Po river was blocked by 5-meter-high walls. The local government agency in charge of historical buildings did not complain since removing them would be rather costly. These inner walls were meant to be light and moveable, but in reality they turned into

something that was close to permanent. Hall C, which is nearby, is better maintained in its original form.



Figure 33 The Palazzo delle Esposizioni ITALIA 61 in the Parco del Valentino during the Turin 2006 Olympic Games. The vault of Luigi Nervi [31]

In connection with the restoration work, a comprehensive program of structural evaluation, inspection, and non-destructive testing on structural concrete was conducted in 2006. The basic structural idea and design was correct, according to the structural analysis tests performed on the vault by F.E.M. In terms of tensile strength, tests demonstrating a practically absent carbonation were able to attest to the high quality of the concrete cover, and an inspection of the vault revealed exceptionally high-quality preservation of the ferrocement roof elements, despite rare defects of carbonation and corrosion being discovered in traditional reinforced concrete parts in the structure's exterior zones.

Serious preservation issues are starting to arise as a result of poor upkeep. The Municipality of Turin, which owns the Centre, is looking for a new purpose. Reuse programs, which are still being discussed in part, envision where the City Library will be. It is envisaged that the project would preserve the impression that the building's major feature is its expansiveness. Today is mostly abandoned.

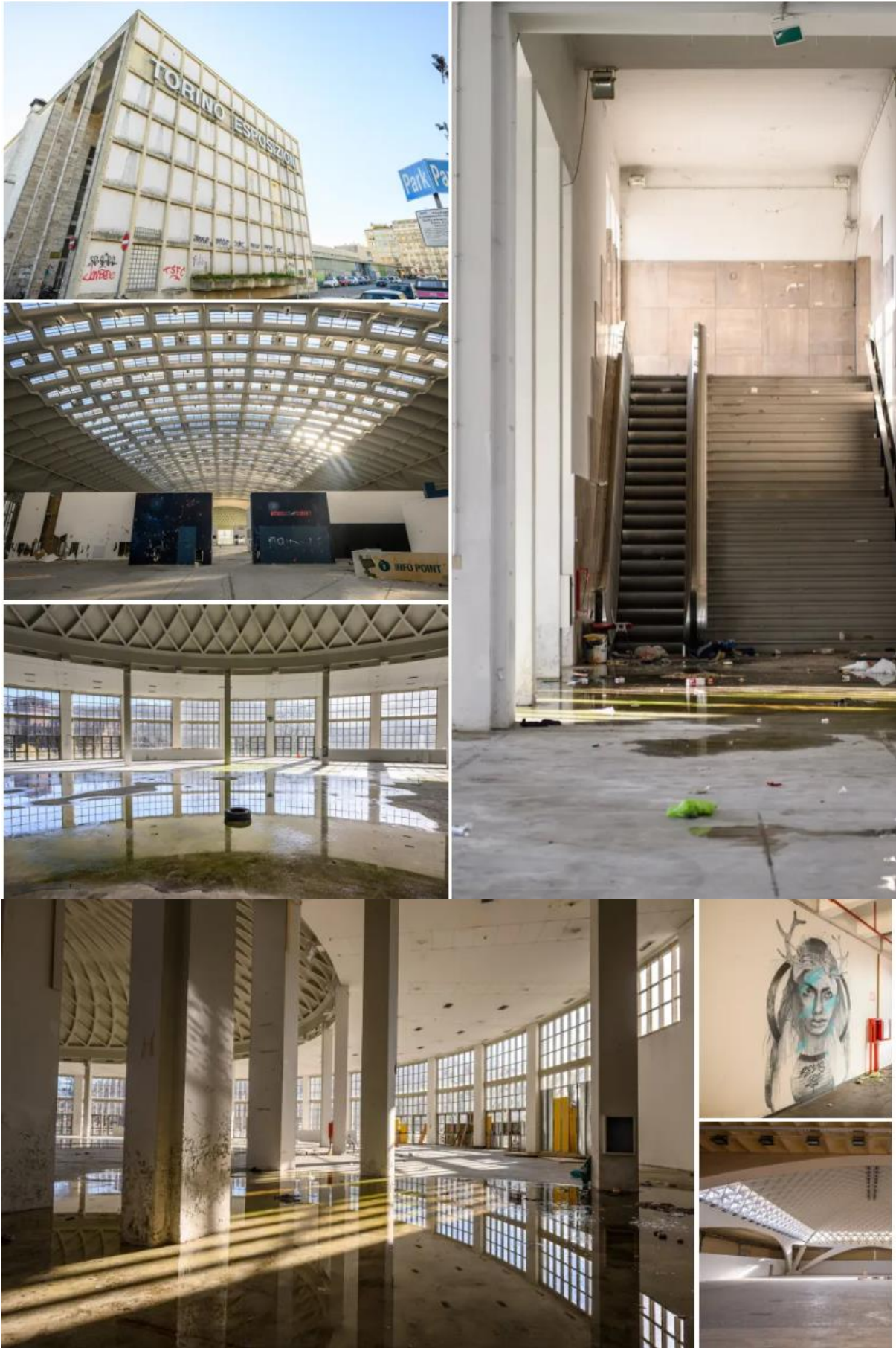


Figure 34 state of Torino Esposizioni centre from the pictures taken between January 2020 to July 2021

4. CASE STUDY

4.1. Pier Luigi Nervi: Shell and Spatial Structure Construction System

Pier Luigi Nervi is credited with creating the "Nervi System," a brand-new approach to erecting massive structures that he perfected through years of continuous research into statics and building. The System was built on genuine inventions, including structural prefabrication, ferrocement special parts, and a number of unique technical solutions, with the aim of minimizing cost and time: Pier Luigi Nervi is credited with creating the "Nervi System," a brand-new approach to erecting massive structures that he perfected through years of continuous research into statics and building. The System was built on genuine inventions, including structural prefabrication, ferrocement special parts, and a number of unique technical solutions, with the aim of minimizing cost and time. [32]

After starting his research, Nervi narrowed his attention to two crucial issues. The first was that less concrete needed to be used in order to save on steel since thinner layers of densely reinforced concrete are more effective and cost less than bigger sections of weaker concrete. The second was that further money might be saved by lowering the amount of wooden formwork used for onsite casting, which was not only incredibly wasteful but also significantly limited the ability of reinforced concrete to be shaped. He experimented with "structural prefabrication," a prefabrication process, to get rid of wood from his construction sites. [33] [23]

4.2. Ferrocement Slabs

Nervi started experimenting with paper-thin slabs of steel-reinforced concrete. These slabs were initially described by Nervi as "evenly wired," "evenly reinforced," and finally "ferrocement felt." Nervi laid down many layers of metal mesh before squeezing cement and sand mortar into them with a trowel or float (the metal mesh had to be a few millimetres thinner than the slab once it was finished, generally 3 cm thick). By pushing the mortar against one side of the mesh, the cement was driven out on the opposing side, filling the whole reinforcement. The mortar has to be carefully molded in order for it to be suitably polymeric, as needed by the method (even with additives such as diatomaceous earth or

bentonite). Making a horizontal or vertical slab no longer required the use of wooden formwork to mould the mortar until it cured. A material considerably distinct from regular reinforced concrete was produced by the great subdivision of the reinforcements, the extremely thin wires, and the uniform distribution. Homogeneous, isotropic, elastic, and ductile described ferro-cement. On Danusso's scale, it lies halfway between "just concrete" and "only iron." Despite the fact that Nervi copyrighted his invention in April 1943 (Italian patent no. 406296, Fig. 32,) (another patent no 429331, Fig 33, in June 1944)

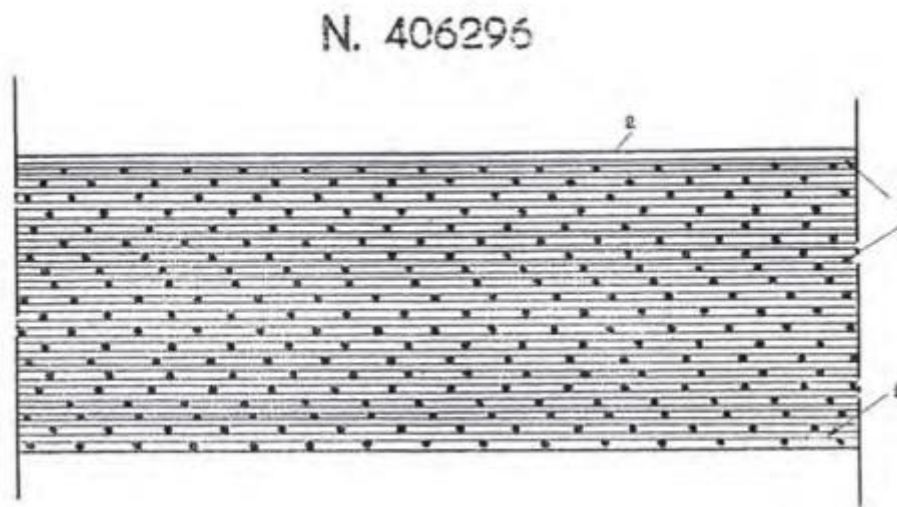


Figure 35 Italian patent n. 406296, "Ferro-cement", 1943 (Archivio Centrale dello Stato, Roma: Fondo Brevetti).

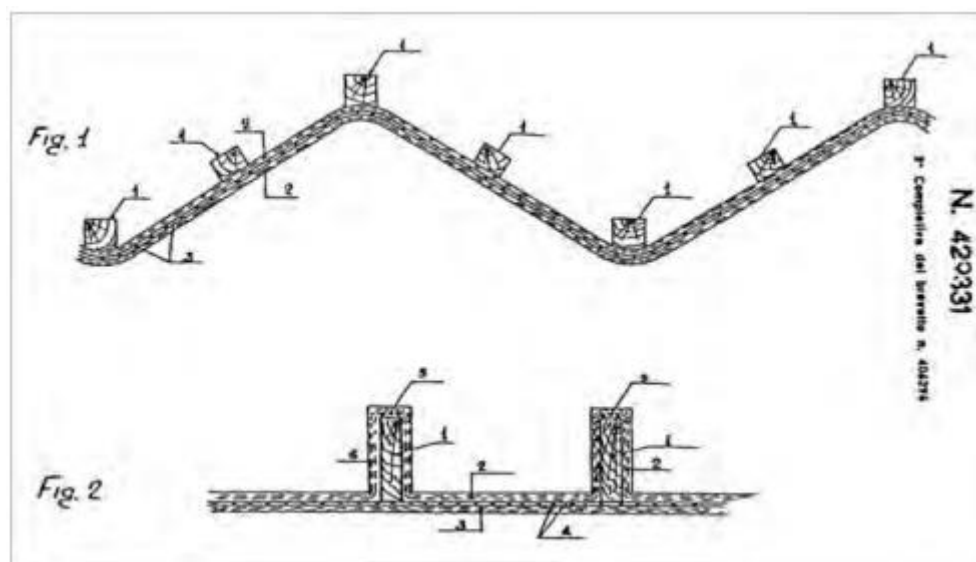


Figure 36 Patent No. 429331 from Italy, "Ferro-cement warehouse," 1944 (Archivio Centrale dello Stato, Roma: Fondo Brevetti).

At the Magliana Nervi & Bartoli facility in Rome, a warehouse was the first structure made with the novel material. It was constructed completely of ferrocement, including the three-centimeter-thick ceiling, and was shaped in waves to fully use the substance's innate ability to retain form.

Ferrocement was drastically simplified for its initial use; the numerous layers of steel mesh were quickly thrown away. The steel inner weave in the curly slabs of the Magliana warehouse (Fig. 34) was prepared with a few 8 mm diameter vertical bars and a few 6 mm diameter shaped horizontal bars spaced 20 cm apart. Within these rebars, numerous wooden squared strips helped to make the composition more stable and supported only two layers of mesh, one for each side. Nevertheless, the construction of the complete structure on site took a long time and was challenging since it was challenging to repair issues as dense concrete was being poured on the mesh. The Magliana Warehouse was the first and only structure to be completely designed in this manner. After that, it was preferable to prefabricate smaller pieces of ferrocement for the roof and ordinary reinforced concrete for vertical structures.

4.3. Shape resisting structures

Reinforced concrete, a substance made of cement, water, sand, and aggregates, was widely employed in civil engineering projects due primarily to its strengths and versatility as a construction material, which made it one of the most innovative building materials of its time. As a result of the cementitious material's complete compliance with the static rules governing the stability and strength of the buildings themselves, satisfactory results in the building industry also contributed to adaptation. However, more than just the straightforward technical aspect was evident, as cement also contributed creatively by realizing straightforward statically resistant aspects by opting for "resistance by form" and substituting elements that were challenging to materialize. [34]

A shape-resistant structure is anything that, from a structural standpoint, is self-supporting, capable of carrying specific loads, and may span considerable distances employing flexible or even rigid pieces with limited curved surfaces [35]. Since total overlap is not attainable, it is conceivable to assume loading conditions that take advantage of the structure's pressure and tensile curves that practically correspond with the shape of the material.

As a result, the form resistance is described as "the increase in the load-bearing capacity of an element achieved by two methods, which can be applied independently of one another or jointly on the same element" in technical jargon

- I. Assigning a curvature.
- II. Moving the material away from the neutral plane

By more properly distributing the pressures along the entire resistive body, these two processes both aim for an uniform exploitation of the entire material. By bending, one can, on the one hand, change the stresses on the material from bending stresses to only compressive or tensile stresses, which are typically less taxing on the material; on the other hand, one can reduce the bending stresses along the section by taking advantage of the regions that offer a greater contribution to resistance (those far from the neutral plane). [32]

Surface-resistant structures are created by combining the components of shape-resistant structures: the structural surface is created by the path that forces travel through it to reach the ground; the surface's capacity to change the direction of forces, i.e., to carry loads, depends on its location in relation to the force's direction. There are two alternative resistance methods, or combinations of them, for flat structural surfaces, depending on the direction of the force: the plate mechanism (force parallel to the surface), and the slab mechanism (force perpendicular to the surface). The two resistive planes indicated above can be made more effective by bending or curving the surface in the direction of the applied force in order to build a more evenly distributed and effective structure that can support the loads.

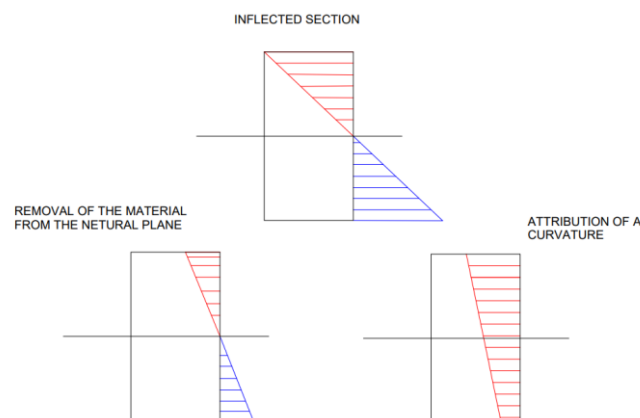


Figure 37 In the case of constructions with shape resistance, the resistant region.

It's important to note that this choice of construction is not without issues; all structures that exhibit these static-architectural traits face design challenges, such as those caused by resistance checks on double curved surfaces, which from a mathematical perspective make it difficult to perform static calculations and develop equations. Even though this issue arose from a precarious sensitivity to shape-resistant constructions, application examples like barrel vaults and conical vaults demonstrated that the creative decision made would ultimately result in vast possibilities and an effective use of reinforced concrete. [34]

Thanks to Pier Luigi Nervi, a civil engineer who rose to reputation specifically for the advancements he made to classical architecture, a construction system and a building choice geared at the use of form-resistant buildings were established in the first half of the 20th century. Additionally, it demonstrated how well these decisions optimized production times, prices, and material selection, but more importantly, how well they organized the site, enabling the building of innumerable reinforced concrete works. According to P.L. Nervi, "for more than ten years, all my efforts, both as a designer and a builder, have been dedicated on overcoming the financial challenges and formal limitations of timber formwork." [34].



Figure 38 Full size model of a portion of the Magliana Warehouse's curly wall, 2013 (Photo Sergio Poretti, SIXXI Project) (LEFT), Magliana Warehouse. Restoration works, 2013 (Photo Sergio Poretti, SIXXI Project). (RIGHT)

To celebrate the end of the war, in May 1945 Nervi published a book titled *Scienza o arte del costruire* [33]. The text recounted his experience with construction: one chapter (6 Pages) is

devoted to explaining potential applications of ferrocement. Ferrocement is a very poor material, and an unskilled labourer can easily prepare it to use very simple equipment. Moreover, structural prefabrication is an artisanal technique that requires careful and much more complex planning than an ordinary technique; however, it can easily be implemented on a traditional worksite. Nervi did not suggest factory-made standard construction elements; in each building he simply used prefab elements, made onsite. The main idea was to build sturdy surfaces from tiny, incredibly light components that were statically linked. This made sure that money, time, and most importantly, energy, were saved. Additionally, the prefabricated components' chosen surfaces benefited from systems whose resistance capabilities were closely related to the implementation of certain curvatures or section corrugations with thinner walls than those of the entire element, covering significant spans. Despite its pompous and misleading name (prefabrication) it is just a very old technique, in continuity with the tradition of stereometry and the art of scribing. It was a perfect technique for post-war Italian construction worksites. Nervi tested his inventions on various minor works in the years leading from reconstruction to the economic boom. [36]. The best chance he had to test ferrocement and structural prefabrication together was the construction of the exhibition halls at the Turin Expo (Hall B and Hall C). During the very rapid construction of this building (construction on Hall B began in June 1947 and inauguration took place on September 1948; Hall C began in early November 1949 and ended on 15 April 1950), Nervi was able to fine tune all the construction processes he would use in his future works: the so-called "Nervi System".

According to Nervi, who emphasized the significance of ferrocement in this project, *"ferrocement, due to its independence from formwork, its inherent lightness (...) and its resistant capacity, provided the simplest and most satisfactory solution to the complex problem. I would add that, without the constructive qualities of ferrocement, the entire architectural and structural concept of the work would have had to be abandoned or drastically changed"* [34].

As far as the ferrocement is concerned as well being discussed in the above section of this thesis it is "a composite structural material made of thin cement mortar sections strengthened by several layers of steel wire mesh positioned closely together."

FERROCEMENT

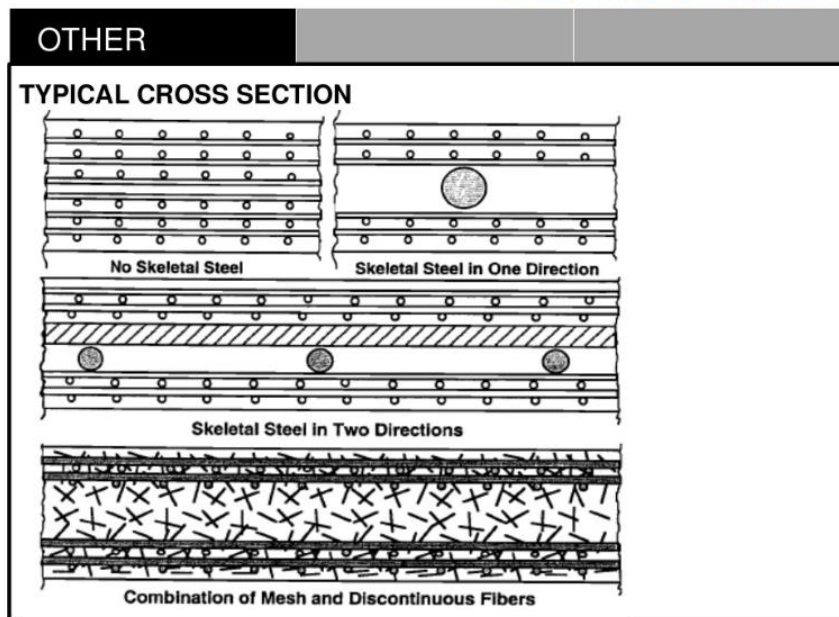


Figure 39 cross section of ferrocement with the wire mesh and the steel rebars [37]

According to Table 1's characteristic strength characteristics, which were determined by academics conducting research at the Politecnico di Milano, the yield stress for steel nets must not be greater than 690 N/mm² and the strength limit for the matrix must not be greater than 35 N/mm² [38]. Additionally, it was noted that the load stress borne by the section's bending moment surpassed 400 kg s/m once the first cracking phase had begun, and that the good material features were directly related to the local plasticity phenomena.

Sample	N. layers	P kg/m ²	d mm	L mm	s mm	g %	ε _r E-05	σ _r kg/cm ²	σ _r ^f kg/cm ²
1	3	0.4	0.57	10	17	0.45	12.5	25	270
2	6	0.4	0.57	10	16	0.95	11.5	20	250
3	4	0.4	0.57	10	17	1.35	11.5	20	250
4	20	0.4	0.57	10	18	2.83	60	42	1290
5	10	1	0.9	10	17	3.74	66	60	1420
6	10	1	0.9	10	17	3.74	67	60	1440
7	10	1	0.9	10	16	3.98	64	60	1380
8	10	1	0.9	10	16	3.98	64	60	1380

Table 1 Oberti & Grandori established characteristic values for ferrocement components in 1949. [38]

Due to the high iron content, this material was intended to be used to make flat or curved slabs that were a few centimetres thick and had previously been unattainable geometries. It also demonstrated increased elasticity and crack resistance in the structures made out of ferrocements.

5. MECHANICAL BEHAVIOR OF FERROCEMENTS.

5.1. Constituent Materials of Ferrocement

Initially ferrocement was defined as being made of a cement-based matrix and steel mesh reinforcement. A broader definition of ferrocement would include the use of skeletal steel in addition to the mesh system, and a cementitious matrix with and without short discontinuous fibers. Typical reinforcement armatures for ferrocement with and without skeletal steel are shown in Fig.37. An overview of ferrocement composition, reinforcing parameters and properties is given in Table 2. [6]

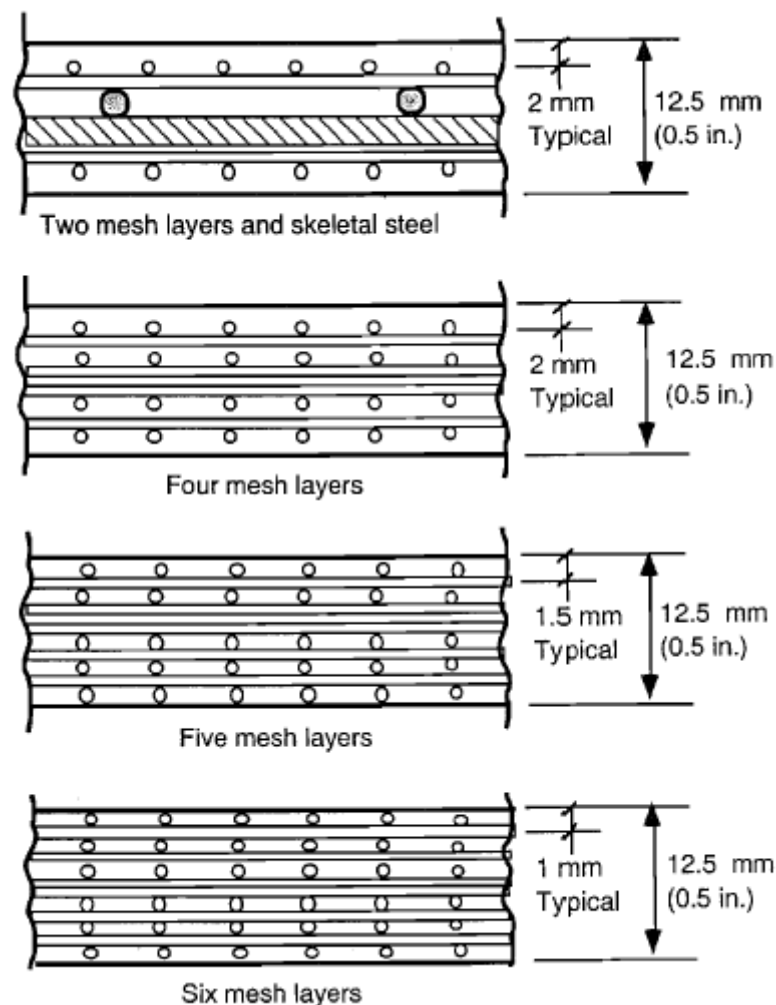


Figure 40 typical cross section of ferrocements [6]

Thus far steel meshes have been the primary mesh reinforcement for ferrocement. However, research on fibres reinforced polymeric or plastic meshes will bring additional alternatives to ferrocement.

WIRE-MESH REINFORCEMENT	<ul style="list-style-type: none"> • Wire Diameter: • Type of Mesh: • Size of Mesh Openings: • Number of Mesh Layers: • Volume Fraction of Reinforcement: • Specific Surface of Reinforcement: 	<ul style="list-style-type: none"> • $0.5 \leq d_w \leq 1.5$ mm; ($0.020 \leq d_w \leq 0.062$ in.) • Square woven or welded galvanized wire mesh; aviary (chicken) wire mesh; or expanded metal mesh • $6 \leq D \leq 25$ mm ($1/4 \leq D \leq 1$ in.) • Up to 6 layers per cm of thickness (Up to 14 layers per in. of thickness) • Up to 8% in both directions corresponding to up to 630 kg/m³ (40 lb per ft³) of steel mesh reinforcement • Up to 4 cm²/cm³ in both directions (up to 10 in.²/in.³ in both directions)
INTERMEDIATE SKELETAL REINFORCEMENT	<ul style="list-style-type: none"> • Type: • Diameter: • Grid Size: <p>Skeletal reinforcement not always present.</p>	<ul style="list-style-type: none"> • Wires; wire fabric, rods; strands • $3 \leq d_b \leq 10$ mm; ($1/8$ to $3/8$ in.) • $5 \leq G \leq 15$ cm; ($2 \leq G \leq 6$ in.)
TYPICAL MORTAR COMPOSITION	<ul style="list-style-type: none"> • Portland Cement: • Sand-to-Cement Ratio: • Water-to-Cement Ratio: • Recommendations: 	<ul style="list-style-type: none"> • Any type depending on application • $1 \leq S/C \leq 2.5$ by weight • $0.35 \leq W/C \leq 0.6$ by weight • Fine sand all passing U.S. sieve No. 16 (1.5 mm) and having 5% by weight passing No. 100 (0.25 mm), with a continuous grading curve in-between. • Additives: (Fly Ash / C) = 0.2 Air entraining agent; Corrosion inhibitor; Water reducing agent, or Superplasticizer, as needed.
COMPOSITE PROPERTIES	<ul style="list-style-type: none"> • Thickness: • Steel Cover: • Ultimate Tensile Strength: • Allowable Tensile Stress: • Modulus of Rupture: • Ratio Bending/Tension: • Compressive Strength: 	<ul style="list-style-type: none"> • $6 \leq h \leq 50$ mm ; ($1/4 \leq h \leq 2$ in.) [mostly < 30 mm] • $1.5 \leq \text{cover} \leq 3$ mm; ($1/16 \leq \text{cover} \leq 1/8$ in.) • Up to 35 Mpa (5,000 psi) • Up to 14 MPa (2,000 psi) • Up to 70 MPa (10,000 psi) • From 2 to 2.5 • 21 to 96 MPa (3,000 to 12,000 psi)

Table 2 Ferrocement in a nutshell: ranges of composition, reinforcing parameters, and mechanical properties. [6]

Steel meshes for ferrocement include square woven or welded meshes, chicken (or aviary) wire mesh of hexagonal shape, and expanded metal lath or sheet similar to those used in plaster and stucco applications (Figs. 1.13a-b). Except for expanded metal mesh, all meshes used are preferably galvanized.

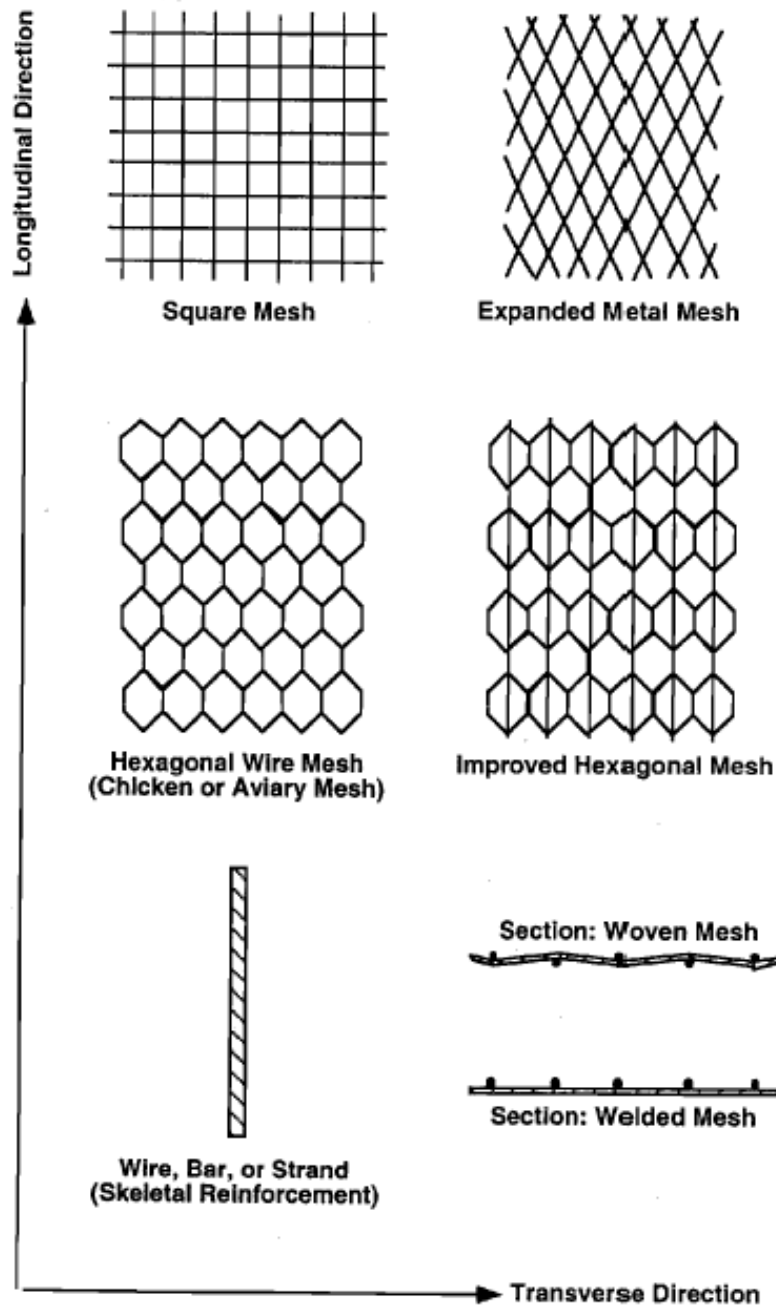
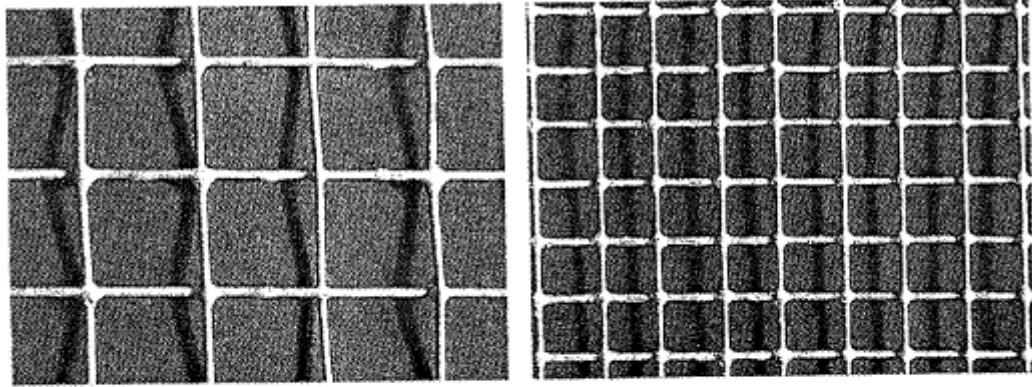
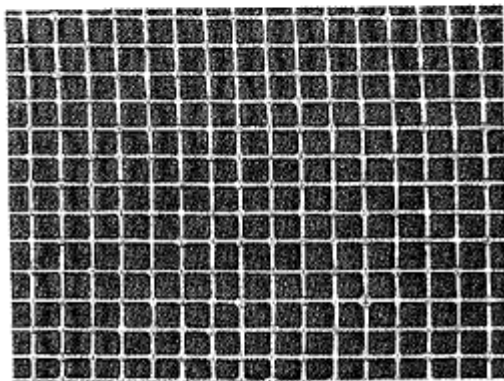


Figure 41 Typical steel mesh used in ferrocements [6]

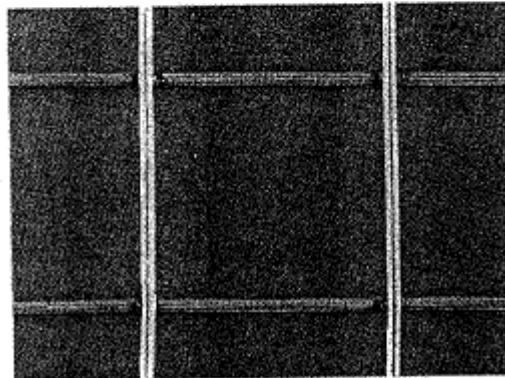


Square woven mesh: D = 12.7 mm, galvanized

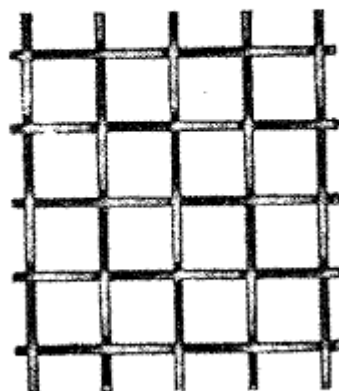
Square woven mesh: D = 6.35 mm, galvanized



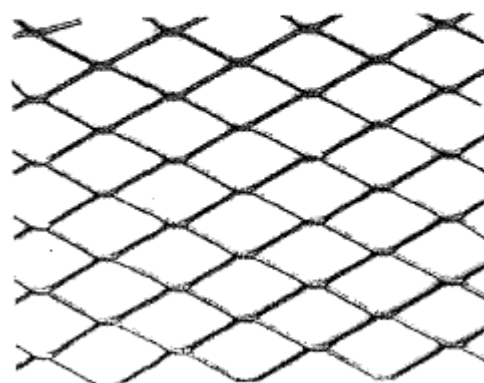
Square woven mesh: D = 3.18 mm, galvanized



Square welded mesh: D = 25.4 mm, non-galvanized



Square woven mesh: D = 12.7 mm, non-galvanized



Expanded metal mesh, non-galvanized

Figure 42 typical steel mesh used in ferrocement applications [6]

Non-metallic meshes composed of fibre reinforced plastics or polymers (FRP) are often not intended for use in ferrocement applications because their apertures are too tiny to allow the matrix to pass through. Fabrication of FRP meshes designed particularly for ferrocement is possible.

While comparing the ferrocement with the reinforced cement concrete they differ in various aspects the mechanical characteristics of ferrocement can be summaries as follows.

- Ferrocement can have homogeneous, isotropic qualities in both directions; in uncertain systems, two-way action and a high level of redundancy are anticipated.
- Ferrocement typically has a high rupture modulus and high tensile strength. Its compressive strength and tensile strength may be on the same scale.
- The reinforcing ratio in ferrocement is typically high in both tension and compression. For square meshes, the reinforcement ratios in each primary direction vary from 1 to 4 percent based on the 2 to 8 percent volume fraction of reinforcement. However, these ratios aren't significantly greater than those of columns or beams made of reinforced concrete.
- • Compared to reinforced concrete, ferrocement has a one to two orders of magnitude higher specific surface of reinforcement.
- • The extensibility of ferro cement—that is, its elongation to failure in tension or its deflection to maximum load—increases with an increase in the number of mesh layers used. This is equivalent to stating that it gets more ductile as the reinforcement's volume % and specific surface rise.
- Because of the two-dimensional reinforcement of the mesh system, ferrocement has a better impact and punching shear resistance. than reinforced concrete, on a per volume basis

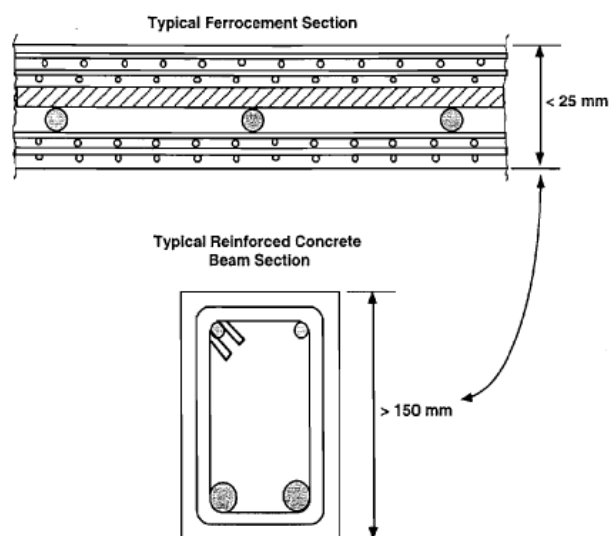


Figure 43 typical cross section of reinforced concrete against ferro cement. [6]

5.2. Behaviour Of Ferrocement In Tension

Figure 42 illustrates the load-elongation curve of a typical reinforced concrete tensile prism. The tensile stress-strain response of the reinforcing steel is assumed to be elastic perfectly plastic. Several stages of behaviour can be identified: [6]

1. Stage I corresponds to the ascending linear elastic portion of the curve (OA); this portion leads to a small plateau region where the structural cracks does not occur.
2. Stage II (AB) multi cracking region can be so extensive so as to completely take over Stage III in particular, after first cracking, cracks keep forming with increasing load.
3. Stage III (BC) A region where gradual yielding of the steel reinforcement occurs; gradual yielding occurs even when the steel mesh has a definite yield point, because Several layers of mesh placed at different depths of the section, undergo yielding at different loading levels.
4. post-yielding plastic or strain-hardening region during which the maximum or ultimate load is attained.
5. A post-peak portion where failure occurs either due to mortar failure in compression or due to failure of the extreme layer of mesh. [6]

Due to the fact that ferrocement appears to gently adjust to increased load by increasing its extensibility, the behaviour of ferrocement under tension is incredibly fascinating. Crack widths tend to stay less than would be expected by reinforced concrete theory when cracks continue to grow because they do not widen proportionally to the applied load. The stabilization stress is the pressure at which new fractures stop forming. The breadth of existing fractures rises with loading beyond the stability stress (at crack saturation), and the behaviour of the composite is governed by that of the reinforcement. Usually others reasons for the breaking of ferrocement and the reinforcing concrete in general is the corrosion of the reinforcements and the incomplete penetration of the cement mic in the metal mesh. Armor rust thus results in increasing the volume which then becomes the reason for the cracking of concrete. [9]

The inevitable result is a cycle of degradation that eventually results in collapse because, once injured, the concrete enables the introduction of further corrosive substances. Two of the primary factors affecting the corrosion process are the presence of air bubbles and exposed reinforcements. Concrete can be successfully vibrated to eliminate air bubbles,

and by galvanizing the nets, which further shields them from corrosion in a harsh environment, the concrete can be further protected from corrosion. [9]

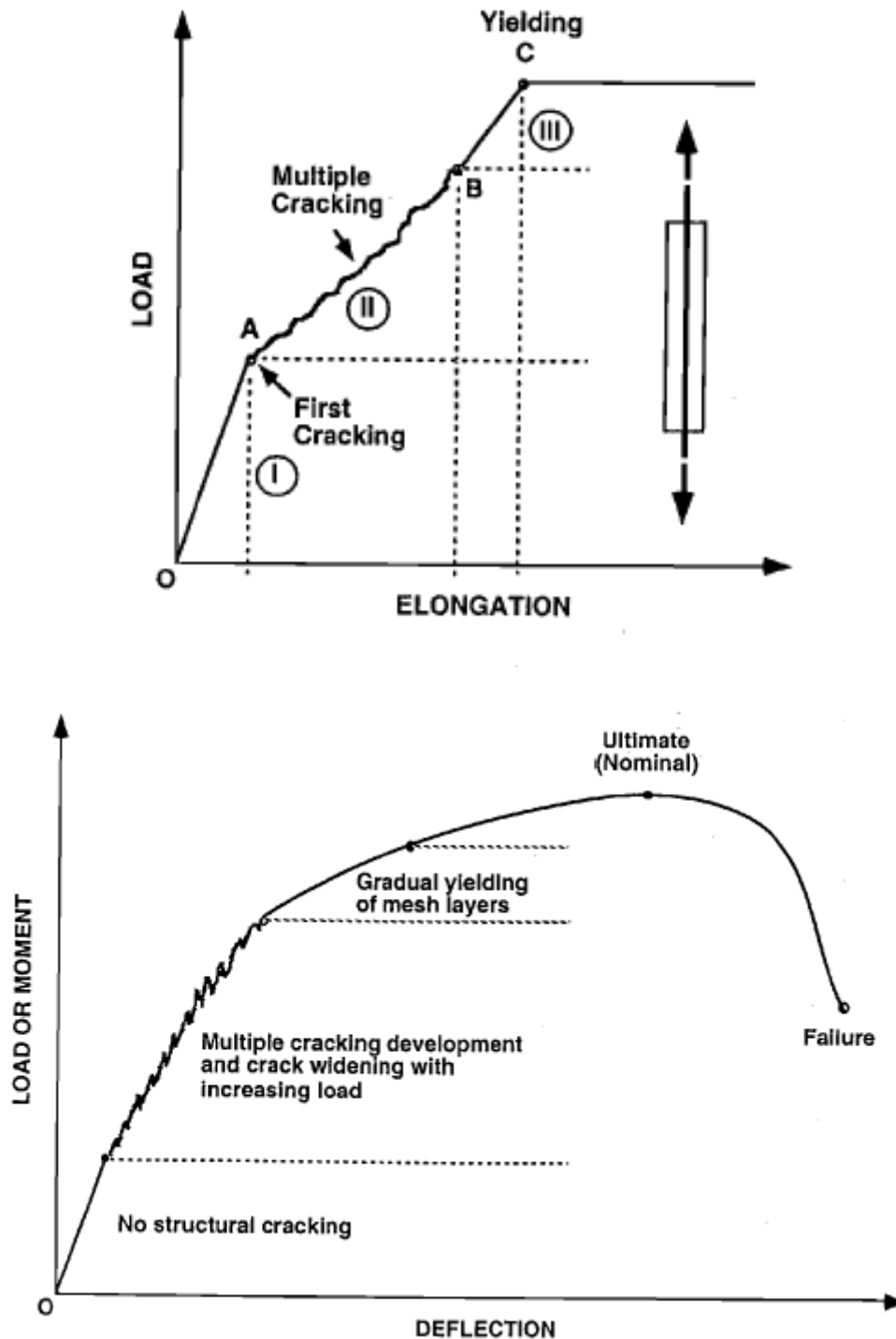


Figure 44 Diagram of the load-elongation curve of tensioned ferro cement illustrating the various stages of behaviour [6]

The yield stress values for the steel mesh used as the reinforcements is much close to the value of rebars use in the reinforced concrete it is summarised In the table

		<i>Woven square mesh</i>	<i>Welded square mesh</i>	<i>Hexagonal mesh</i>	<i>Expanded metal lath</i>	<i>Longitudinal bars</i>
Yield Strength σ_{ry}	MPa	450	450	310	310	414
	(ksi)	(65)	(65)	(45)	(45)	(60)

Table 3 minimum yield values for reinforcements source: A. Naaman

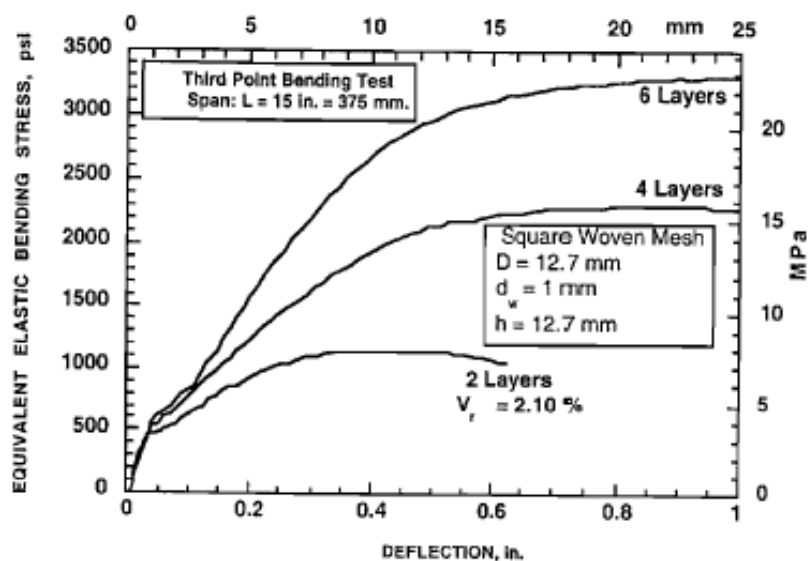


Table 4 Typical bending response of ferrocement beams using square woven mesh [6]

5.3. Stress Strain Law

In order to understand the behaviour of ferrocements made from brittle matrix in the loading conditions it was assumed that steel is used as reinforcement and that the matrix is mostly made of cement. According to the aforementioned assumption, the term "brittle" denotes a load carrying capacity that ends at the maximum stress and a linear elastic tensile stress-strain response up to failure. The contribution of the reinforcement only becomes important after matrix cracking because it is further assumed that the matrix strain to failure is significantly lower than that of the reinforcement. The assumption is that the reinforcement is elastic and fully flexible, as in the case of steel with a distinct yield plateau.

5.3.1. Elastic modulus of cracked and uncracked section

A simplified and a rational approach in order to estimate the approximation of stress strain response and thus the modulus of the continuously reinforced composite undergoing the multiple cracking under the tensile loads. The ferrocement mockup is assumed to be reinforced in the direction of the loading and to take into the effect of transversal reinforcement can be simulated by using a substantially higher value of bond strength, t . This is because either the weaving of the mesh, or its welding, introduces a mechanical component to the bond strength and thus improves overall pull-out resistance. [6]

For the uncracked member

For the uncracked tensile member of (Fig. 42 a), the elastic modulus of the composite in the loading direction can be obtained from the law of mixtures (upper bound solution of equal strains) as: [6]

$$(E_c)_{ub} = E_r V_r + E_m V_m = E_r V_r + E_m (1 - V_r)$$

where $V_r = V_{rL}$ is the volume fraction of longitudinal reinforcement, V_m is the volume fraction of matrix, E_r is the elastic modulus of the reinforcement in the longitudinal (loading) direction, and E_p is the elastic modulus of the matrix assumed isotropic. The numerical value of V_r and V_m can be obtained from: [6]

$$V_r = \frac{A_r}{A_c}$$

$$V_m = \frac{A_m}{A_c}$$

For Cracked Member

Assuming that a tensile member is cracked with numerous closely spaced cracks and that the bond at the interface between the matrix and the reinforcement is destroyed, the tensile member will stretch under load as if only the reinforcement resisted the load (Fig. 42 b). Thus an equivalent elastic modulus of the composite can be obtained from:

$$(E_c)_{lb} = E_r \frac{A_r}{A_c}$$

This modulus is the same as if the reinforcement had a sufficiently high strain capacity to eventually induce total debonding between matrix and reinforcement.

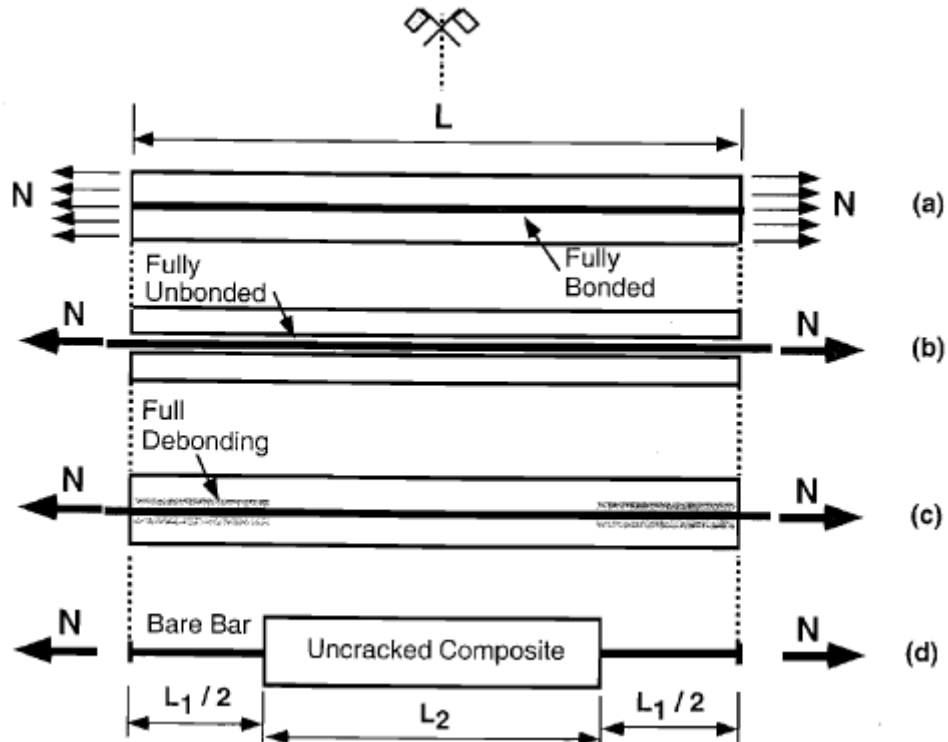


Figure 45 Model of tensile prism: a) uncracked composite; b) unbonded reinforcement; c) partial debonding; d) assumed model between two cracks

5.3.2. Prediction of stress strain response for the ferrocement mockup

Let us assume the reinforcements is lumped into a single bar with the notations adopted

A_c = cross sectional area of composite

A_m = cross sectional area of matrix

A_y = cross sectional area of reinforcement in the direction considered

A_{tr} = area of transformed section

E_m = elastic modulus of matrix

E_r = elastic modulus of (longitudinal) reinforcement

$n = \frac{E_r}{E_m}$ = modular ratio

N = externally applied tensile load

N_m = tensile load resisted by the matrix

For the prediction we considered a small ferrocement mockup that was made in the lab with the with the following specifications

$$A_c = 7.5 \times 3.0 = 22.5 \text{ cm}^2$$

$$L = 60 \text{ cm}$$

Reinforced with 49 longitudinal wire of 1mm dia so,

$$A_r = 0.384 \text{ cm}^2 = 6.7 \text{ mm dia}$$

$$E_r = 200 \text{ GPa}$$

$$E_m = 20 \text{ GPa}$$

Tensile strength of matrix $\sigma_{mu} = 3.5 \text{ Mpa}$

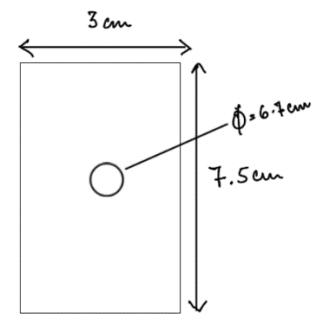
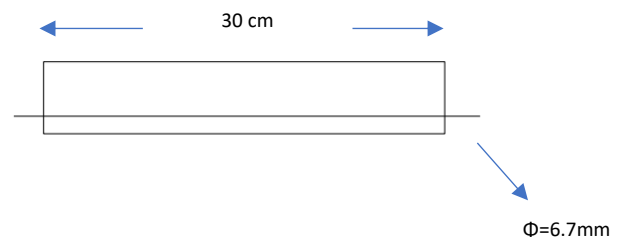


Figure 46 ferrocement matrix dimension

The strain curve for the bar is assumed to be elastic perfectly plastic with a yield strength

$$\sigma_{ry} = 480 \text{ MPa}$$

$$\sigma_{uy} = 655 \text{ MPa}$$



As to take into account the effect of transverse reinforcements the value of $\tau = 4.2 \text{ MPa}$

And ratio of $\frac{\tau}{\sigma_{mu}} = 1.75$

$$n = \frac{E_r}{E_m} = 10$$

$$A_m = A_c - A_r = 22.5 - 0.384 = 22.116 \text{ cm}^2$$

$$A_{tr} = A_c + (n-1)A_r = 22.5 + (10-1) \times 0.384 = 25.956 \text{ cm}^2$$

$$V_m = A_m / A_c = 22.116 / 22.5 = 0.982$$

$$V_r = A_r / A_c = 0.384 / 22.5 = 0.0156$$

From the equations

$$(E_c)ub = E_r V_r + E_m V_m = E_r V_r + E_m (1 - V_r L)$$

$$(E_c)_{ub} = (200 * 0.0156) + (20 * 0.982) = 23.16 \text{ GPa}$$

To find the embedded length of the bar L_e needed to develop yielding in the bar is obtained from the pull-out load equation

$$f_y A_y = \pi d_b L_e = 480 * 0.353 = \pi * 0.67 * 4.2 * L_e$$

$$L_e = 19.16 \text{ cm}$$

Let's assume the length as 1st approximation to be 19 cm

It will be assumed for the purposes of modelling the composite of the ensuing examples that a length of bar = $L_e / 2 = 9.58$ cm on either side of a fracture is typically entirely deboned from the matrix. This is the same as claiming that the matrix does not extend that far.

For the following situations, identify the pivotal points of the composite's stress-strain curve (σ_c versus ϵ_c) in direct tension up to the yielding of the reinforcing bar.

One crack at the midsection

Assume that when the stress in the matrix reaches only, there will only be one crack in the middle of the prism (Fig. 44 (b)). Find the coordinates of the curve's important landmarks.

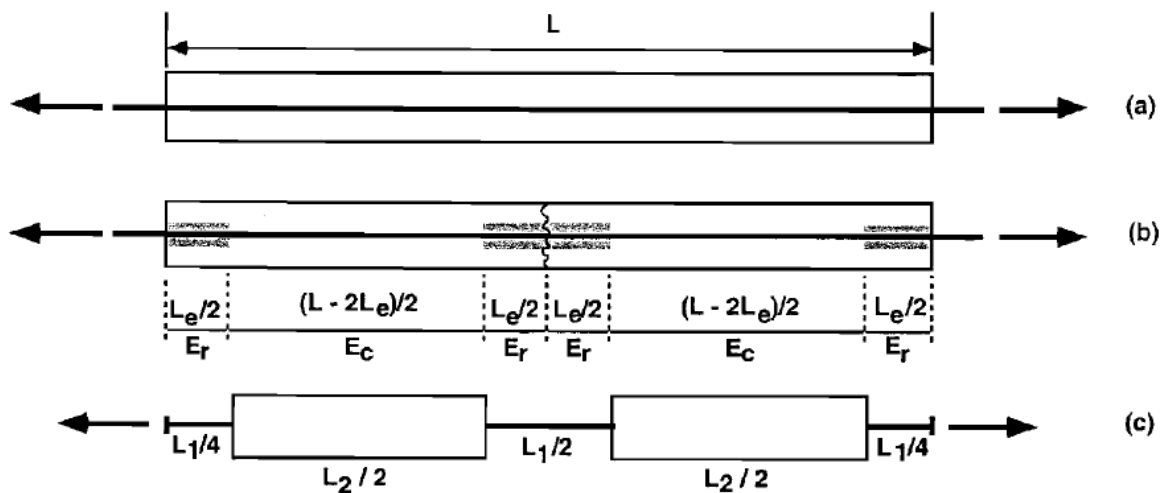


Figure 47 (a) Tensile element that hasn't cracked; (b) cracked element; (c) an assumed cracked element model

It is assumed that a crack exists at each end boundary and that each contributes half a crack width. Thus the tensile model acts as if it had two full cracks. For this example, the model of Fig. 44 (c) leads to a total length of bare bar $L_1 = 9.58 \times 4 = 38.33$ cm, and a total length of uncracked composite $L_2 = 60 - 38.33 = 21.66$ cm

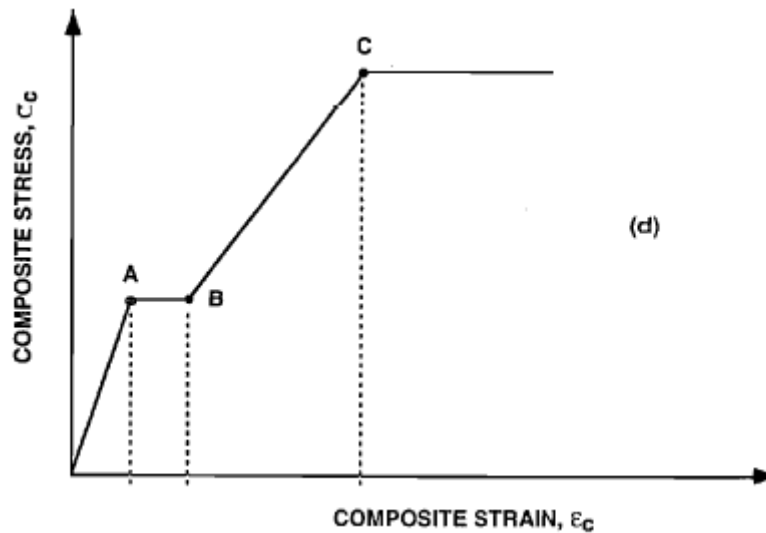


Figure 48 Typical tensile stress strain response assuming only one crack occurs

The tensile stress-strain curve of the composite is schematically depicted in Fig. 49 since it is anticipated that there will only be one break. Point A is where there is cracking, which leads to point B. Point C will finally be reached with additional loading. Next, these points' coordinates are found.

Point A corresponds to the stress in the composite at onset of cracking in the matrix. The composite stress is obtained from Eq

$$(\sigma_c)_A = \sigma_{mu}(v_m + nv_r) = 4.053 \text{ MPa}$$

The corresponding strain is given by:

$$(\varepsilon_c)_A = \frac{\sigma_{cr}}{(E_c)_{ub}} = \frac{2.73}{22.806 * 10^3} = 175 * 10^{-6}$$

Point B corresponds to where the composite is immediately after cracking assuming the external load is kept same. The stress at point B is same as that at point A. However, the strain is obtained from the model of Fig. 44 c

$$(\varepsilon_c)_B = \frac{\sigma_c}{(E_c)_{equivalent}}$$

$$(E_c)_{equivalent} = 4.932 \text{ GPa}$$

$$(\varepsilon_c)_B = \frac{2.73}{4.54 * 10^3} = 821.77 * 10^{-6}$$

Since it is assumed that no additional cracks occur up to yielding, the coordinates of point C are obtained as follows:

$$(\sigma_c)_c = \frac{A_r \sigma_{ry}}{A_c} = \frac{0.352 * 480}{22.5} = 8.192 \text{ MPa}$$

$$(\varepsilon_c)_c = \frac{(\sigma_c)_c}{(E_c)_{eq}} = \frac{7.50}{4.54 * 10^3} = 1660.98 * 10^{-6}$$

Thus the curve obtained from the values of the stress strain profile is shown in Fig 46.

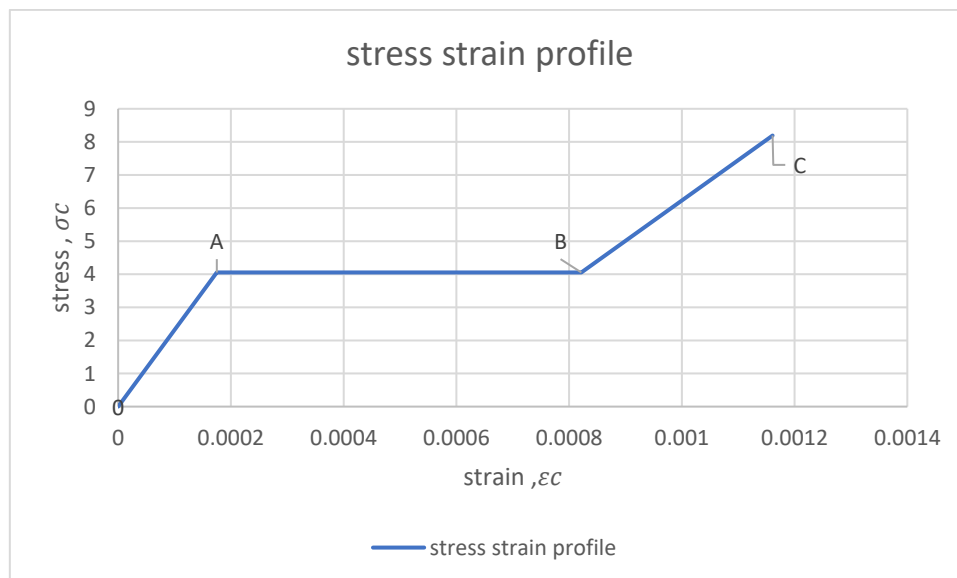


Figure 49 stress strain profile obtained for ferrocement model

5.4. Typical moment-curvature response

Consider the moment curvature relationship of a typical ferrocement section (Fig. 47). Several portions of the curve can be defined as

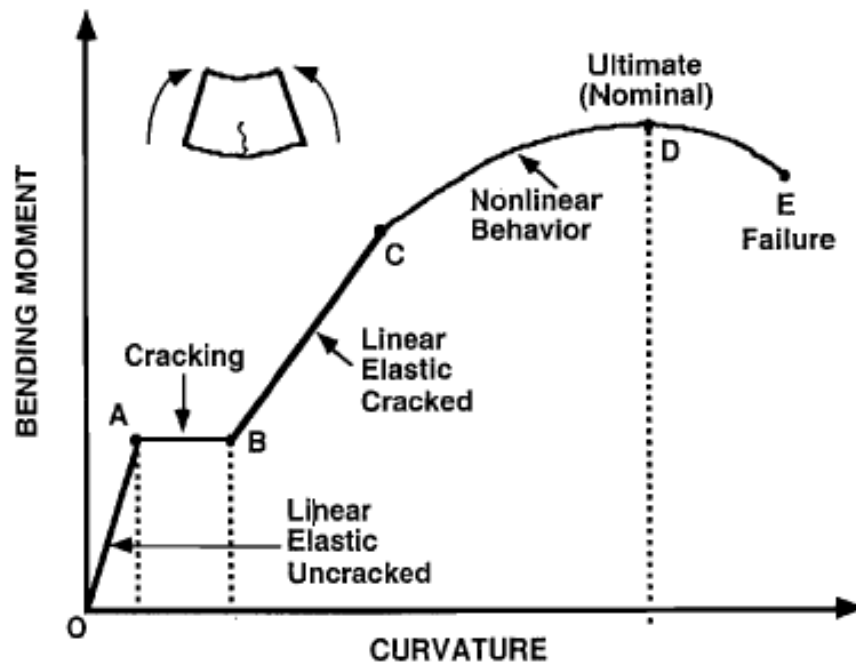


Figure 50 Schematic moment-curvature response of a ferrocement section.

1. the first linear segment When the part is not cracked, the condition is OA.
2. At A, cracking begins, increasing curvature at constant moment (segment AB),
3. A linear elastic region BC where the mortar matrix in compression and the reinforcement both maintain their linear elastic properties.
- 4, A part of a CD that is nonlinear in which one or both materials are nonlinear.
5. A peak point D where the highest or nominal level of bending resistance is reached.
6. A falling branch DE where failure of one of the materials takes place. Failure could be caused by the excessive mesh layer or the concrete.

5.5. Calculation Of Cracking Bending Moment

The area of reinforcement is a crucial piece of information when designing concrete constructions. A typical ferrocement section with its three loading axes described is shown in Figure 48. In general, the Z axis is intended to be the axis about which the bending moment is applied, and the X axis is intended to be the axis of the member for tensile loading. As shown in Fig. 48, the effective area of tension-resisting reinforcement connected to a typical mesh layer in a ferrocement section is defined as follows:

$$A_{ri} = \eta_o V_{ri} A_c$$

where V_{ri} is the total volume fraction of reinforcement due to layer of mesh i and A_c is the cross sectional area of the ferrocement composite section. The value of η_o can be taken in the longitudinal direction (η_L), transverse direction (η_T) or any other direction if available (η_θ) for which the section resistance is being calculated.

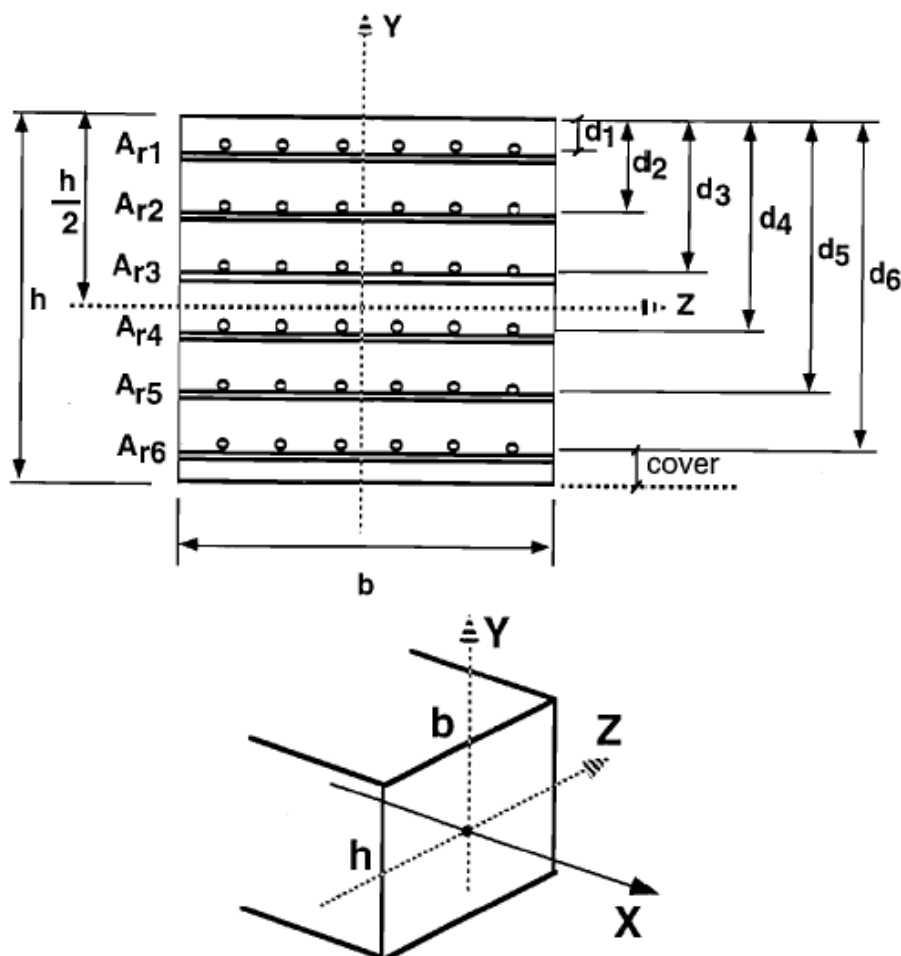


Figure 51 cross section of a ferrocement member.

Consider the ferrocement section of dimensions $b = 300 \text{ mm}$ and $d=30\text{mm}$, shown in Fig. 49 reinforced with seven identical layers of welded mesh, with wire spacing = 4 mm and wire diameter = 1 mm . The value of moduli ratio $n = 10$ and the depth to the various layers of wires in the loading direction are given by

$d_1(\text{mm})$	3
$d_2(\text{mm})$	7
$d_3(\text{mm})$	11
$d_4(\text{mm})$	15
$d_5(\text{mm})$	19
$d_6(\text{mm})$	23
$d_7(\text{mm})$	27

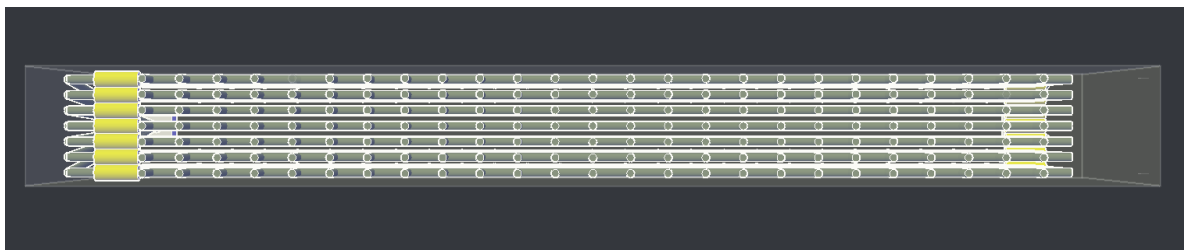


Figure 52 cross section view of ferrocement mockup

Assume the tensile strength of the matrix $\sigma_m = 2.45 \text{ MPa}$, its allowable stress in compression is 14 MPa , the allowable stress in the reinforcement under maximum service load is 210 MPa , the elastic modulus of the reinforcement $E_r = 200 \text{ GPa}$ and the elastic modulus of the matrix $E_y = 20 \text{ GPa}$.

Cross section area of 1 wire = $= \frac{\pi}{4} * d^2 = 0.7854$

Area of one layer of mesh = 18.0642 mm^2

And the corresponding volume

fraction of the reinforcements

$V_{rL} = 0.01405$ and $V_r = 0.0281$

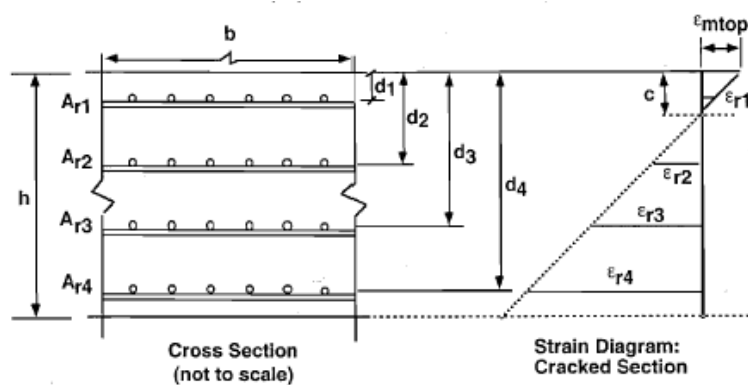
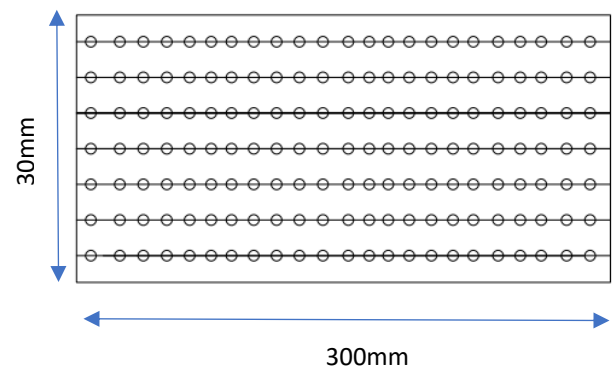


Figure 53 cross section with detailed area of beam

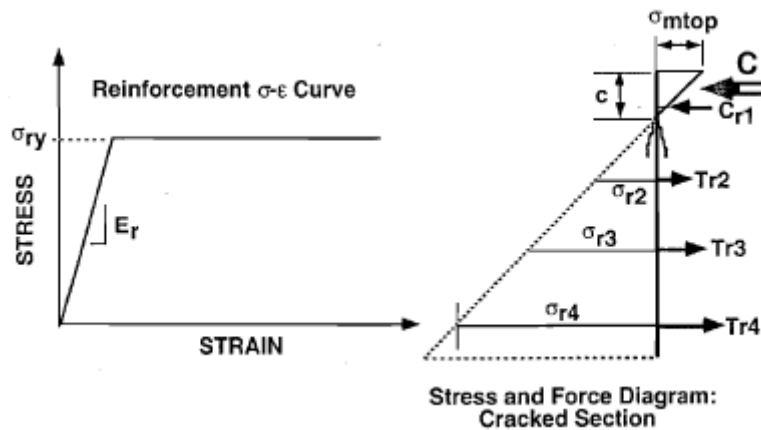


Figure 54 linear stress and linear strain diagram

Determine the cracking bending moment and corresponding curvature

At first the MOI (moment of inertia) of the uncracked section is needed to be calculated 1st

From the equation $(I_{tr})_{uncracked} = \frac{bh^3}{12} + (n - 1) \sum A_{ri} \left(\frac{h}{2} - d_i\right)^2$

$$(I_{tr})_{uncracked} = 70393mm^4$$

The above calculated value was about 4.2% higher than the gross moment of inertia which was about to be = 675000 mm⁴

The moment leading to cracking $M_{Cr} = \frac{2\sigma_m \cdot (I_{tr})_{uncracked}}{h}$

$$M_{Cr} = 114.971 N - m$$

Now, for calculating the elastic modulus for the uncracked section is calculated as

$$(E_c)_{ub} = E_r V_{rI} + E_m V_m$$

$$(E_c)_{ub} = 22.248 GPa$$

The curvature of the section just before cracking at point A shown in figure 47 is given by

$$(\varphi)_A = \frac{M_{Cr}}{E_c (I_{tr})_{uncracked}}$$

$$(\varphi)_A = \frac{114.971}{22.248 * 10^9 * 703903 * 10^{-12}} = 7.34 * 10^{-3} = 7.3415mm$$

Determine the Maximum Service Moment and corresponding Curvature

The area should be changed into a mortar matrix. Consider that the neutral axis of bending of the transformed section lies between the first and second layers of the reinforcing mesh; the neutral axis, c, is determined from the first moment of the section with respect to the neutral axis:

$$bc \frac{c^3}{2} + (n - 1) * Ar1(c - 3) + nAr2(7 - c) = nAr3(11 - c) + nAr4(15 - c) + nAr5(19 - c) + nAr6(23 - c) + nAr7(27 - c)$$

Solving for c we get the value to one positive root

$$c_{neutral\ axis} = 7.82mm$$

The value of c indicates that the neutral axis of bending lies in between the 1st and 2nd layer of mesh and the assumption $d1 < c < d2$ is correct. If the $c > d2$ we have to revise the procedure to find the correct value according to the assumption made. The moment of inertia of the transformed section can then be calculated as:

$$(l_{tr})_{cracked} = bc \frac{c^3}{2} + (n - 1) * Ar1(c - 3) + nAr2(7 - c) + nAr3(11 - c) + nAr4(15 - c) + nAr5(19 - c) + nAr6(23 - c) + nAr7(27 - c)$$

$$(l_{tr})_{cracked} = 143459\ mm^4$$

from the value obtained for the moment of inertia the maximum service moment is obtained:

$$M_{service} = \frac{l_{tr}(\sigma_r)_{all}}{n(d_i - c)} = 157.072\ N - m$$

the curvature for the cracked section can then be calculated as calculated for the point A for point B and point C

$$(\varphi)_B = \frac{M_{cr}}{E_c(l_{tr})_{cracked}} = 0.036022\ m^{-1}$$

$$(\varphi)_C = \frac{M_{service}}{E_c(l_{tr})_{cracked}} = 0.049213\ m^{-1}$$

6. SELECTING THE TYPE OF MOCK-UP

While working out the types of mockups required to find out the properties of the ferrocement used the two kind of mockups were realized and out of which it was decide that 36 smaller mockups would be used to find the mockups strength categories and the progression of the corrosion potential and a bigger 6 meter slab of the ferrocement identical to the one used in the Torino Esposizioni would be made and casted in the laboratory for further bending test.

All these works were started by casting the smaller mockups with the woven steel mesh. A series of 7 layers of steel mesh were places parallel to each other and cut and placed in precise manner and separated with a 0.2 cm spacing between then and then the mixture of the cement was poured above it. The cement mixture used was a cement with fine sand and a water cement ratio of 0.20.

6.1 Realization of smaller mock-ups.

Six samples were just created to examine the mechanical characteristics of cementitious materials, while the other thirty samples were constructed to be treated and aged to study their performance and durability The sample has seven layers of metal mesh measuring 270x55 mm and has dimensions of 300x30x75 (h) mm. Six samples, which measure 160x35x35(h) mm, is used to assess the mechanical characteristics of concrete (this sample does not include metal mesh layers).



Following Pier Luigi Nervi's design and in conformity with ACI Standard PRC-549-18, the ferrocement samples were produced. Cutting the layers of metal mesh to size was the first stage in preparing the samples. A big bundle of steel was divided into smaller pieces, and each piece was straightened and bent by hand to lessen the curvature impact of the metal bundle.

Next after flattening the sheets and getting the curvature required, they were cut in smaller dimensions of 240mm*50mm steel mesh layer and number of sheets in one sample were kept to be 7.

Each sample's seven metal layers were put together using clay. To enable for the proper placing of each metal layer, a clay bed was constructed. The spacing between each metal sheet was 2 mm, resulting in a 2 mm concrete. The location of the steel mesh remained unchanged when it was leaned against the clay layer. This process took a lot of work. Seven wood sticks were then attached within the metal layers to create more rigidity when this stage was finished. In order to lessen deformation during the concrete pour, four wood sticks were placed: three on the sides and one in the centre.

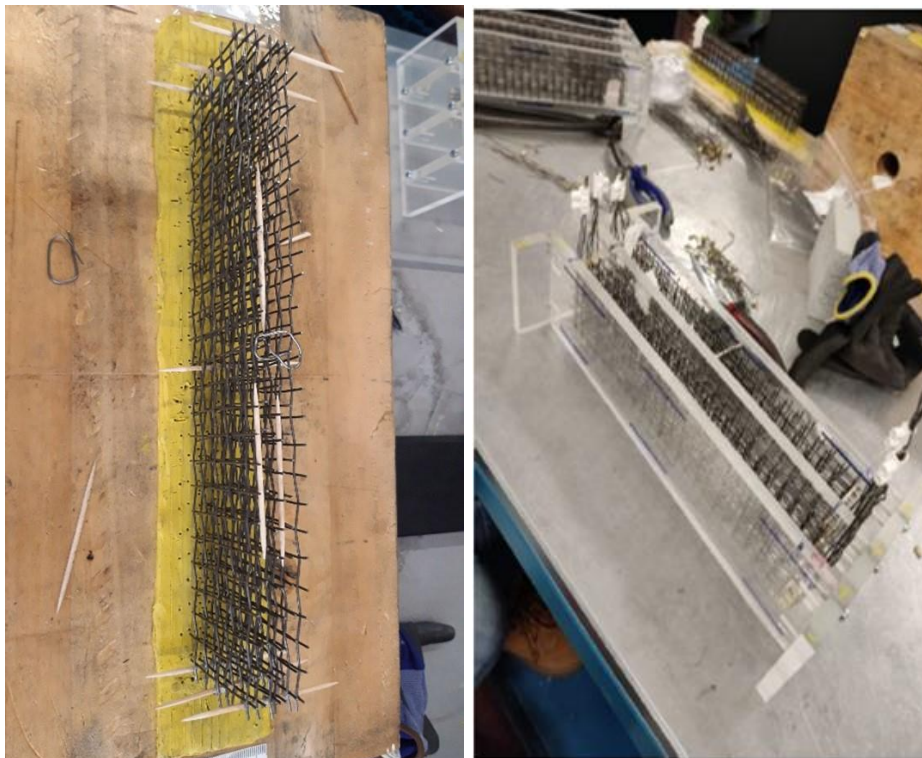


Figure 55 steel woven wire mesh in smaller mock-ups

After the mesh layers were in place, electrical connections were made using faston terminals, enabling the creation of a reliable connection between each mesh layer for the purpose of conducting electrochemical tests. On each net, from the point where a steel wire was attached to it, on both short sides of the steel mesh package, in the bottom and in the top, a faston was positioned.

Following the completion of the electrical connections, the samples were set in a plexiglass formwork in order to prepare for casting. Plexiglass rectangles were cut and then bored to provide screw holes, resulting in the plexiglass formwork (A type: 130x320x85 (h) mm, B type: 90x320x85 (h) mm). There were two separate formworks made: Type A for simultaneous casting of three samples, and Type B for simultaneous casting of two samples.

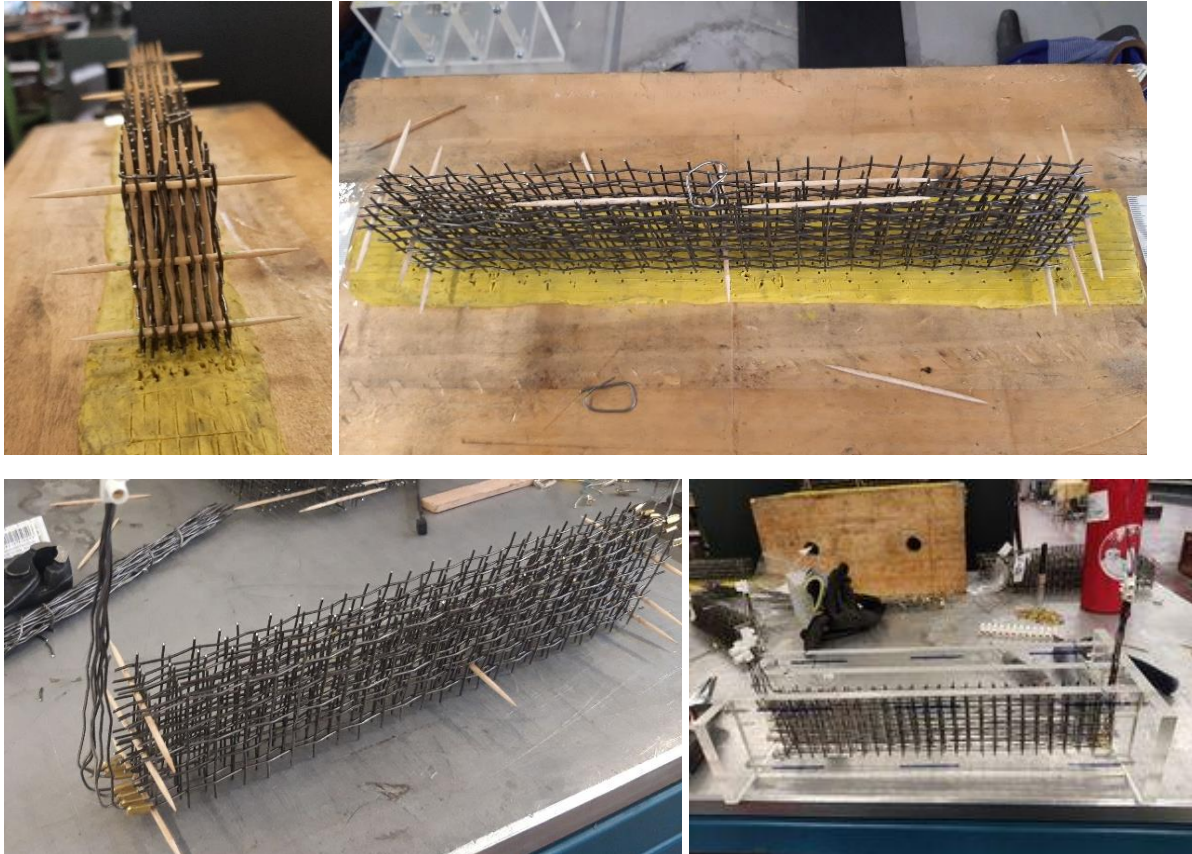


Figure 56 7 layers of steel mesh separated with wooden sticks to avoid sticking and proper spacing and end connectors attached.

The samples were dried or cured for 28 days under water in a humidity-controlled setting. The samples were first cured on December 20, 2021 and were finished on January 20, 2022.

6.2 Realization of bigger Mock-up

The bigger mock-ups are 1:1 scale replicas of the interior beams of Turin's Hall C. And the next step was to make up these larger mock-ups formwork in order to cast the concrete and make a larger beam which could be tested on in later stages for the properties required and different test could be carried out.



Figure 57 ferrocement realization as done by Nervi

On a scale of 1:1, a wavy beam supporting pavilion C's perimeter floor was selected as the component to be created in the lab. One of the core components of salon C is the corrugated floor. It is made out of 9.5 m-long ferrocement pieces that are then finished by an opera cast.

One of its static tasks would be to provide a correction to the horizontal thrust of the vault in the regions of connection with the arches, especially in the corner sections. To replicate 2/3 of the entire length, it was determined to create a specimen that was 0.94 m wide and 6 m long, including a mid-length diaphragm. The procedure for locally preparing the material to have both intact and intentionally damaged sections is still up for debate.

The generic section which was to be used were designed by Eng. Nervi and has been documented and were shown on the pictures below.

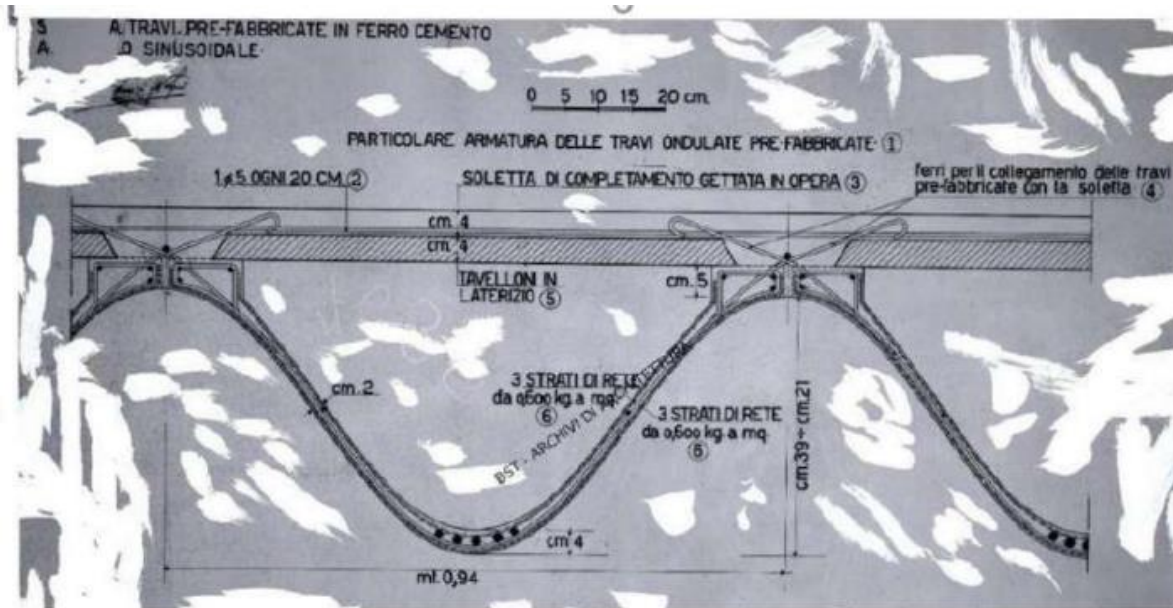


Figure 58 typical cross section of the ferrocement beam [27]

The wavy beam's section is not constant; rather, it changes, increasing in height as it moves from the outside inside toward the arches.

It is a modular, monolithic element with excellent resistance properties when paired with other components of the same kind.

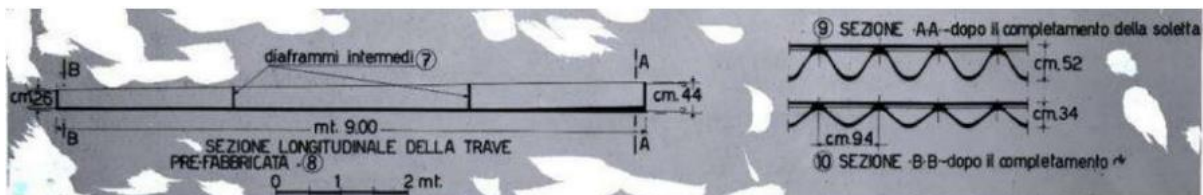


Figure 59 lateral view of beam with the continuous wavy shaped beam [27]

The corrugated beam which was used in the hall C presents as the 4 layers of wires mesh placed one above the other two layer at the bottom and two layers at the top and within them encased the longitudinal reinforcement and transversal reinforcements forming the curved characteristics, almost analogous to the wavy vault of salon B. [39].

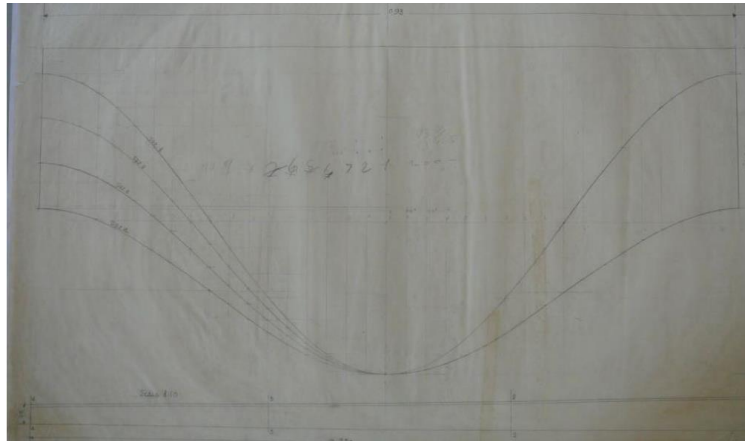


Figure 60 4 steel nets to be placed and curvature of the beam. [27]

In order to make the bigger mockup there were many steps which were involved, and they were needed to be carried out in a specific manner. There are specific circumstances where the beams shorten and taper along the corner beam because the longitudinal reinforcements vary depending on the piece being evaluated. For the beam designated "Normal" in the table of Figure 52, there are five longitudinal reinforcing bars, three of which have a diameter of 10 mm and two of which have a diameter of 12 mm, as illustrated in Figure 52. [40]

Additionally, we can see in the image that there are additional longitudinal bars with a diameter of 5 mm, the same dimension as the transversely bent bars. These longitudinal bars are important for constructing a cage with metal nets so that cement mortar may be distributed afterwards.

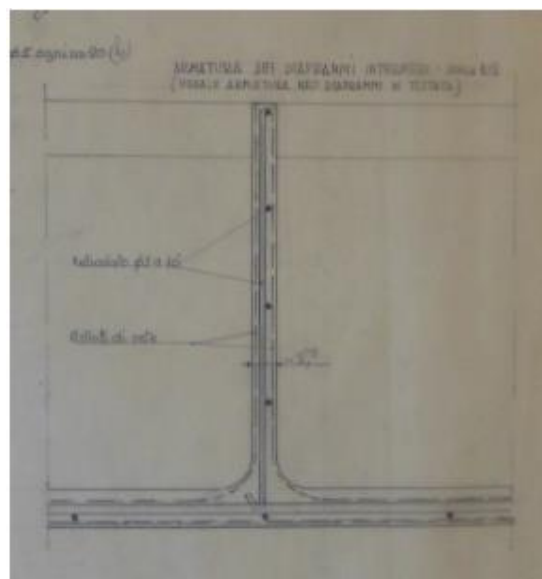


Figure 61 side view of diaphragm [27]

shape pushing them towards the rigid mould then the mortar was poured cementitious and made to adhere by hand to the previously laid layers of mesh. The supported wooden formwork used to make these beam is shown in figure 52.

If we talk about the beam which was made as the 1:1 sample of the beam used in the hall C, included various steps. The 1st thing which was done was placing the lower supporting longitudinal beams on which the 13 MDF panels were cut and placed. These MDF sections which have a thickness of 30mm were placed at a distance of 50cm from each other. The total length of beam which was obtained after placing these MDF panels was 6m in total but an additional length of 30cm was also included at the end of each side of the beam which constitute the diaphragm of the beam. These diaphragms also have a reinforcement and have a thickness of 15cm on either side of the beam making the total length of the beam to be 6.3m in total. In the figure shown below are a step-by-step process which includes the progress made while placing the panels at 50cm distance and the base beam.

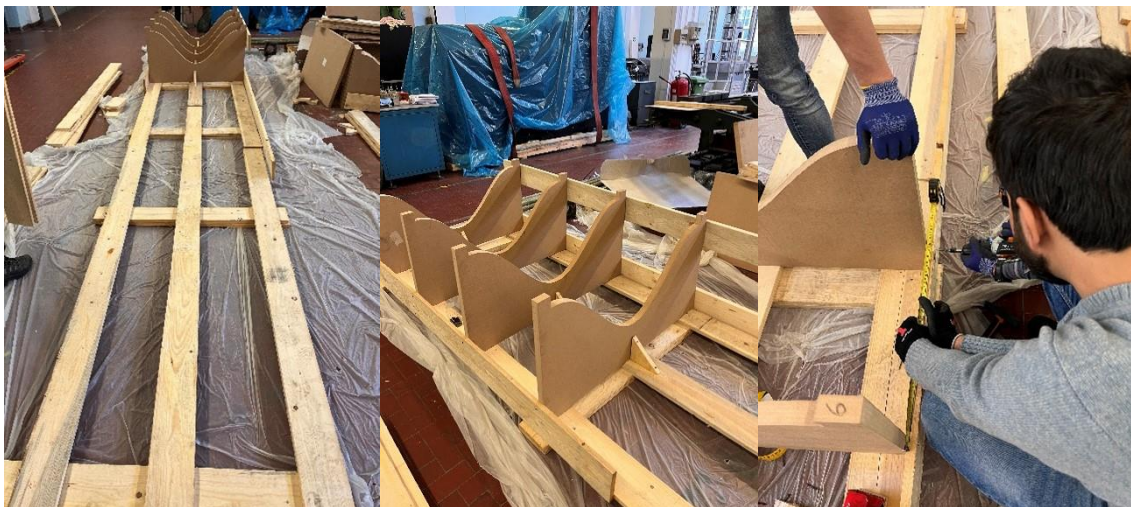


Figure 63 base beam and the curved panels placed.

The panels are positioned on three horizontal longitudinal wood beams before being positioned on six pairs of horizontal transverse wood beams, creating a thickness under the formwork that may accommodate any movement-related device. Once all the curved panels were placed at a distance of 50 cm apart the from each other they were screwed with the screws at the side of the formwork by placing a side wooden panel, this panel kept the panels in a straight line and helped to withstand their own weight. After all the panels were placed in the longitudinal direction two side wooden rails which run all the way from one and to the

other were placed and panels were bolted to them. So in total of 4 side rails two on either side where placed to provide the rigidity to the formwork.



Figure 64 side rails and curved panels placed.

Once all the panels and the rails were added it was found later that the curved panels are not that rigid and they need to be fixed at the bottom with the bottom wooden longitudinal bar in order to do so a triangular support was placed to provide the rigidity to the panels required as shown in the figure 60. Once everything was rigidly fixed the formwork was ready to place the upper aluminium sheet.

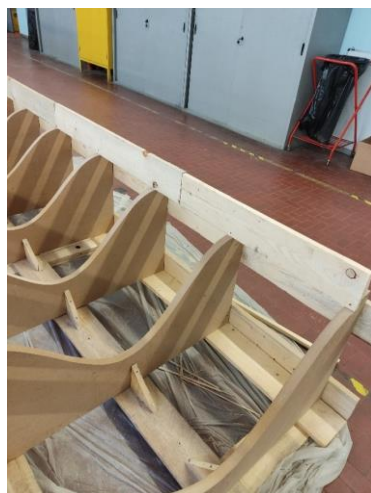


Figure 65 placing of the triangular shaped support

6.3.1. Aluminium Curved Sheet Placement

The next step in the process was the placement of the aluminium sheet on these curved MDF panels. The aluminium sheet of an approximate size of 600 c in length and following the shape of the curved beam the two sides of the beam have a different length on either side, one side being of the length of 106cm, and the other side be of 120cm this increment in the length is because of the tapered shape of the beam where the depth of the beam increase as the we progress deeper in the beam along the length.



Figure 66 placing steel sheet

To place this aluminium sheet, the first thing was placing the sheet on top of the formwork and above the panels of the wood which were fixed to the beam at the bottom. Once the sheet was placed the next step was shaping it down to the perfect curved shape of the beam and to follow the shapes if each panel. To do so the aluminium sheet was pushed down with the hands at 1st and then the gravel bags with weights were placed on top of the beam. To provide a downwards weight on the sheet so that it gets costume to the shape of the panels. Once the sheet gets the shape the next step was to nail the middle part of the sheet all along the length of the beam. The sheet was nailed to the diaphragm and then with each MDF panel

the nails were placed along the length of the panels transversely. Fixing it one by one all along the length of the beam. Once the sheet attains the side curvature of the beam placing a heavy bar helped with keeping the shape of the aluminium sheet to be in shape while putting the nails.



Figure 67 placing of the aluminium sheet



Figure 68 marking the diaphragm and placing the sheet with nails.

6.3.2. Shaping and placement of the reinforcements

The wave part of the beam is followed by the steel reinforcement, and the steel bars are bent using a specialized tool. The bending operation is carried out in accordance with the beam's shape. Thirty steel rebars and sixty anchoring bars are ready for each beam.

The steel reinforcements have two kinds of reinforcement longitudinal one and the transversal one the longitudinal reinforcements are 5 in number and placed at the bottom of the beam and the transversal reinforcements and at every 20cm in the curved shaped of the beam. The shaping of the transversal reinforcements is done in the lab with the tools with a curved and rectangular shape reinforcements which need to be placed at the side end of the beam a detailed section is also shown below in order to understand all type of reinforcements required to be placed.

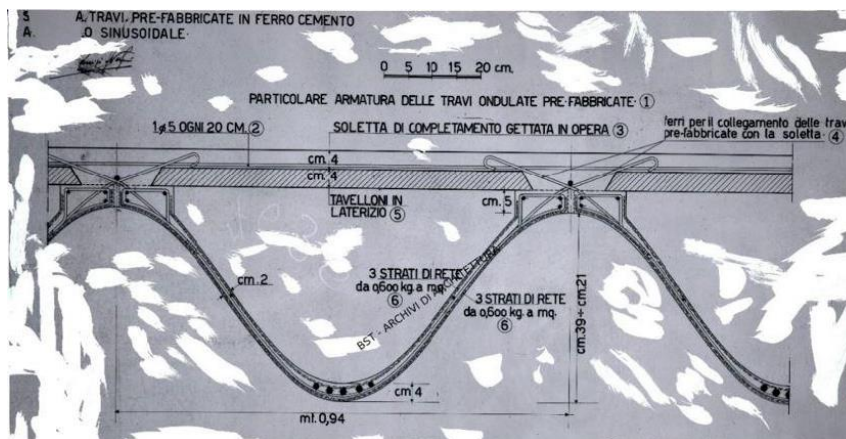


Figure 69 cross section view of the beam [27]





Figure 70 bending the transverse reinforcements

Once all the reinforcements were shaped in the required curvature the next step was placing them on the aluminium sheet, but before that we need to place the steel mesh.

The steel mesh which has a 4 layers on the sheet was de rolled and cut in the required shape at 1st two layers where cut and placed at the bottom of the beam and then the transversal reinforcements were placed. The procedure includes the steps of cutting the steel mesh at a length of 6m and pacing them, after placing them the steel mesh were cut from on side in order to inure the shape of the beam as the beam is trapezoidal shape and varies with depth. The next was placing the transversal reinforcements at every 20cm from the previous one. Once placing the reinforcements, they were tied down to the steel mesh with the wires to hold them in position.

The next step was placing the longitudinal reinforcement along the length and tie them up with the transversal reinforcement and the stell mesh. Also, these longitudinal reinforcements are spaced at 5cm from each other, to reach the length of 6m the longitudinal reinforcements were also welded at the certain distance. After placing all the reinforcements,

the next layer of steel mesh were to be put in position and tied down firmly to attain the required shape of the beam as suggested by nervi in the concept of ferrocement.

The next step after this was the positioning of the diaphragm, the total length of the beam contains 3 diaphragms of which one diaphragm is in the centre to the beam and the other two diaphragms are the extreme ends of the beam. These diaphragms are two end diaphragms have a different reinforcement than the one in the middle they are shaped as rectangular engulfing the front and rear end of the beam which constitute the running beam in which these wavy shaped beams are positioned next to each other. In order to make it clearer a picture is shown below to understand the positioning of the beam.

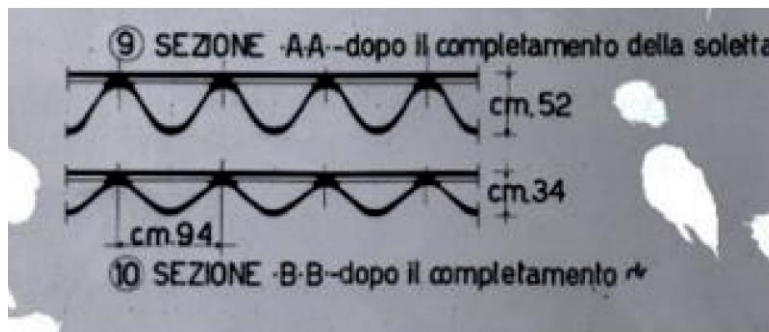


Figure 71 continuous curved beam setup [27]

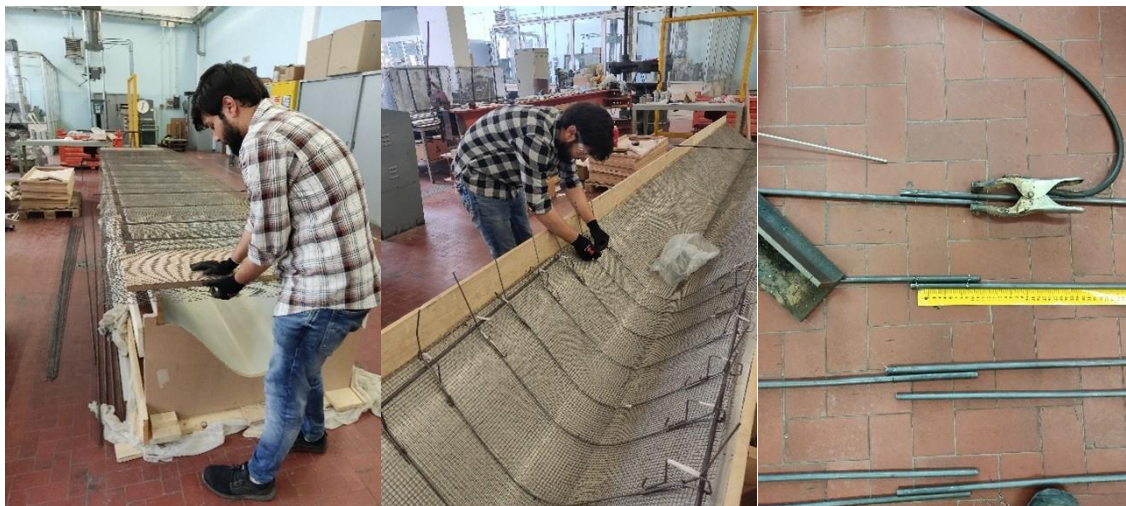


Figure 72 steel mesh placements and transversal reinforcements

The longitudinal reinforcements which are positioned in the middle part of the beam was not of the same length so to achieve a length of 6m the longitudinal reinforcements were welded against each other creating an overlapping bond, and the other reinforcements which runs in the side parts were overlapped against each other with a overlapping distance of 4 times the diameter of the bar.



Figure 73 transversal reinforcements and longitudinal reinforcements with wire mesh layers.

6.3.3. Trial testing of the beam.

In order to check the curvature of the beam and the cement mortar a trail test of the beam was conducted. As the curvature of the beam was not the usual rectangular shaped and also the curved aluminium sheet is placed in a right position these things were needed to be checked before casting the whole beam. Also the cement mixture available was mixed with the fine sand this mixture has to be tested for the water cement ratio.

In order to check the water cement ratio, the previous data was used. While casting the smaller mock-ups which were to be used in the process of corrosion potential testing required the water cement ratio of 0.20, the same water cement ratio was also used in the trail beam casting.

In order to cast the trail, beam the previously placed reinforcements were shifted to the other end, the aluminium sheet was brushed with the oil so that concrete could not stick with the plate, just the wire mesh was placed. 4 layers of wire mesh were cut and placed the one above the other and held down with the curvature of the aluminium sheet. The mortar mix was prepared with the cement water ratio of 0.2 and was placed and spread out evenly on the surface. And to avoid the segregation of the concrete slight tapping on the base of the beam were done so that cement could get between all the layers of the mesh. Once casted it was left for 5 days to dry and was lifted out after words to check the trial beam.



Figure 74 weighing the cements to add the required water and application of the scotch tape.

In order to avoid the cement leaking out of the side gaps the scotch tape was made was used on all the open edges as seen in the pictures above. The cement was measured to the required quantities and so the water to have a uniform mix required and within the workable limits. Two batches of the concrete were prepared.



Figure 75 trail casting of the beam

6.3.4. Making Of Diaphragms

Once all the transverse and longitudinal reinforcement are placed the next steps were attaching the diaphragm in the sides and middle of the beam, as these diaphragms have different reinforcements it was seen to customize the shape of diaphragms additional shape of formwork were needed the reinforcements were made in rectangular shape with a mesh of reinforcement of 10cm x 10cm and encircling this mesh reinforcements. The thickness being equals to 15cm and height being equal to 77cm. also this diaphragms will be connected

with the reinforcement that is in the longitudinal direction these longitudinal direction reinforcements were meant to be bent in L shape one end of the reinforcement is connected to the longitudinal reinforcement of the main beam and the second L should be connected with the reinforcements in the diaphragm. The reinforcement is welded on one side and tied on the other side in the diaphragms as for the middle diaphragm the reinforcement was cut down in the curved shape of the beam and was attached with the four layers of wire mesh.

7. ANALYSIS OF CURVED SHAPED BEAM

After building the model in laboratory we the FEA analysis of the beam was also carried out. In order to do the FEA analysis of the beam I choose the ANSYS software as being a good software and availability of the student licence from Polito. The 1st step was to make the model in some designing software for which I chose the RHINOCEROS 7.0.

7.1 Modelling the beam in RHINO

To model the beam the curved shape of the beam, it was 1st divided in two parts, in other words the beam of 6m was modelled as 3m and the design was carried out it was done so as to reduce the computation analysis of the software.

At 1st the curved beam was modelled as shell elements with a variable thickness of 4cm in the middle centre part of the beam and gradually decreasing on the sides with a thickness of 2cm. in order to achieve a smooth shape of the curve arch methods were used to model it.

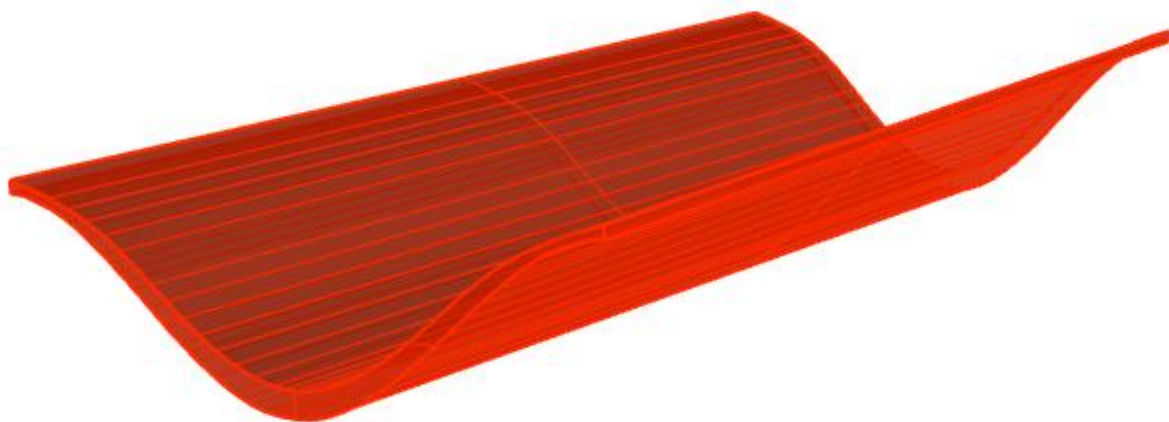


Figure 76 curved shaped beam modelled in rhino

In order to add the wireframe as per the drawings there were 4 layers of wire mesh and this mesh were modelled as a surface with an equivalent thickness of 4mm. this equivalent thickness was assumed thinking about the thickness of wires in the mesh as 1mm in dia.

Once the mesh was placed above the curved shape beam the next step was placing the transversal reinforcement and longitudinal reinforcements for the transversal reinforcements the curve of the beam was used to make the shape and a solid surface were modelled as the reinforcements with a thickness of 5mm in dia. And 3 longitudinal reinforcements with diameter of 10mm and two other longitudinal bar of 12m making in total of 5 bars in the centre.

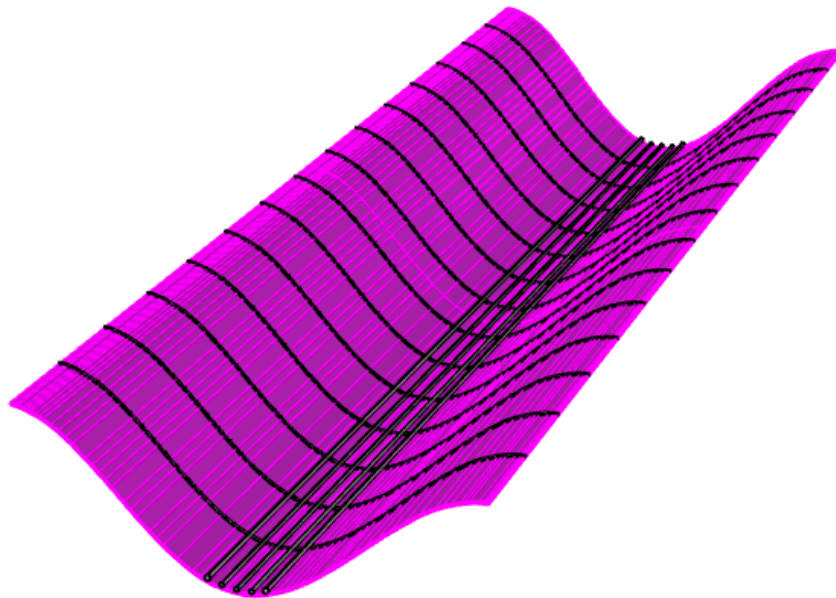


Figure 77 equivalent layer of steel mesh and reinforcements in transversal and longitudinal direction

Once this part was modelled the diaphragms were added, as we know the beam was divided in 2 parts the diaphragms which was supposed to be in centre became the extreme ends diaphragm these diaphragm have a thickness of 15cm on either side of the beam.

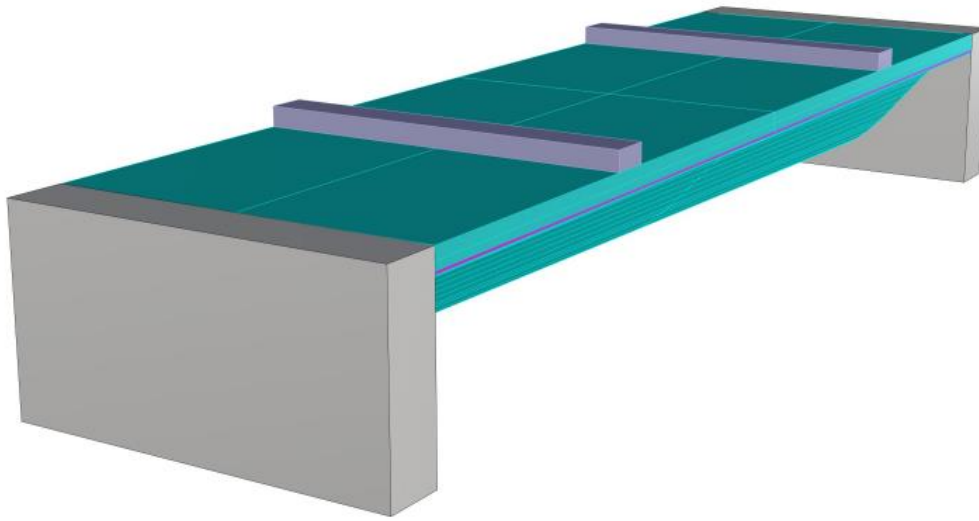


Figure 78 diaphragm placements

After the placement of the diaphragms the upper slab was modelled as solid surface. Making the complete model of the curved shaped beam. Also, a steel stirip of 20cm thick was placed in the middle in order to simulate the 4-point bending test.

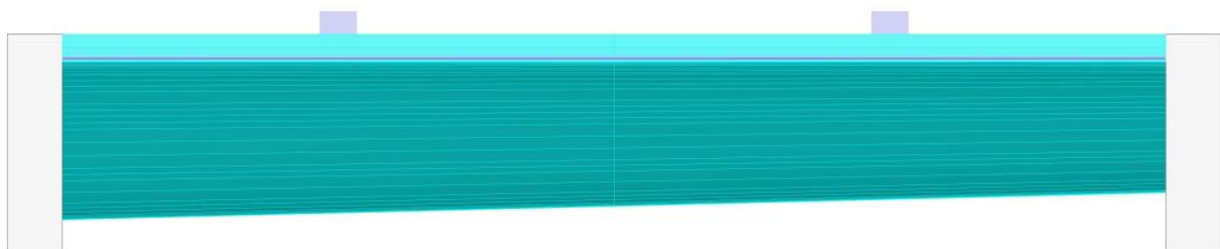


Figure 79 full modelled curved shape beam

7.2 4-point bending test.

The four-point bending flexural test provides values for the modulus of elasticity in bending E_f flexural stress σ_f flexural strain ε_f and the flexural stress–strain response of the material. This test is very similar to the three-point bending flexural test. The major difference being that with the addition of a fourth bearing the portion of the beam between the two loading

points is put under maximum stress, as opposed to only the material right under the central bearing in the case of three-point bending. [41]

This difference is of prime importance when studying brittle materials, where the number and severity of flaws exposed to the maximum stress is directly related to the flexural strength and crack initiation. Compared to the three-point bending flexural test, there are no shear forces in the four-point bending flexural test in the area between the two loading pins. The four-point bending test is therefore particularly suitable for brittle materials that cannot withstand shear stresses very well. It is one of the most widely used apparatus to characterize fatigue and flexural stiffness of asphalt mixtures. [41]

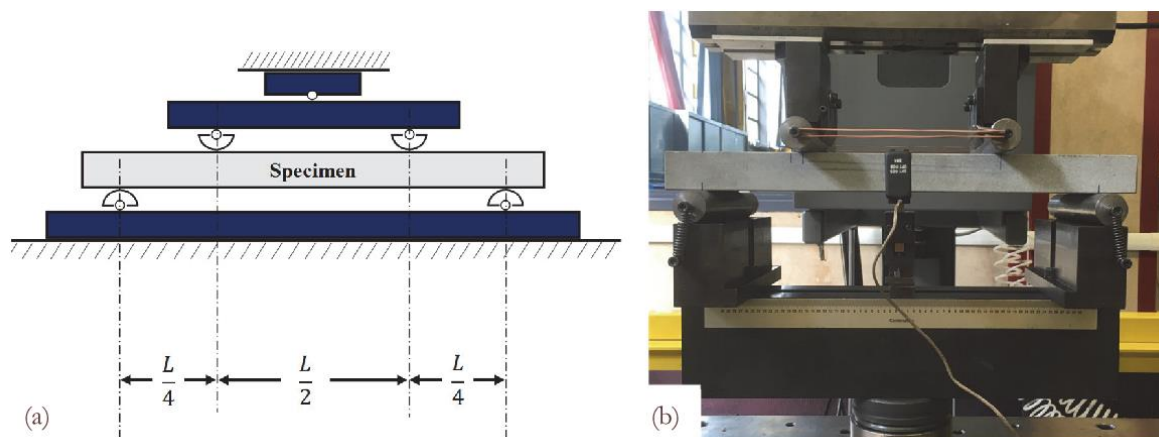


Figure 80 four-point flexural test

Calculation of the flexural stress σ_f

$$\sigma_f = \frac{3FL}{4bd^2} \text{ for a rectangular cross section}$$

$$\sigma_f = \frac{FL}{bd^2} \text{ for a circular cross section [1]}$$

7.3 Finite Element Modelling and Analysis

A common technique for numerically resolving differential equations that appear in engineering and mathematical modelling is the finite element method (FEM). The conventional topics of structural analysis, heat transfer, fluid flow, mass transport, and electromagnetic potential are typical issue areas of interest. Using two or three spatial variables, the FEM is a generic numerical technique for solving partial differential equations (i.e., some boundary value problems). The FEM breaks down a complex system into smaller,

more manageable pieces known as finite elements in order to solve an issue. The numerical domain for the solution, which has a limited number of points, is accomplished by creating a mesh of the object using a specific space discretization in the space dimensions. In the end, a set of algebraic equations emerges from the formulation of a boundary value problem using the finite element approach. The technique makes domain-wide approximations of the unknown function. [42] The small system of equations that describes these finite components is then combined with other equations to model the full issue. The calculus of variations is used by the FEM to minimize an associated error function and then estimate a solution. [43]

To accurately record and collect any relevant data for architectural historic buildings, as well as to elucidate their most contentious elements, many disciplinary approaches are necessary. The finite element methods in used in this thesis, In order to correctly determine the curved beams used in the hall C many pervious original drawings and data were collected from the archives. And based on the data available the best possible approach was used to create and carry out the model analysis of the beam. The beams dimensions and geometrical features as well as components classifications were matched with the original beam and used.

7.3.1 Numerical Modelling and Analysis.

The original documentation was used as the foundation for creating the finite element model (FEM) in the ANSYS program (see Figure 82). Due to the paucity of experimental data on material characteristics, linear models were selected to carry out the final element modelling. the whole beam was 6m which was reduced to 3 meters because of the symmetry of the beam.

The whole beam is made of out of various elements which includes the curved beam following the curvature of the beam as designed by Nervi, in real beam there were 3 diaphragms two at the extreme corners and one in the middle with reinforcements. But in the model two diaphragms were included at both extreme ends. Also the beam contains 4 layers of wire mesh in order to simulate the 4 layers of wire mesh a surface element of 4mm thick was encased inside the beam.

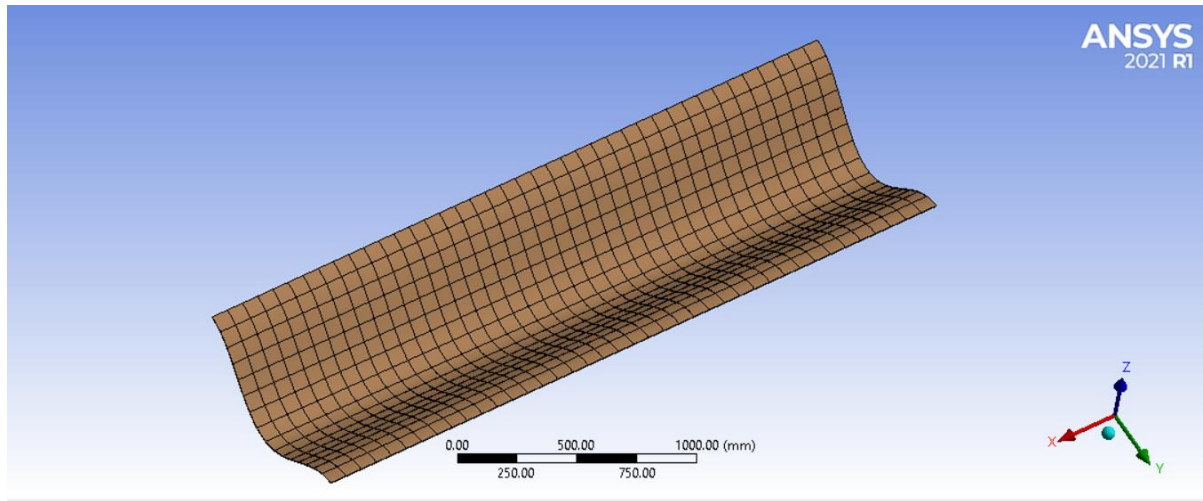


Figure 81 steel mesh with meshing

The steel mesh contains 5 longitudinal reinforcements with equally spacings, two of the reinforcements having diameter of 12mm and 3 bars with diameter of 10mm. The ferrocement slabs which have a curved shaped regime also have a top surface in order to provide the rigidity and structural stability, these elements were modelled as bi-dimensional elements (SHELL).

The properties of the materials which were used to define the different materials can be summaries in table 5.

Material	$\frac{E}{GPa}$	Poisson's Ratio	$\frac{\rho}{Kg/m^3}$
Ferrocement	20	0.2	2500
Steel mesh	138	0.3	7850
Transversal reinforcement	200	0.3	7900
Longitudinal reinforcements	200	0.3	7900

Table 5 materials and properties

In order to simulate the 4-point bending test setup the whole beam have a different constraints or boundary conditions. The base of the diaphragms was treated as fixed supports. The contacts between the different were fixed as bonded in ANSYS. To apply the displacement in the vertical direction in the point of loading a roller was placed at the top surface of the beam.

The meshing was done and in order to simulate the curved surface of the ferrocement beam the method of meshing was chosen as tetrahedron as it is much more efficient on the curved

surfaces. For the reinforcements and the steel mesh and diaphragms the square normal mesh was used with element size of 75mm. The whole setup of the beam is shown in figure 82.

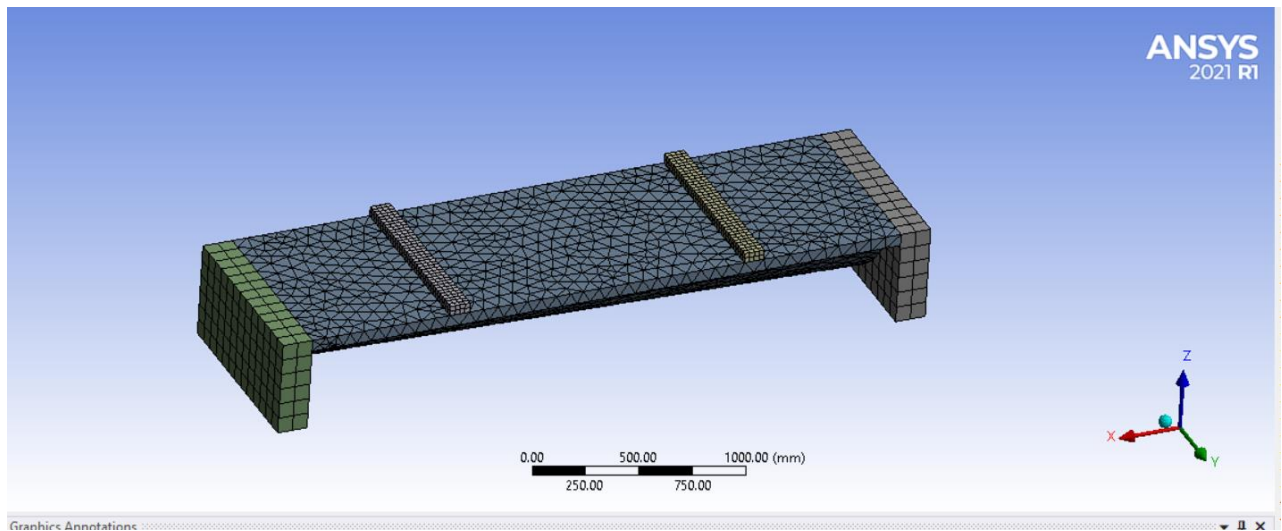


Figure 82 ferrocement beam with meshing

As we have seen in the previous sections of the stress strain law which was calculated for the smaller mock-up a similar calculation can be calculated in order to find the stress and strain profile at which the first crack would develop in the matrix. The general properties which were used In the analysis on Ansys includes maximum tensile stress $\sigma_{mu} = 3.5 \text{ Mpa}$, $E_r = 200 \text{ GPa}$, $E_m = 20 \text{ GPa}$. Volume of matrix = $2.1 \times 10^5 \text{ cm}^3$ and Volume of reinforcement = 11234 cm^3

From the above data

$$V_c = \text{volume of matrix} - \text{volume of reinforcements}$$

$$\text{volume of concrete} = 210700 - 11234 = 119536 \text{ cm}^3$$

$$V_m = \frac{\text{volume of matrix}}{\text{volume of concrete}} = \frac{119536}{210770} = 0.9467$$

$$V_r = \frac{\text{volume of reinforcements}}{\text{volume of concrete}} = \frac{11234}{210770} = 0.0532$$

The elastic modulus of the composite in the loading direction can be obtained from the law of mixtures (upper bound solution of equal strains) as:

$$(E_c)_{ub} = E_r V_r + E_m V_m = E_r V_r + E_m (1 - V_r)$$

where $V_r = V_{r1}$ is the volume fraction of longitudinal reinforcement, V_m is the volume fraction of matrix, E_r is the elastic modulus of the reinforcement in the longitudinal (loading) direction, and E_m is the elastic modulus of the matrix assumed isotropic.

$$(E_c)_{ub} = (200 * 0.0532) + (20 * 0.9467) = 29.574 \text{ Gpa}$$

In order to calculate the stress at which the first crack would develop we need to calculate the σ_c

$$\sigma_c = \sigma_{mu}(v_m + n * v_r)$$

$$\sigma_c = 3.5(0.9467 * (10 * 0.0532)) = 5.175 \text{ Mpa}$$

So the stress at the point of first cracking of concrete is estimated to be around 5.17 MPa. Once the displacement applied at the top pad of the beam and the matrix reaches the stress of $\sigma_c = 5.175 \text{ Mpa}$ the first crack could be observed in the matrix. The similar linear elastic model was also calculated in the Ansys, and the results obtained were similar to the one obtained analytically.

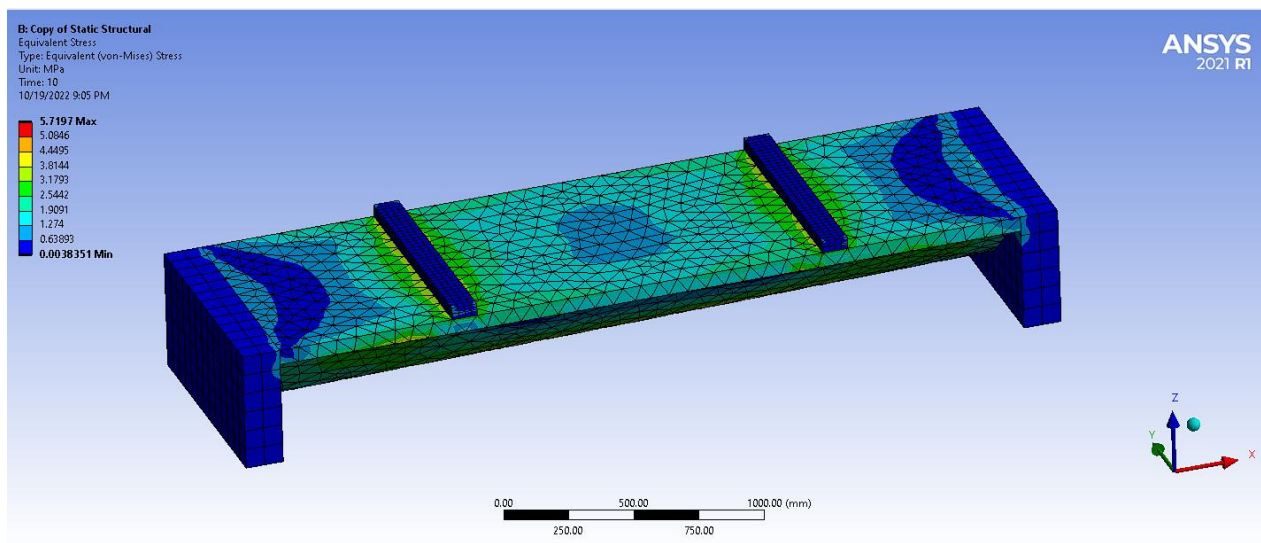


Figure 83 equivalent stress obtained from Ansys

As we know since this is a linearly elastic modelling the behaviour of the beam under the applied displacements is also linear the point which was discussed above the point A at which the first cracking in the ferrocement beam, after point A or first cracking in the beam the structure starts to behaviour nonlinearly and sudden increment in the strain are observed. The equivalent elastic strain can be seen in figure 85.

The Equivalent stress and strain if plotted shows the linear behaviour up to the point A. these results could be used further in the physical testing of the beam when the first cracking in the beam starts to occur. And after that the non-linear behaviour of the beam can be observed.

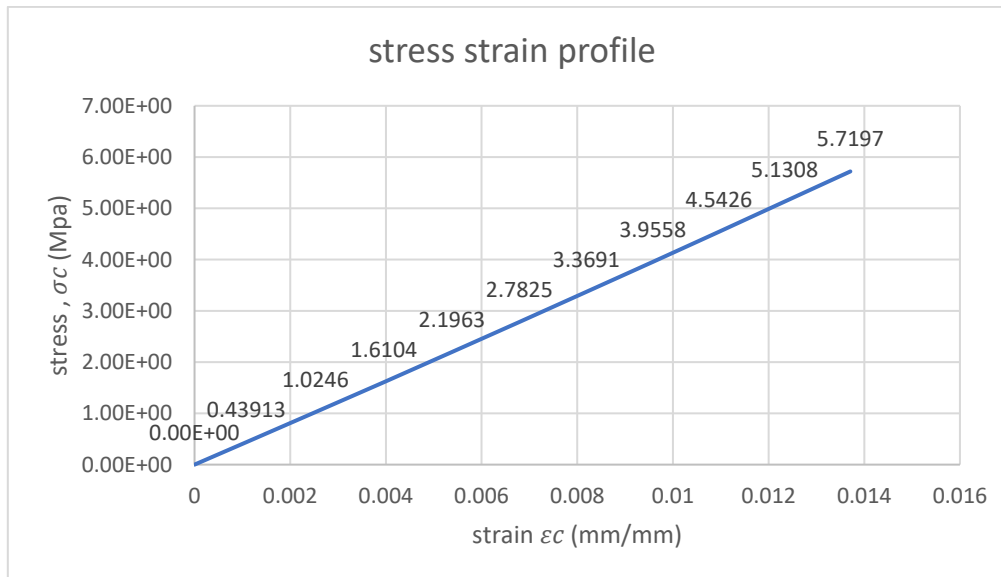


Table 6 stress strain profile of the beam

8. CONCLUSION AND FUTURE DEVELOPMENTS

This dissertation analysed ferrocement buildings, demonstrating the composition and primary applications of this little-known material, which is sometimes mistaken for traditional reinforced concrete.

Thanks to its simplicity of manufacture and accessibility of materials, its qualities and how it was employed in many sectors of application were discussed. Its greatest advantage is the ability to reproduce any shape without the need for intricate formwork, and it can achieve extremely thin thicknesses while still having excellent mechanical strength and impermeability. For this reason, it has found extensive use in the construction of tanks and other structural components that resist taking on a particular shape.

Also, the famous works of Eng. Pier Luigi Nervi was discussed in this dissertation and exploring the Nervi system of ferrocement. The focus of this dissertation was the choice of the mock-up's and building the bigger mock-up of a corrugated ferrocement beam of 1:1 scale in

laboratory and testing them in order to better understand the behaviour of the ferrocements slabs used in Torino Esposizioni centre.

The numerical analysis of the beam included the modelling of the corrugated beam in a drafting and design software for which Rhino was used and making the numerical linear analysis of the beam, the finite element software Ansys and used in order to carry out the linear analysis and find the stress at which the propagation of the first cracks develops in the beam.

Future work will also include to model the nonlinear behaviour of the ferrocement after the propagation of the first crack developers in the beam with the help of any finite element analysis software, also as for the experimental study the construction of 4 beams will be carried out in future, which will be evaluated under two distinct conditions—one where the beam is artificially conditioned to replicate the corrosion deterioration of the reinforcing bars, and the other where it is completely intact—to correlate the impact that corrosion has on ferrocement parts.

References

- [1] "The Getty Foundation," [Online]. Available: https://www.getty.edu/foundation/initiatives/current/keeping_it_modern/grants_awarded_2019.html.
- [2] "TORINO ESPOSIZIONI: THE POLITECNICO PROJECT WINS FUNDING FROM THE GETTY FOUNDATION "KEEPING IT MODERN"," [Online]. Available: [https://www.dad.polito.it/news/\(idnews\)/13445](https://www.dad.polito.it/news/(idnews)/13445).
- [3] "Ferrocement," [Online]. Available: <https://en.wikipedia.org/wiki/Ferrocement#:~:text=Ferrocement%20originated%20in%20the%201840s,sculpture%20and%20prefabricated%20building%20components..>
- [4] "ACI Committee 549-1R-88, "Guide for Design Construction, and Repair of Ferrocement"".
- [5] "Bingham, B., Ferro-cement Design, Techniques, and Applications, Cornell Maritime Press,".
- [6] in *Ferrocement & laminated cementitious composites*, 2000.
- [7] "What Is Ferrocement | Properties of Ferrocement | Uses of Ferrocement | Process of Ferrocement Construction | Advantages & Disadvantages of Ferrocement," [Online]. Available: <https://civiljungle.com/uses-of-ferrocement/>.
- [8] in *how the world is built today* , 1995.
- [9] "Ferrocement and properties," [Online]. Available: <https://www.civilclick.com/ferrocement/>.
- [10] "Vacuumatic Concrete: From Boats to Architecture," [Online]. Available: https://www.researchgate.net/publication/322255623_Vacuumatic_Concrete_From_Boats_to_Architecture.
- [11] "wikipedia," [Online]. Available: https://en.wikipedia.org/wiki/Pier_Luigi_Nervi#cite_note-3.
- [12] "expedition workshed," 1973. [Online]. Available: <https://expeditionworkshed.org/workshed/sydney-opera-house/>.
- [13] "SYDNEY OPERA HOUSE," [Online]. Available: <https://expeditionworkshed.org/workshed/sydney-opera-house/>.
- [14] "Pier Luigi Nervi," in *Olympedia* , retrived 11 august 2020.

- [15] "wikipedia," 2022. [Online]. Available: https://en.wikipedia.org/wiki/Palazzetto_dello_Sport.
- [16] C. Correttamente, "Il Percorso creativo di Pier Luigi Nervi attraverso 13 Opere - Schede informative, Palazzetto dello Sport, Roma 1956-57," [Online]. Available: http://costruirecorrettamente.org/site/approfondimento/informative_detail.php?do_c_id=108.
- [17] wikipedia, "Palazzetto dello Sport (Roma)," [Online]. Available: [https://it.wikipedia.org/wiki/Palazzetto_dello_Sport_\(Roma\)#Bibliografia](https://it.wikipedia.org/wiki/Palazzetto_dello_Sport_(Roma)#Bibliografia).
- [18] "Pier Luigi Nervi per le Olimpiadi di Roma: un sistema mai eguagliato," [Online]. Available: <https://www.teknoring.com/news/progettazione/pier-luigi-nervi-per-le-olimpiadi-di-roma-un-sistema-mai-eguagliato/>.
- [19] S. P. Tullia Iori, "Pier Luigi Nervi's Works for the 1960 Rome Olympics," 2005.
- [20] "THE HIDDEN GEM OF FLORENCE: THE ARTEMIO FRANCHI STADIUM," [Online]. Available: <https://www.innovaconcrete.eu/the-hidden-gem-of-florence-the-artemio-franchi-stadium/>.
- [21] I. ISC20C, "ICOMOS Heritage Alert for the Stadio Artemio Franchi (Pier Luigi Nervi, 1929-31) in Florence, Italy".
- [22] P. Nervi, "La struttura portante del nuovo Salone del Palazzo di Torino Esposizioni., Atti e rassegna," 1950.
- [23] N. P.L, "Structures," 1956, F.W. Dodge Corp, New York.
- [24] "Minimum Documentation Fiche composed by regional working party of LOMBARDIA, Italy," [Online]. Available: https://www.docomomoitalia.it/register/MF_02.pdf.
- [25] R. C. C. C. Erica Lenticchia, "Damage scenario-driven strategies for the seismic monitoring of XX century spatial structures with application to Pier Luigi Nervi's Turin Exhibition Centre".
- [26] G. C., "Pier Luigi Nervi. Dai primi brevetti al Palazzo delle Esposizioni di Torino 1917-1948," 2008.
- [27] p. guarino, "Analysis of the state of conservation of ferrocement structures by Eng. Pier luigi nervi," *politecnico di torino web thesis portal*.
- [28] "Turin Exhibition Palace," [Online]. Available: <https://www.domusweb.it/en/from-the-archive/2011/04/28/turin-exhibition-br--palace.html>.
- [29] "international hockey wiki," [Online]. Available: https://internationalhockey.fandom.com/wiki/Torino_Esposizioni.

- [30] " Olimpiade Invernale Torino 2006," [Online]. Available: https://www.gazzetta.it/Speciali/Torino_2006/impianti/79.shtml.
- [31] "MARCO SAROLDI PHOTOGRAPHER," [Online]. Available: <https://photoit.photoshelter.com/image/I0000wZyAn.fdpvl>.
- [32] "Costruire Correttamente," 2B.COM SPRL, [Online]. Available: http://costruirecorrettamente.org/site/approfondimento/informative_detail.php?doc_id=106.
- [33] N. P.L, "Scienza o arte del costruire? Caratteristiche e possibilità del cemento armato," Rome, Edizioni della Bussola, 1945.
- [34] G. Colonnetti, "Tecnica delle costruzioni: sezioni sottili. Realizzazioni di P. L. Nervi, E. Torroja e G. Oberti.," 1957, Edizioni Scientifiche Einaudi.
- [35] S. L. e. L. Consolini, "Percorsi per un metodo progettuale tra forma e struttura,," 2007, Roma: ARACNE editrice S.r.l.
- [36] S. P. TULLIA LORI, "Pier Luigi Nervi: His construction system for Shell and Spatial Structures," 2013.
- [37] "slideshare ferrocement," [Online]. Available: <https://www.slideshare.net/prabhatchhirolya/ferrocement-65375247>.
- [38] D. Abruzzese, "A model for ferrocement thin walled structures,," rome.
- [39] C. Greco, "The ferro concrete of Pier Luigi Nervi," 1995.
- [40] "Calcoli statici, salone C,Torino," 1950.
- [41] "Four-point flexural test," [Online]. Available: https://en.wikipedia.org/wiki/Four-point_flexural_test.
- [42] D. L. Logan, "A first course in the finite element method.," no. Cengage Learning, 2011.
- [43] "Finite element method," [Online]. Available: https://en.wikipedia.org/wiki/Finite_element_method.
- [44] "Three-point flexural test," [Online]. Available: https://en.wikipedia.org/wiki/Three-point_flexural_test.
- [45] "THE GETTY FOUNDATION KEEPING IT MODERN ARCHITECTURAL CONSERVATION GRANTS 2017," [Online]. Available: <https://www.stadioflaminio.org/index.php?lg=en#home>.

INDEX OF FIGURE

Figure 1 typical cross section of ferrocement beam [7]	8
Figure 2 Joseph Louis Labot (right) ferrocement boat (left).....	8
Figure 3 Ferrocement and its constituents, mortar, and steel, being given a cylindrical	9
Figure 4 Types of wire mesh used in ferrocement applications; (a) welded wire mesh; (b) hexagonal wire mesh; (c) woven wire mesh; (d) expanded metal [6]	10
Figure 5 typical ferrocement housing units.....	12
Figure 6 ferro-cement panels that have been prefabricated and installed for a house [6] ...	12
Figure 7 ferrocement wall in construction [7]	13
Figure 8 ferrocement walls and shell in India [9]	14
Figure 9 ferrocement dome shaped house [7]	14
Figure 10 Ferro-cement fishing boat 'La Giuseppa', designed by Nervi, 1967 Image source: ericafirpo.com (left): ferrocement boat name PRISCILLA (right) [10]	15
Figure 11 Typical section through bulwark showing fitting out detail.....	16
Figure 12 ferrocement boat Ambrym dating 1985 [10]	16
Figure 13 large size boat of ferrocement in China (left); medium size ferrocement boats (right) source A Naman [6].....	17
Figure 14 Sydney opera house built with ferrocement shell elements [13]	18
Figure 15 Sydney opera house (Australia) [13]	19
Figure 16 Arup, O and Zunz, J 1969, 'Sydney Opera House', Structural Engineer, March 1969. Reprinted in The Arup [13].....	20
Figure 17 Palazzetto dello Sport (Rome) [15]	22
Figure 18 (A) interior view Palazzetto dello Sport; (B) Exterior view of the Palazzetto (Source: Pier Luigi Nervi Project); Aerial view of the Flaminio Stadium; (D) Flaminio shelters; (E) Interior view of the Palazzetto; (F) Aerial view of the Sports Palace [18]	23
Figure 19 Pier Luigi Nervi, drawing of the covered stand, section of the heading part, undated (1931). Private Archive of Pier Luigi Nervi, Rome [21]	24
Figure 20 External view of the Stadium shortly after its completion, © Ferdinando Barsotti, 1932 [21].....	25
Figure 21 One of the helical staircases, © Marco Menghi, 2018 [21]	25
Figure 22 scaffolding for the building's prefabricated components (from The Norton Lectures, Courtesy Pier Luigi Nervi Knowledge and Management project Asbl) [24].....	27
Figure 23 Proposed hall b in 1948.....	28
Figure 24 The Salone B of Torino Esposizioni under construction in 1948: assembly of the prefabricated ferrocement waves that make up the arches of the great vault. [24]	29
Figure 25 Drawings of the prefabricated system (from The Norton Lectures, Courtesy Pier Luigi Nervi Knowledge and Management project Asbl) [24]	29
Figure 26 Plan of the Turin Exhibition: Hall B, the huge rectangular area in the; Hall C, the smaller rectangular shape in the upper right corner, was constructed a year later; (B) Pier Luigi Nervi's plan and section of Hall C from the (Rassegna tecnica della Società degli ingegneri e architetti in Torino.) [25]	30
Figure 27 original drawings of the short bow (left) and longbow (right) reinforcement design [27].....	32

Figure 28 phase of assembling the diamond shape slabs on the vault before casting the ribs [28].....	32
Figure 29 Hall C's half-plank outline as seen in the source : CSAC Parma Archives	32
Figure 30 Planks in Hall C are shown in silhouette in this image from the CSAC Parma Archives.	33
Figure 31 Section of the perimeter floor in ferrocement source CSAC Archive Parma	33
Figure 32 Realization of a practical roofing board.....	34
Figure 33 The Palazzo delle Esposizioni ITALIA 61 turin olympic games 2006 [29] [30]	35
Figure 34 The Palazzo delle Esposizioni ITALIA 61 in the Parco del Valentino during the Turin 2006 Olympic Games. The vault of Luigi Nervi [31].....	36
Figure 35 state of Torino Esposizioni centre from the pictures taken between January 2020 to July 2021	37
Figure 36 Italian patent n. 406296, "Ferrocement", 1943 (Archivio Centrale dello Stato, Roma: Fondo Brevetti).	39
Figure 37 Patent No. 429331 from Italy, "Ferrocement warehouse," 1944 (Archivio Centrale dello Stato, Roma: Fondo Brevetti).	39
Figure 38 In the case of constructions with shape resistance, the resistant region.	41
Figure 39 Full size model of a portion of the Magliana Warehouse's curly wall, 2013 (Photo Sergio Poretti, SIXXI Project) (LEFT), Magliana Warehouse. Restoration works, 2013 (Photo Sergio Poretti, SIXXI Project). (RIGHT)	42
Figure 40 cross section of ferrocement with the wire mesh and the steel rebars [37]	44
Figure 41 typical cross section of ferrocements [6].....	45
Figure 42 Typical steel mesh used in ferrocements [6]	47
Figure 43 typical steel mesh used in ferrocement applications [6]	48
Figure 44 typical cross section of reinforced concrete against ferro cement. [6].....	49
Figure 45 schematic load-elongation curve of ferrocement in tension illustrating the various stages of behaviour [6].....	51
Figure 46 Model of tensile prism: a) uncracked composite; b) unbonded reinforcement; c) partial debonding; d) assumed model between two cracks.....	54
Figure 47 ferrocement matrix dimension.....	55
Figure 48 (a) Tensile element that hasn't cracked;(b) cracked element; (c) an assumed cracked element model	56
Figure 49 Typical tensile stress strain response assuming only one crack occurs	57
Figure 50 stress strain profile obtained for ferrocement model	58
Figure 51 Schematic moment-curvature response of a ferrocement section.	59
Figure 52 cross section of a ferrocement member.	60
Figure 53 cross section view of ferrocement mockup.....	61
Figure 54 cross section with detailed area of beam	61
Figure 55 linear stress and linear strain diagram	62
Figure 56 steel woven wire mesh in smaller mock-ups.....	65
Figure 57 7 layers of steel mesh separated with wooden sticks to avoid sticking and proper spacing and end connectors attached.....	66
Figure 58 ferrocement realization as done by Nervi	67
Figure 59 typical cross section of the ferrocement beam [27]	68

Figure 60 lateral view of beam with the continues wavy shaped beam [27]	68
Figure 61 4 steel nets to be placed and curvature of the beam. [27]	69
Figure 62 side view of diaphragm [27]	69
Figure 63 cross section view of the beam with diaphragm reinforcement and longitudinal reinforcements(top), example of a longitudinal section of a reinforced corrugated beam (bottom) [27]	70
Figure 64 base beam and the curved panels placed.	71
Figure 65 side rails and curved panels placed.	72
Figure 66 placing of the triangular shaped support	73
Figure 67 placing steel sheet.....	73
Figure 68 placing of the aluminium sheet	74
Figure 69 marking the diaphragm and placing the sheet with nails.	74
Figure 70 cross section view of the beam [27]	75
Figure 71 bending the transverse reinforcements	76
Figure 72 continuous curved beam setup [27]	77
Figure 73 steel mesh placements and transversal reinforcements	77
Figure 74 transversal reinforcements and longitudinal reinforcements with wire mesh layers.	78
Figure 75 weighing the cements to add the required water and application of the scotch tape.....	79
Figure 76 trail casting of the beam.....	80
Figure 77 curved shaped beam modelled in rhino	81
Figure 78 equivalent layer of steel mesh and reinforcements in transversal and longitudinal direction.....	82
Figure 79 diaphragm placements.....	83
Figure 80 full modelled curved shape beam	83
Figure 81 four-point flexural test	84
Figure 82 steel mesh with meshing.....	86
Figure 83 ferrocement beam with meshing	87
Figure 84 equivalent stress obtained from Ansys	88

INDEX FOR TABLE

Table 1 Oberti & Grandori established characteristic values for ferrocement components in 1949. [38].....	44
Table 2 Ferrocement in a nutshell: ranges of composition, reinforcing parameters, and mechanical properties. [6]	46
Table 3 minimum yield values for reinforcements source: A. Naaman	52
Table 4 Typical bending response of ferrocement beams using square woven mesh [6]	52
Table 5 materials and properties	86
Table 6 stress strain profile of the beam.....	89